Toxicogenomic Fingerprint Identification in Springtails to Assess Pesticide-Contaminated Soils

Bakker, Ruben Rob

2022

DOI (link to publisher)
10.5463/thesis.44

document version
Publisher's PDF, also known as Version of record

Toxicogenomic Fingerprint Identification in Springtails to Assess Pesticide-Contaminated Soils

Ruben Bakker

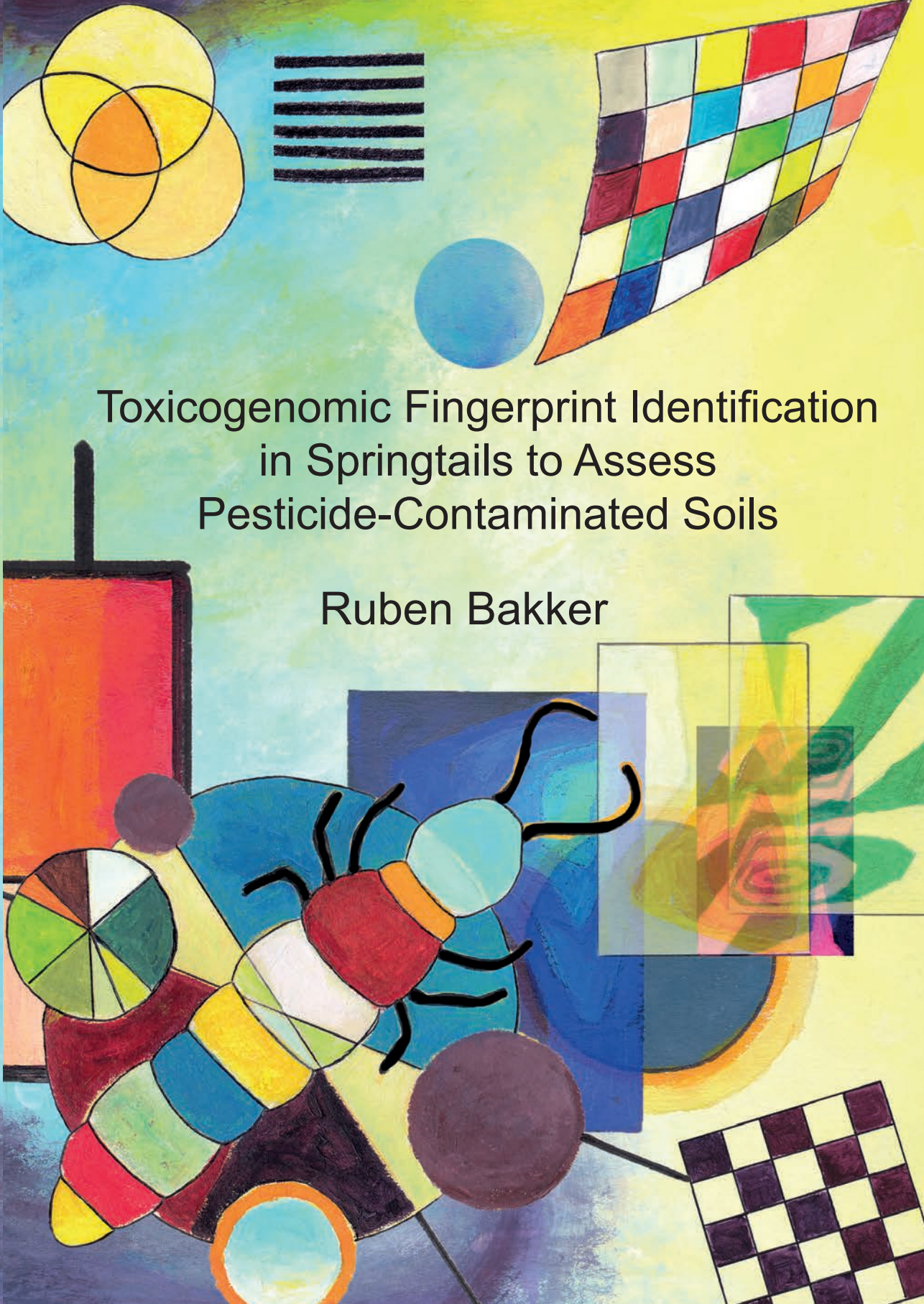

Toxicogenomic Fingerprint Identification in Springtails to Assess Pesticide-Contaminated Soils

Ruben Bakker

ISBN: 978-94-6458-779-1
Cover design: Janine Mariën
Lay-out: Publiss | www.publiss.nl
Print: Ridderprint | www.ridderprint.nl

VRIJE UNIVERSITEIT

Toxicogenomic Fingerprint Identification in Springtails to Assess Pesticide-Contaminated Soils

ACADEMISCH PROEFSCHRIFT

ter verkrijging van de graad Doctor of Philosophy aan
de Vrije Universiteit Amsterdam,
op gezag van de rector magnificus
prof.dr. J.J.G. Geurts,
in het openbaar te verdedigen
ten overstaan van de promotiecommissie
van de Faculteit der Bètawetenschappen
op vrijdag 16 december 2022 om 11.45 uur
in een bijeenkomst van de universiteit,
De Boelelaan 1105

door
Ruben Rob Bakker
geboren te Haarlem

promotoren:	prof.dr.ir. C.A.M. van Gestel prof.dr. J. Ellers
copromotoren:	dr.ir. T.F.M. Roelofs dr. K.M. Hoedjes
promotiecommissie:	prof.dr. K. Borgå dr. B. Campos prof.dr.ir. P.J. Van Den Brink prof.dr. L. Posthuma dr. S. Hughes prof.dr. N.M. van Straalen

Foreword

During a friend's Ph.D. thesis defense ceremony, one of the opponents recited a poem. He said, "I hold a pebble and lay it in a river; now the river runs a different course." He asked my friend to speak his mind: "was his Ph.D. thesis a pebble in the river, and did it diverge its course?" My friend was bewildered and unable to answer the opponent well. Such a question is not typically asked during a Ph.D. thesis defense ceremony. After giving it much thought, I would like to provide my answer. For me, the key to viewing this parable is not the pebble but the river. I see the river as human curiosity, forever meandering down the mountain and its hills, pooling in its depth and creating rapids on its slopes. The river bed, the universe around us, is everywhere different, and everywhere the water seeks to explore its shapes and finds its way through. Or in other words, our curiosity explores our universe. Just like human curiosity, the river cannot be stopped. At an obstacle, it may break off rock chunks. The river currents in its rapids grind the rocks, eventually returning them as smooth pebbles somewhere on the river bed. During my Ph.D., my curiosity, together with that of many other scientists, friends, and consortium partners, has grounded down a rough stone into a pebble. Now I hope someone might find my pebble and return it to the river. Hopefully, it will be ground down until it can no longer be recognized as my pebble, worn by human curiosity to its elemental parts. Hopefully, someone will find its remnants somewhere down the river's stream. Hopefully, someone will find it useful; it would be the greatest honor for me. Are you that person?

Table of Contents

Chapter 1

General Introduction

The Green Revolution

The period between 1960 and 2000 witnessed the widespread adoption of agricultural (agro-)chemicals, such as pesticides and artificial fertilizers, among other innovations. The result was a tripling of agricultural productivity and, in tandem, a doubling of the world population (Ruttan, 2002). Therefore, this period is called "the Green Revolution." Besides the historical relevance of agrochemicals, they also play a vital role in supporting future population growth while maintaining, or in some areas increasing, the human standard of living (Godfray et al., 2010). Meanwhile, climate change will strain agricultural productivity by rising sea levels, increasing temperature, and more frequent extreme weather events such as heatwaves, droughts, and wildfires (Gornall et al., 2010).

The environmental impact of agrochemicals

Besides the beneficial aspects of agrochemicals, they also disrupt the globally interlinked ecosystems and cause biodiversity loss (FAO, ITPS, GSBI, 2020). The aspects of ecosystem functioning that contribute to human wellbeing are called "ecosystem services," and some are essential for agriculture (Wall et al., 2015). Pastures and most crops grow in the soil, bar in the horticulture sector. Here plants come in contact with a diverse community of organisms, the soil ecosystem. The plant's first contact with this ecosystem is with the soil microbes. The majority of this group lives in or directly on the roots of plants but can also live freely and consists of, among others, bacteria, fungi, viruses, algae, and Archaea (Dastogeer et al., 2020). In particular, the bacteria and fungi form symbioses with plant roots and exchange nutrients for sugars and other energy sources. These microbial symbionts are crucial for the plant's survival (Dastogeer et al., 2020). Another important organism group of the soil ecosystem are the invertebrates, such as nematodes, mites, beetles, springtails, ants, and, chief among them, the earthworms. Earthworms feed off dead plant litter and tunnel through the soil, preventing land erosion and promoting nutrient cycling.

Collectively, the soil invertebrates feed on the microbes, dead plant litter, and each other. They aerate the soil, cycle nutrients, control pest species, and spread, maintain and reshape the soil microbiome (FAO, ITPS, GSBI, 2020; Pathiraja et al., 2022). Even invertebrates that provide ecosystem services above ground can spend a life stage or part of the day underground, where they come in contact

with agrochemicals. For example, solitary bees nest in the soil and, here, can come in contact with agrochemicals (Willis Chan et al., 2019). Moreover, the above- and belowground parts of an ecosystem are intimately intertwined and comprise many more relevant groups of organisms. Arguably, however, invertebrates and microbes are omnipresent in every agricultural system and, therefore, deserve to be mentioned explicitly. The risk agrochemicals pose to the soil ecosystem services can have repercussions far beyond the soil and impact every part of human wellbeing.

Assessing the environmental risk of pesticides

Agrochemicals, especially pesticides, are necessary to maintain the growing human population and standard of living in a rapidly advancing and developing world while also posing a real threat to global ecosystem services and natural resources the world population equally relies on to sustain itself. Because of this duality, efforts should be made to gradually reduce the quantity of applied pesticides and improve our understanding of what makes them toxic to organisms by themselves and in mixtures. Meanwhile, we must enhance analytical methods to monitor pesticides and their environmental risk to (soil) invertebrates.

Traditionally, the environmental risk assessment of agrochemicals is based on highly standardized tests and statistical methods that determine the effective concentration (EC_x), indicating by what percentage a pesticide reduces reproduction or increases mortality of the test species (van Gestel, 2012). The strength of these EC_x-toxicity tests is their simplicity, reproducibility, and global standardization. It is difficult, however, to extrapolate the results of these standardized tests to field-relevant conditions. First, most agricultural soils are contaminated with mixtures of pesticides (Pelosi et al., 2021; Silva et al., 2019) and innumerable other contaminants such as (veterinary) pharmaceuticals, metals, microplastics, and nanoparticles. The (synergistic) interaction effects between these contaminants are ill-understood. Second, soil characteristics, i.e., its physicochemical properties, influence how much of the pesticide remains bound to the soil and how much is absorbed by organisms, i.e., its bioavailability (van Gestel, 2012). Therefore, EC_x values for pesticide toxicity obtained in one soil type cannot directly indicate toxicity in other soils with different properties. Third, the enforcement of EC_x-based policy requires the measurement of environmental concentrations of a

alarge panel of pesticides. Assessing a myriad of pesticides is labor-intensive and requires chemical references, i.e., pure pesticide standards. Therefore, chemical analysis of environmental samples is costly and limited to well-studied pesticides. If pesticides degrade by natural forces, such as the temperature or soil microbes, potentially toxic metabolites may be formed, which often are not determined in routine chemical screening. Due to these factors, traditional chemical analysis underestimates the toxicity of complex environmental mixtures of contaminants (Escher et al., 2020). A range of bioanalytical tools can supplement conventional chemical screening and EC_x-based pesticide monitoring to improve the accuracy of the risk assessment of environmental pollution mixtures (Escher et al., 2020).

Bioanalytical methods

Pesticides and other toxicants trigger a cascade of responses in the organisms at various levels of biological organization, molecular, biochemical, cellular, tissue, organ, body (behavior), and population. At the lowest level, chemical reactions start the response cascade. A toxicant, for example, a pesticide, disrupts the steady state of all chemicals and bodily functions, called homeostasis. The stress caused by the disruption of homeostasis leads to the reallocation of energy to reestablish it. Reallocation of energy is primarily affected by altering the number and type of proteins. Proteins form complex networks called pathways in which many hundreds of proteins can be involved. Speeding up or slowing down these pathways by altering proteins in critical positions is pivotal for maintaining homeostasis. With this information, scientists can develop bioanalytical tools to monitor the response cascade and determine the reallocation of the energy budget to determine the type of toxic exposure and its intensity.

Ecotoxicogenomics seeks to provide a link between the cause and consequence of a toxic exposure along the response cascade by studying its molecular components. These components can, then, be used as bioanalytical tools. In turn, the bioanalytical tools may support a prognosis or diagnosis of the risk of a (single) pollutant or a case of environmental contamination, respectively (van Gestel, 2012). For a prognosis, scientists identify the mechanisms that mediate toxic exposure to predict its effects on organisms, and this is then used to predict the risk of ecological effects occurring in the field. The opposite is diagnosis in which scientists survey the triggering of mechanisms explaining the effects observed in

organisms exposed to a (sample of a) contaminated medium, e.g. soil, to identify the cause of these effects and with that the type of exposure. Therefore, both the prognosis and diagnosis of pollutants rely on understanding the mechanisms that mediate toxicity. However, for a diagnosis, an additional assessment is required of the reliability of these mechanisms in indicating the type and intensity of toxic exposure under various conditions, as most organisms are exposed to a mixture of pollutants and a range of stressors.

Advances in molecular biology have led to an increasing number of bioanalytical tools and their accuracy since the 1990s (Rehberger et al., 2018). The first generation of bioanalytical tools were bioassays, providing a simple read-out of toxicity based on phenotypic responses (van Gestel, 2012). The second-generation bioanalytical tools were *in vivo* assays based on, for example, histological staining, metabolite concentration, or enzymatic activity (Rehberger et al., 2018). These *in vivo* assays allow for assessing the effects of chemical pollution on key processes of concern. Although first and second-generation bioanalytical tools help generating a general overview of toxic effects, they cannot provide a comprehensive mechanistic understanding necessary for diagnosing mixtures of contaminants (Escher et al., 2020). Arguably, early generation bioanalytical tools provide information only on the prognosis of toxic exposure. The triggering of key processes of concern can only provide information on mechanisms that mediate the toxicity of a (novel) pollutant in isolation. Under mixture exposure, the triggering of key processes of concern does not identify the mixture components or their toxic properties.

The lack of relevance of quantifying individual biomolecules for diagnosing complex environmental pollution is particularly relevant for pesticide monitoring. Pesticides overstimulate or inhibit endogenous pathways in organisms (Hawkins et al., 2019). Also, pesticides commonly synergize with key processes of concern, such as detoxification enzymes (Hawkins et al., 2019). For example, one of the only *in vivo* bioanalytical tools to assess pesticide exposure in invertebrates, currently accepted by regulators, is the enzymatic activity of a cytochrome P450 in the honey bee (Haas & Nauen, 2021). However, this enzyme does not respond specifically to any particular exposure and is a point of synergistic interaction with other pesticides (Haas & Nauen, 2021). Its relevance for diagnosing pesticide exposure is dubious as measuring the cytochrome P450 enzymatic activity cannot help deducing any relevant information on the exposure's culprit or the stress.

Because the toxic effects of pesticides and other environmental toxicants are so varied, any bioanalytical tool for their diagnosis should allow for the monitoring of numerous processes of concern (Fontanetti et al., 2011; Lionetto et al., 2019).

The use of omics in environmental risk assessment

In the 2000s, a new generation of high-throughput methods was developed, referred to as the "omics." In a single assay, omics provide thousands of measurements on biological molecules (biomolecules), such as DNA, RNA, proteins, or metabolites. For example, genomics, transcriptomics, proteomics, and metabolomics. Each omics data type can only provide information on a single level of biological organization, even though toxicity acts simultaneously on all levels of biological organization. However, the molecular functions associated with biomolecules affected by toxic exposure can be identified (Roelofs et al., 2008). The annotation of the molecular functions is the same per gene, transcript, or protein. Thereby, identifying the shifts in molecular functions on one level of biological organization indicates effects at other levels of biological organization. Together with a certain degree of human interpretation, molecular functions from one omics type allow scientists to map the effects of toxic exposure on a large part of the response cascade.

For the implementation of omics data in diagnosing pesticide mixtures, the concept of the reallocation of the energy budget to maintain homeostasis is essential. This concept is not commonly discussed in the academic literature, probably due to limitations on the number of words. However, I believe it should be our discipline's core concept for future endeavors. Omics data obtained under circumstances that compare control and exposure conditions are useful in prognosis. Under these conditions, energy reallocation is directly observed by relating individual biomolecule abundances to their collective total in the two conditions. For diagnosis, we require an extra step. In diagnosis, reallocation of energy should be tracked under control conditions (no stress) and various stress conditions. By tracking the reallocation of energy in this way, scientists can determine the reliability of this energy reallocation in identifying the type and intensity of toxic exposure. In light of the energy budget, the stability of energy distribution over various conditions is crucial in applying omics in diagnosing environmental toxicants.

The central open question is thus: "how to relate shifts in biomolecule abundance at different levels of biological organization to reallocation of energy and, therefore, stress?" I will focus my discussion on transcripts and proteins as they can be related to a single locus in the genome, a gene. Fold-changes in transcript and protein abundances between conditions have different meanings. Transcript abundances increase and degrade quickly after exposure and at similar rates for any transcript in the order of minutes (Canzler et al., 2020), see Figure 1.1. Even though it is some of the most rapid responses to toxic exposure, gene transcription is considered to have predictive qualities for the effects of toxic exposure on the phenotype weeks later (van Straalen & Roelofs, 2008). Moreover, roughly 80 % of the entire transcriptome can be measured in one assay, and over 85 % of all raw transcriptomic data is commonly refined into the final dataset (based on chapters in this thesis). Although there are exceptions, the rate at which transcripts increase in their abundance is also roughly equal to the rate at which they increase their function, i.e., the synthesis of more protein. Proteins, in contrast, have highly varying synthesis and turnover rates, varying over hours, days, or, in rare cases, even months (see Figure 1.1). Moreover, an increase in protein abundance does not strictly relate to an increase in its functioning, as protein functioning depends commonly on a complex set of factors, e.g., substrate levels, phosphorylation, and cofactor availability. Moreover, a smaller portion of the proteome can be assessed in one assay, roughly 10 – 15 %, and typically only 20 to 40 % of raw proteomic data is refined into the final dataset (Bielow et al., 2016). Succinctly, shifts in transcript and protein abundances have very different meanings: it is an unspoken assumption that responses to toxic exposure in the transcriptome reflect energy expenditure, and the proteome reflects energy investment due to their rapid or relative slow turnover rates, respectively.

By combining transcriptomic and proteomic data in one statistical framework, scientists hope to provide a comprehensive account of the reallocation of the energy budget after exposure. The integrative analysis of multiple omics data types is currently a trending topic in the academic literature (Canzler et al., 2020; X. Zhang et al., 2018). Scientists commonly assume that shifts in biomolecule abundances that are conserved between levels of biological organization provide more relevance to their associated molecular functions (Rohart et al., 2017; Yugi et al., 2016). However, a critical assessment is required of the validity of this

assumption as shifts in transcript and protein abundance should be interpreted differently. Nevertheless, combining the results is certainly a worthwhile endeavor to determine both energy expenditure and investment in reshaping the response cascade under toxic exposure. This endeavor allows for a more accurate prognosis and diagnosis of the exposure and effects of environmental contaminants.

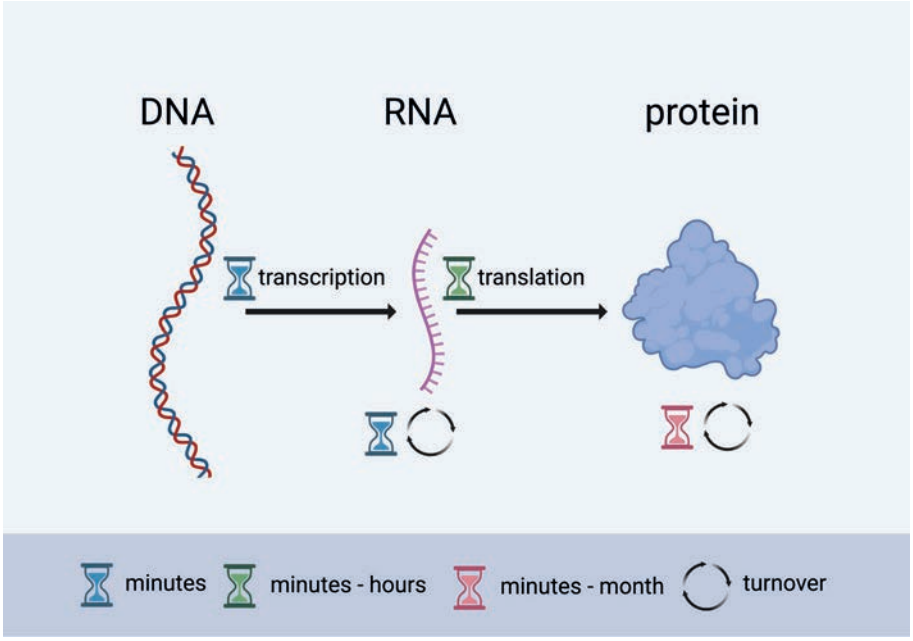

Figure 1.1: a schematic depiction of the transcription, translation, and turnover rates, after exposure to toxicants. Gene transcription responds rapidly, in the order of minutes. Translation responds slower, typically in the order of minutes to hours. Transcript (RNA) turnover is in the order of minutes while protein turnover can take minutes up to months. The information flow is from left to right, from DNA to proteins, indicated by the black arrows in the Figure. The actual regulation of transcription and translation consists of many feedback loops and is directed both ways. This has been omitted from the Figure for the sake of simplicity, along with the action of proteins. The Figure was generated by BioRender.com

In the previous section, I concluded that bioanalytical tools for diagnosing pesticide pollution should accommodate the monitoring of numerous processes of concern. Previous applications of omics to soil pollution monitoring focused on heavy metals (G. Chen et al., 2014). However, metals are exogenous; therefore, a clear baseline condition can be assigned (i.e., no expression of metal detoxification genes). Pesticides, in contrast, affect endogenous pathways, and baseline can be

lower or higher compared to no control conditions depending on stress exposures (Hawkins et al., 2019). Hence, in this section, I have highlighted the concept that the stability of energy reallocation is essential in applying omics in the diagnosis of pesticide pollution. In a practical sense, these findings are reported on the level of the molecular functions of biomolecules affected by toxic exposure. Hence, the stability of shifts in molecular functions over various stress conditions forms the basis for diagnosing pesticide pollution.

Toxicogenomic fingerprints

The molecular stress response is commonly categorized into two parts, the universal and the specific stress response (Roelofs et al., 2008). The universal response consists of molecular functions that are consistently increased or decreased under stress, such as diverging energy away from reproductive organs or removing damaged cell parts. The specific stress response includes the organism's actions unique to the toxic exposure, such as upregulation of a detoxification enzyme or a fast turnover of a receptor. Both stress responses occur at the same time. However, the energy budget predicts that under severe stress, the universal stress response is prioritized and receives a larger portion of the total energy budget (Roelofs et al., 2008). Under low to mild stress intensities, the specific stress response is most pronounced. For the diagnosis of pesticides, the specific stress response has greater applicability.

The molecular functions that entail the specific-stress response can help identifying "toxicogenomic fingerprints" from toxicological and genomic fingerprints. Their use is akin to fingerprints left at a crime scene. However, in diagnosis, we seek to identify the type of toxic exposure and its intensity instead of a suspect. Gene-regulation biomarkers can be designed based on these toxicogenomic fingerprints. In that sense, a toxicogenomic fingerprint is a concept, and biomarkers are its implementation as a bioanalytical tool.

Another way of diagnosing contaminated soils is by applying an effect-directed analysis (EDA), which aims at identifying the (group(s) of) chemical(s) causing the effect and uses a combination of high-throughput (in vitro) bioassays and sophisticated chemical analyses to achieve this aim (Brack, 2003; Simon et al., 2013). EDA is beyond the scope of this thesis, which focuses on using toxicogenomic

fingerprints, and derived biomarkers, for assessing pesticide exposure. However, these biomarkers may also be applied as part of EDA.

Toxicogenomic fingerprints consist of the parts of the response cascade to toxic exposure that is both necessary and relevant for the progression of intoxication. These responses are a source for the identification of Key Events. Linking the various Key Events from the onset of exposure to a phenotypic adverse outcome is called an adverse outcome pathway (AOP) (Ankley et al., 2010). A distinction feature of an AOP compared to a toxicogenomic fingerprint is that an AOP accepts information from any level of biological organization and is a tool designed explicitly for multi-disciplinary collaboration in risk assessment (OECD, 2018). Toxicogenomic fingerprints identify the specific-stress response, independently whether this information is used in environmental risk assessment. Again, biomarkers can provide a tool for monitoring pesticide pollution by indicating the triggering of Key Events in an AOP.

Toxicogenomic fingerprints to assess pesticide contamination

Under toxicogenomic-fingerprint pesticide monitoring, soil samples are sent to a testing facility where lab-reared animals are added. These sentinels can provide a read-out of the type and intensity of their toxic exposures and function as a living probe to assess the bioavailable and -active part of the pollution mixture. The springtail *Folsomia candida* has been an ecotoxicological model species since the 1960s, and its genome has been annotated, providing a valuable resource for the development of bioanalytical tools (Faddeeva-Vakhrusheva et al., 2017; van Gestel, 2012). Additionally, *F. candida* can easily be reared in the lab and its testing requires only a small amount of soil (Fountain & Hopkin, 2005). Hence, *F. candida* is an ideal sentinel species for biomarker-based monitoring of pesticide pollution mixtures in soil.

Toxicogenomic fingerprints for neonicotinoids

For soil invertebrates, insecticides are the most toxic pesticide class (Gunstone et al., 2021), as they are specifically designed to kill insects or insect-related species. The most commonly applied insecticide group of the past three decades are the neonicotinoids (Borsuah et al., 2020). Neonicotinoids mimic the endogenous

neurotransmitter acetylcholine, but cannot be degraded by the enzyme acetylcholinesterase (AChE), see Figure 1.2. Thereby neonicotinoids circumvent limits on neurotransmission and over-stimulating the signal over the nicotinic acetylcholine receptor (nAChR) (Simon-Delso et al., 2015). Neonicotinoids are more toxic to invertebrates (especially insects) due to their higher binding affinity to their nAChR compared to those of mammals or birds (Bonmatin et al., 2015). The genes involved in the neuron transmission as mediated by nAChR are potential targets for toxicogenomic fingerprinting.

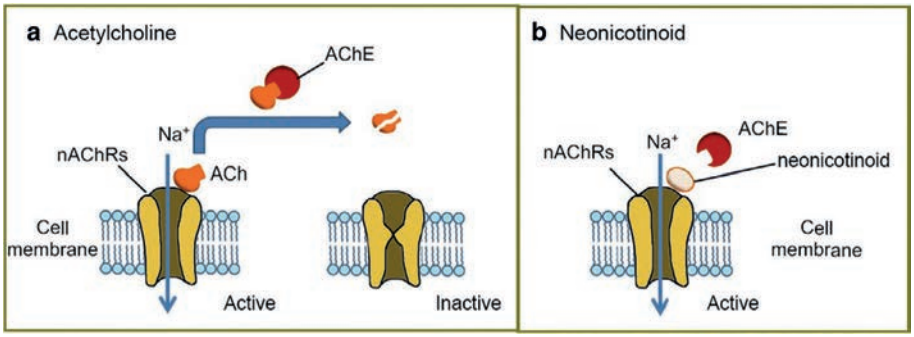

Figure 1.2: schematic depiction comparing cholinergic neurotransmission (a) to the mechanism of toxic action of neonicotinoids (b). Under endogenous circumstances, acetylcholine (ACh) binds the nicotinic acetylcholine receptors (nAChR) which opens up allowing potassium ions (Na^+) to pass the cell membrane. The influx of positively charged potassium ions relays a signal through the neuron that can ultimately, among other things, contract muscles and enables memory formation. The signal is stopped when ACh is released from nAchRs and degraded by acetylcholinesterase (AChE) (a). Neonicotinoids bind strongly to nAChR and cannot be broken down by AChE (B). Hence, the nAchRs continuously pass potassium ions, leading to a loss in memory formation, tremors and paralysis of invertebrates, in particular those relating to insects. Picture from Buszewski et al. (2019).

Toxicogenomic fingerprints for azole fungicides

Although less toxic to invertebrates than neonicotinoids, fungicides are applied in greater quantities. Hence, they are commonly found in combination with neonicotinoids. Most have indirect effects on invertebrates, in particular azole fungicides. These fungicides inhibit the fungal cell wall formation by inhibiting the enzyme cytochrome P450 5A1 in fungi. In invertebrates, azole fungicides might inhibit the cytochrome P450 counterparts of fungi. Thereby, azole fungicides amplify the effects of neonicotinoid toxicity on invertebrates compared to the effects of neonicotinoids by themselves (Glavan & Bozic, 2013; Raimets et al., 2017; Sgolastra

et al., 2017). Especially the toxicity of neonicotinoids with low toxicity to invertebrates becomes enhanced in the presence of azole fungicides (Feyereisen, 2018).

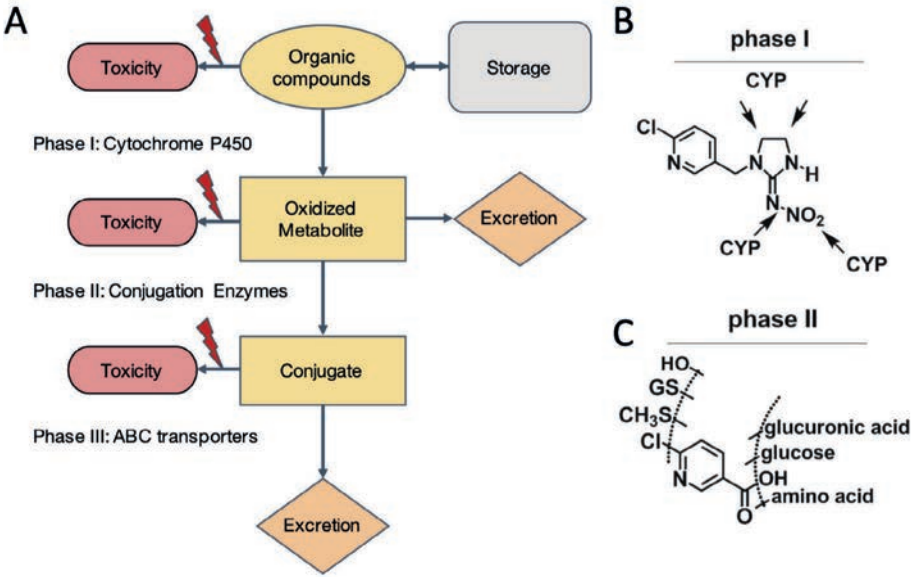

Figure 1.3: biotransformation breaks down organic compounds, such as neonicotinoids. Biotransformation consists of three phases oxidation (I), conjugation (II) and excretion (III), see panel A. The most prominent enzyme group for neonicotinoid biotransformation is listed for each phase. In phase I, various cytochrome P450 (CYP) enzymes oxidize the compound into transformation products. In panel B, known sites for CYP activity are shown for the neonicotinoid imidacloprid. In phase II, various conjugation enzymes are facilitating the binding of endogenous compounds to phase I biotransformation products, see panel C, in this way making them ready for excretion in phase III. The Figure has been adapted from van Straalen & Roelofs (2011), for panel A, and Casida (2011) for panel B and C.

These cytochrome P450 enzymes are part of a large family of genes that play an essential role in Phase-I biotransformation, see Figure 1.3. Due to the inhibition by azole fungicides of CYP genes, toxicogenomic fingerprints based on biotransformation genes might not provide a reliable read-out for neonicotinoid exposure.

Aims and objectives

My Ph.D. research aims to identify toxicogenomic fingerprints to assess pesticide contamination in soils. I focused on neonicotinoids and an azole fungicide, cyproconazole. A key aspect of the applicability of toxicogenomic fingerprints is

their reliability in indicating the type of pesticide contamination in a mixture with other pesticides.

My research questions are divided into two categories: (1) How to identify toxicogenomic fingerprints? (2) Are biomarkers derived from toxicogenomic fingerprints robust indicators of neonicotinoid exposure under various stress conditions?

Chapter 2

Toxicants, such as pesticides, trigger a response cascade in an organism from the initiation of chemical interactions to shifts in transcripts, proteins, and metabolites, eventually resulting in adverse effects on the phenotype. By combining various omics data types, scientists wish to provide insight into the cause and consequence of toxic exposure (Canzler et al., 2020; X. Zhang et al., 2018). A common assumption for this approach is that shifts in biomolecule abundances across levels of biological organization represent a conserved indication of the mechanisms that mediate toxicity (Rohart et al., 2017; Yugi et al., 2016). However, shifts in transcripts and protein abundances occur at varying time scales (Canzler et al., 2020); see Figure 1.1. In chapter 2, I investigated whether shifts in transcript and protein abundances were delayed in a manner that would inhibit the combined analysis of transcriptomic and proteomic data.

I exposed springtails (*F. candida*) to a concentration of the neonicotinoid imidacloprid and monitored transcript and protein abundances every 12 hours for a total of 72 hours (3 days). I sought to determine the exposure duration with the largest difference in transcript and protein abundances between the imidacloprid exposure and control condition. This timepoint marked the most opportune moment for toxicogenomic fingerprint identification as the effect of the neonicotinoid on transcript or protein abundances would be most pronounced. Finally, I calculated the correlation between transcript and protein abundances from the same gene and determined if shifts in protein abundances were delayed after those of transcripts in a manner that would interfere with their combined analysis.

Chapter 3

For the application of toxicogenomic fingerprints in the diagnosing pesticide contamination, their reliability for indicating the type and intensity of exposure

under varying mixture compositions is essential. Current methods for identifying the transcriptomic response of organisms to toxic exposure are ill-suited in their application on mixture exposure transcriptomic data. The main deficiency of these methods is their reliance on parametric models that poorly assess nonlinear and interaction effects on the gene expression concentration-response relationships (Altenburger et al., 2012; Ren & Kuan, 2020). The interaction effects on gene expression occur predominantly when mixture toxicity is nonadditive, i.e., toxicity is synergistic or antagonistic compared to effects expected based on the toxicity of the individual compounds in the mixture.

In chapter 3, I exposed *F. candida* to two mixtures containing either similar or dissimilar acting pesticides. The first mixture consisted of two neonicotinoids, imidacloprid and clothianidin, with the same mechanism of action and roughly the same toxicity to *F. candida*. The second mixture consisted of the neonicotinoid imidacloprid and the azole fungicide cyproconazole. The aim of this chapter was to determine whether toxicogenomic fingerprints remained indicative to the broader neonicotinoid family, even under mutual exposure with cyproconazole. Moreover, the pesticide mixtures were finely resolved for stress intensities with slight increases in the concentration of the pesticides. Over 33 unique pesticide concentration combinations were tested. Together with Dr. Yuliya Shapovalova of the Radboud University in Nijmegen, we developed a custom-made statistical framework to find genes that could serve as toxicogenomic fingerprints. In a separate experiment described in this chapter, I tested the assumption that biomarkers derived from these toxicogenomic fingerprints remained indicative for either neonicotinoid or cyproconazole exposure. To this end, I spiked soil with known mixtures of imidacloprid and cyproconazole and determined the reliability of the toxicogenomic fingerprints.

Chapter 4

The first two chapters addressed my first research question: “How to identify toxicogenomic fingerprints?” In chapters 4 and 5, I focused on my second research question: “Are biomarkers derived from toxicogenomic fingerprints robust indicators of neonicotinoid exposure under various stress conditions?” Cytochrome P450 (CYP) enzymes have been extensively mentioned in the academic literature as pivotal mediators of neonicotinoid toxicity, see Figure 1.3.

In particular, two classes of neonicotinoids, i.e., nitro- and cyano-substituted, have a different rates in their toxicity to bee species based on varying rates of CYP-mediated detoxification between these classes (Beadle et al., 2019; Manjon et al., 2018). Moreover, neonicotinoids commonly synergize with azole fungicides by the inhibition of CYP enzymes (Glavan & Bozic, 2013; Raimets et al., 2017; Sgolastra et al., 2017). For the implementation of gene-expression biomarkers for the monitoring of neonicotinoid soil contamination, biomarkers should remain robust indicators for the broader neonicotinoid family even under synergistic interaction by CYP inhibition.

In chapter 4, I used the metabolic inhibitor piperonyl butoxide (PBO) to target CYP enzymes specifically and test the reliability of various biomarkers in indicating neonicotinoid exposure. The PBO metabolomic inhibitor is well-studied and therefore I can attribute the experimental results to CYP enzymatic activity. When using another pesticide or pollutant, it would remain unclear to what mechanism the observed effects could be attributed. First, I sought to confirm the potency enhancing effects of PBO on the toxicity of two neonicotinoids to *F. candida* reproduction. The neonicotinoids were imidacloprid and thiacloprid as representatives of the nitro- and cyano-substituted classes of neonicotinoids, respectively. Second, I surveyed the influence of PBO on the gene expression of eight biomarkers to determine their reliability in indicating neonicotinoid exposure.

Chapter 5

Previous research proposed glutathione-S-transferase (GST) enzymatic activity and gene-expression as a biomarker for neonicotinoid exposure in *F. candida* (Sillapawattana & Schäffer, 2017). Moreover, the expression of *heat shock proteins* and *vitellogenin* were proposed as biomarkers in the diagnosis of the type of pollution in *F. candida* (M. E. de Boer et al., 2011, 2013). However, these genes are all involved in mediating oxidative stress, a hallmark of the universal stress response (Roelofs et al., 2008). For their application in assessing neonicotinoid soil pollution, biomarkers should remain robust even under the effects of other stressors. As these genes are part of the universal stress response, I sought to determine their reliability in indicating neonicotinoid exposure.

In chapter 5, I used the metabolic inhibitor diethyl maleate (DEM) that depletes the cofactor of GST enzymes involved in phase II of the biotransformation process (see Figure 1.3). The metabolic inhibitor is well studied and commonly applied in pesticide research to determine the influence of GST enzymes on pesticide detoxification. By choosing DEM over another type of pollution, I ensured the observed effects could be attributed to GST inhibition. First, I surveyed the influence of probable GST inhibition on the toxicity of two neonicotinoids to springtail reproduction, i.e., imidacloprid and thiacloprid. Second, I validated the biomarkers mentioned above to determine their reliability in indicating the exposure of the broader neonicotinoid family even under another stress factor crucial to the oxidative stress response.

Chapter 6

In chapter 6, I discuss the current methods for toxicogenomic fingerprint identification, and place the findings described in this thesis in a broader scientific context.

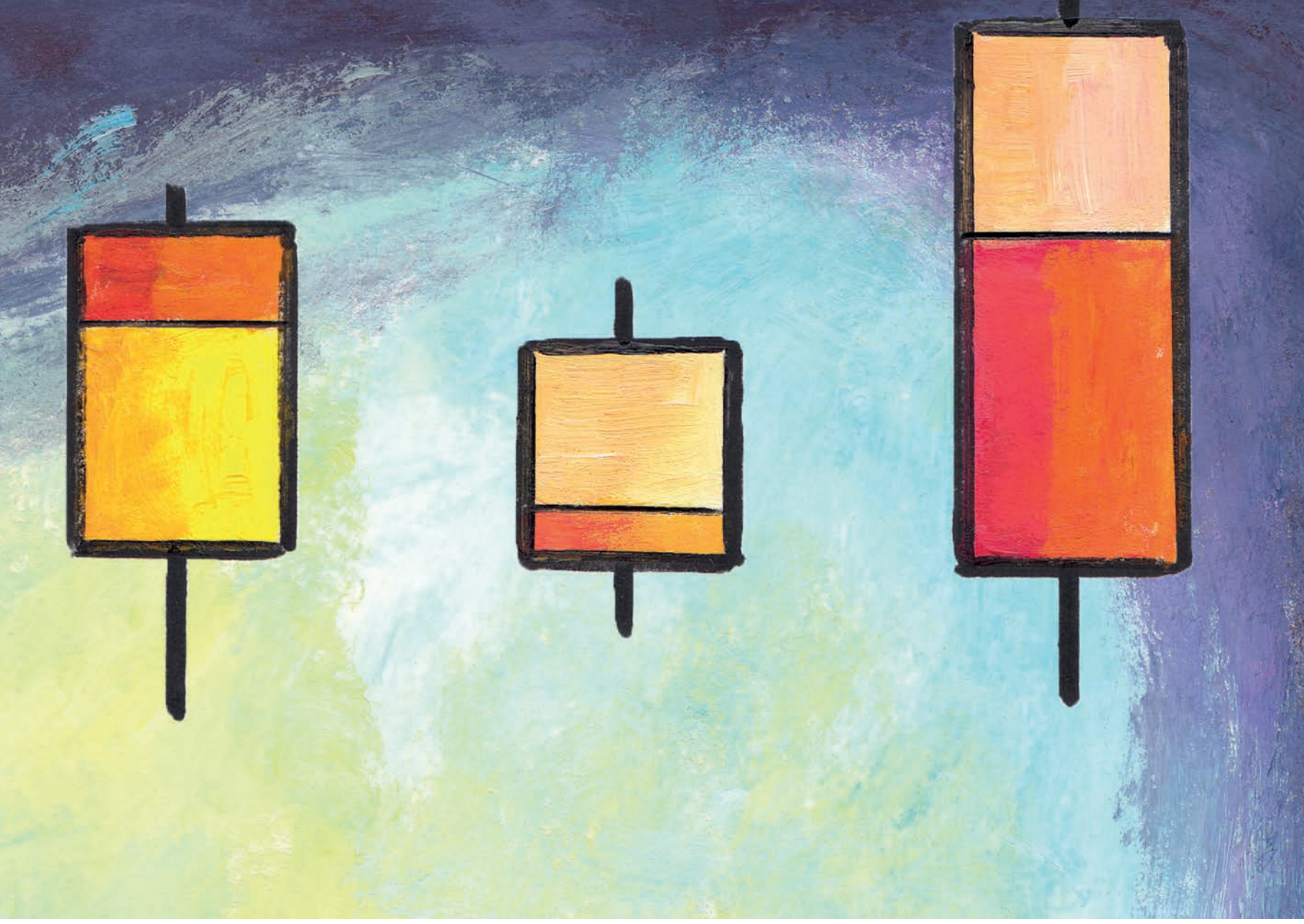

Chapter 2

Combining time-resolved transcriptomics and proteomics data for Adverse Outcome Pathway refinement in ecotoxicology

Ruben Bakker[1*], Jacintha Ellers[1], Dick Roelofs[2], Riet Vooijs[1], Tjeerd Dijkstra[3],
Cornelis A.M. van Gestel[1], Katja M. Hoedjes[1]

[1]Amsterdam Institute for Life and Environment (A-LIFE), Faculty of Science, Vrije Universiteit Amsterdam, De Boelelaan 1085, 1081 HV Amsterdam, The Netherlands
[2]Keygene N.V., Agro Business Park 90, 6708 PW Wageningen, The Netherlands
[3]Max Planck Institute for Developmental Biology, Max-Planck-Ring 25, D-72076 Tübingen, Germany
* corresponding author
Corresponding e-mail: k.m.hoedjes@vu.nl

This manuscript has been submitted to
Science of the Total Environment

Graphical Abstract

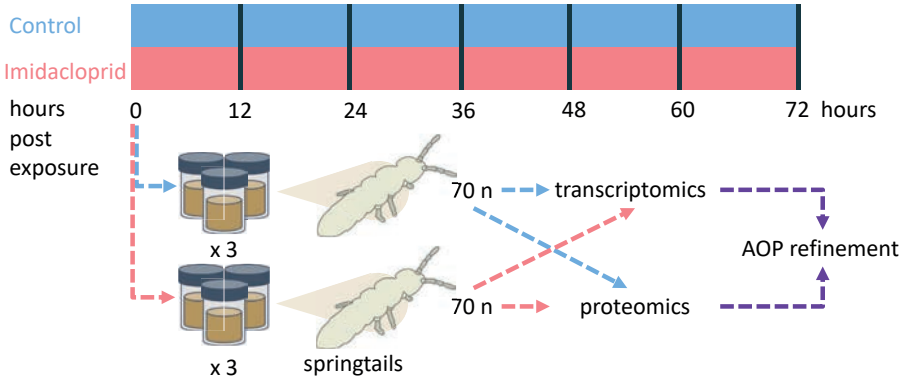

Highlights

- Time-resolved transcriptomic and proteomic responses to imidacloprid in springtails
- Adverse Outcome Pathway (AOP) refined for nicotinic Acetylcholine Receptor binding
- No temporal delay identified between changes in transcript and protein abundances from same gene
- Largest shift in protein and transcript abundances observed at 48 hours exposure
- Results facilitate multi-omics data integration for biomarker and AOP development

Conventional Environmental Risk Assessment (ERA) of pesticide pollution is based on soil concentrations and apical endpoints, such as the reproduction of test organisms, but disregards information along the organismal response cascade leading to an adverse outcome. The Adverse Outcome Pathway (AOP) framework, on the other hand, facilitates the use of response information at any level of biological organization. Transcriptomic and proteomic data can provide thousands of data points on the response to toxic exposure. Combining multiple omics data types is necessary for a comprehensive overview of the response cascade and, therefore, AOP development. However, it is unclear if transcript and protein responses are synchronized in time or time lagged. To understand if analysis of multi-omics data obtained at the same timepoint reveal one synchronized response

cascade, we studied time-resolved shifts in gene transcript and protein abundance in the springtail *Folsomia candida*, a soil ecotoxicological model, after exposure to the neonicotinoid insecticide imidacloprid. We analyzed transcriptome and proteome data every 12 hours up to 72 hours after onset of exposure. The most pronounced shift in both transcript and protein abundances was observed after 48 hours exposure. Moreover, cross-correlation analyses indicate that most genes displayed the highest correlation between transcript and protein abundances without a time-lag. This demonstrates that a combined analysis of transcriptomic and proteomic data can be used for AOP improvement. This data will promote the development of biomarkers for neonicotinoid insecticide pollution in soils or chemicals with a similar mechanism of action.

Keywords: Collembola, nicotinic Acetylcholine Receptor (nAChR), Mechanisms of Action, neonicotinoids, multi-omics data, time series

Introduction

Environmental Risk Assessment (ERA) of soil pollutants is traditionally based on soil concentrations (Effect Concentrations (EC_x)) affecting apical endpoints of test organisms, such as reproduction and survival. As a consequence, conventional ERA effectively only uses information on the effect concentration and the final event of an elaborate response cascade that can include effects on gene transcription, proteins, and metabolites in specific tissues, but also on intermediate phenotypes such as physiology and behavior, among others. Understanding the intermediate steps of the response cascade, therefore, provides opportunities for developing biomarkers that could facilitate more rapid and cost-efficient means of ERA. Ordering relevant and casually linked events in the response cascade is critical to apply this information for ERA, which is what the Adverse Outcome Pathway (AOP) framework aims for (Ankley et al., 2010). AOPs are, ideally, chemically or species agnostic, making them broadly applicable as a tool for ERA, including for emerging contaminants or toxins with a similar Mechanism of Action (MoA) (Ankley et al., 2010; OECD, 2018).

One area of ecotoxicological concern that could benefit especially from AOP-based ERA is pesticide monitoring. Intensified application of pesticides has contributed to a global decline of non-target invertebrates that support sustainable agriculture (FAO, ITPS, GSBI, 2020). This has prompted large-scale chemical analyses of pesticide concentrations in soils, but these analyses are costly and labor-intensive, and pesticide concentrations do not always correlate proportionally with their biological activity and environmental risk. Using biomarkers could provide a more cost-efficient approach to screen large sets of soil samples for the exposure to pesticides and to assess their toxicity to non-target invertebrates (Lee et al., 2015; Lionetto et al., 2019). Robust AOPs for pesticide exposure are critical for the development of such biomarkers.

Successful development of AOPs depends on identifying relevant responses at increasing levels of biological organization, so-called Key Events (KE), that link the onset of effects upon exposure (Molecular Initiation Event (MIE)) to the Adverse Outcome (AO). These KEs can then serve as anchor points for the development of biomarkers that signal the progression of the AOP. Advances in "omics" technologies have made it possible to survey thousands of quantitative measurements that may provide insights on the molecular responses to pesticide

exposure, such as shifts in the expression of genes (transcriptomics), proteins (proteomics), or metabolites (metabolomics). Combining data from these different levels of biological organization is necessary for a comprehensive overview of the response cascade and, therefore, AOP development (Canzler et al., 2020; Leung, 2018). It remains unclear, however, if shifts in transcript and protein expression in response to pesticide exposure are synchronized in time, and (Canzler et al., 2020; Haider & Pal, 2013). A time lagged response of gene and protein expression could complicate combined transcriptomics and proteomics data analysis for AOP refinement, especially if data is obtained from a single or few time points only. Modelling approaches and time-staggered data collection have been proposed to overcome this obstacle (Canzler et al., 2020; Garcia-Reyero & Perkins, 2011). However, both approaches require information on the time lag between correlated transcript and protein expression patterns. Therefore, the temporal dynamics of transcript and protein abundances after pesticide exposure have to be further investigated, before multiple omics datasets can be combined for biomarker identification and AOP refinement.

Neonicotinoids are the most widely used insecticides of the past three decades and are currently the most toxic class of pesticide pollution to non-target soil invertebrates (Borsuah et al., 2020; Gunstone et al., 2021). Neonicotinoids act on the nicotinic Acetylcholine Receptor (nAChR), leading to overstimulation and disruption of its neuronal signal, and eventually resulting in paralysis or death (Simon-Delso et al., 2015). Currently, the only AOP for nAChR activation is taxon specific for the honey bee and, therefore, not species agnostic (MIE 559 AOPWiki) (LaLone et al., 2017). Combined transcriptomics and proteomics studies on bumble bees and water fleas have provided more insights into the response cascade after nAchR activation, but have not resulted in AOP refinement (Camp & Lehmann, 2021; Pfaff et al., 2021). Here, we aimed to test the applicability of the AOP for nAChR activation to non-target soil invertebrates and to further develop it. For this, we studied the molecular responses to neonicotinoid exposure of the springtail *Folsomia candida*, a soil ecotoxicological model species belonging to the prevalent and species-rich soil-dwelling Collembola (Fountain & Hopkin, 2005). Collembola are crucial for sustainable agricultural practices such as nutrient cycling and maintenance of soil plant-microbiomes (FAO, ITPS, GSBI, 2020; Innocenti & Sabatini, 2018). In addition, the *F. candida* genome has been sequenced and time-resolved transcriptomic and proteomic data has previously been collected after

exposure to pesticides and flame retardants (Faddeeva-Vakhrusheva et al., 2017; Simões et al., 2019; Q. Q. Zhang & Qiao, 2020). However, the large time intervals used in these studies (i.e. ranging from 2 to 14 days post the onset of exposure) provide limited information on rapid responses to toxic exposure.

In this study, we exposed *F. candida* to the neonicotinoid insecticide imidacloprid and obtained time-resolved transcriptomics and proteomics data, with 12-hour intervals up to a total exposure time of 72 hours (i.e., 3 days). From these data we aimed to: (1) Identify the timepoint with the most distinctive differential expression in transcript- and/or protein abundances exerted by imidacloprid exposure, (2) identify the ontologies and pathways affected by imidacloprid exposure through time, and (3) determine if a time-delay exists between transcript and protein abundances.

Materials and methods

Test organism, test soil, chemicals, and exposure

For this study, we used the Berlin strain of *Folsomia candida*, which has been reared for over 30 years at the Vrije Universiteit Amsterdam, the Netherlands, as previously described (Pitombeira de Figueirêdo et al., 2019). LUFA 2.2 was used as test soil (Lufa Speyer, Germany), which is a natural loamy sandy soil with approximately 2.1 % organic carbon, pH 5.5. (0.01 M $CaCl_2$) and water holding capacity (WHC) of 46.5 % (w/w). Imidacloprid (98 % purity) was provided by Bayer CropScience, Monheim, Germany.

Imidacloprid was dissolved in ultra-pure water and left to stir at 300 rpm, overnight and in the dark. Soil was thoroughly mixed with an imidacloprid solution to achieve a moisture content of 50 % of the WHC. Soil mixed with demineralized water was used as a control. For the imidacloprid exposure a concentration of 0.25 mg kg^{-1} dry soil was chosen, roughly equal to the Effect Concentration reducing juvenile numbers by 20 % (EC_{20}) (Bakker et al., 2022). The imidacloprid concentration in control and test soil was confirmed by Groen Agro Control, Delfgauw, the Netherlands, following certified analytical methods and with a detection limit of 0.01 mg kg^{-1} dry soil (see supplementary information for results). A sublethal concentration was used to allow for assessing imidacloprid-specific effects without general toxicity effects that may occur at higher concentrations.

Pools of 70 age-synchronized animals, 21-24 days old, were placed in 30 grams of soil with or without imidacloprid in a glass jar at 20 ± 1 °C, 75 % RH, and a 16:8 light:dark regime. Three pools per treatment were harvested every 12 hours for a total duration of 72 hours, i.e. 6 timepoints (12, 24, 36, 48, 60, 72 h). With this set-up we included the 48h exposure duration, which marks a conventional exposure duration for gene-expression assays in *F. candida* (M. E. de Boer et al., 2009, 2011; T. E. de Boer et al., 2010; Nota et al., 2009; Sillapawattana & Schäffer, 2017). To collect the springtails, the soil was waterlogged, the floating animals were scooped from the surface with a fine-mesh, transferred by aspirator to 1.5 ml reaction tubes, snap frozen in liquid nitrogen and stored at -80 °C.

RNA isolation and protein extraction

RNA and proteins were isolated simultaneously from the collected pools of animals using a TRIzol-based extraction procedure. Frozen samples were homogenized manually in a 1.5 ml reaction tube using a pestle. RNA and protein fractions were isolated using a starting volume of 500 µl of TRIzol (Invitrogen - Thermo Fisher Scientific, Breda, the Netherlands), following the manufacturer's instructions. The aqueous phase was incubated with isopropanol (1:1 v:v) followed by incubation for 2 hours at -20 °C to allow RNA precipitation. Subsequently, DNase-I digestion (Roche Diagnostic, Almere, the Netherlands) was carried out following the manufacturer's instructions. RNA quality and quantity were verified by spectrophotometry on a NanoDrop (Thermo Fisher Scientific, Breda, the Netherlands) and Qubit (Thermo Fisher Scientific, Bleiswijk, the Netherlands), and 1 µg of total RNA from each sample was used for RNAseq library preparation using the TruSeq Stranded mRNA Sample Preparation kit following the instructions of the manufacturer (Illumina, Nijmegen, the Netherlands). Libraries with a mean length of 260 base pairs were sequenced on an Illumina Nova Seq 6K instrument, 150 base pairs pair-end, with a sequencing depth of 20 million per library, by Macrogen (Seoul, the Republic of Korea).

The protein pellets were stored in 1.5 ml of 0.3 M guanidine hydrogen chloride at -80 °C until shipment. Immediately before shipment, the supernatant was removed from the pellets and the pellets were shipped semi-dried on dry ice to the Core Facility for Medical Bioanalytics, at the Institute for Ophthalmic Research, Eberhard-Karls University, Tübingen, Germany. The samples were subsequently

resuspended using a Precellys tissue homogenizer, by two bursts of 30 seconds at 5500 rpm in a lysis buffer of 6 M Urea (Roth, Germany) and 0.1 Ammonium bicarbonate (ABC) (Merck, Germany). Protein quantification was performed by a Bradford assay (Biorad, USA) on a Tecan Spark 10M (Tecan, Männedorf, Switzerland). Approximately 10 µg of the original protein pellets was digested overnight at 37 °C, using 0.5 µg of Trypsin (Serva, Heidelberg, Germany), in a buffer consisting of 50 mM ABC (Merck, Germany), 4 µL RapiGest (Waters, Germany), 0.1 M dithiothreitol (Merck, Germany), and 0.3 M 2-iodacetamide (Merck, Germany). The peptides were then precipitated using 5 % of total volume Trifluoroacetic acid (Merck, Germany) and centrifuged at 16,000 g. The lower phase was filtered by C18 Stage Tips (Thermo-Fisher, Germany) and separated over a micro-HPLC before injection into an Orbitrap (Thermo-Fisher, Germany).

Differential gene expression analysis

Trimming of the raw reads was performed by *Trim Galore* v0.6.3 (Ewels et al., 2016), using *Cutadapt* v2.4 (Martin, 2011). Before and after trimming, fastaq files were visually inspected by generating *FastQC* v0.11.8, in parallel using the software package *GNU Parallel* (Tange, 2011), and bundling these into a *MultiQC* v1.7 (Ewels et al., 2016) report. This allows for the visual inspection of Quality Control metrics; such as sequence QC-content, length distribution and duplication events, in all 36 sample files simultaneously and to ensure a comparable quality of the reads in all libraries. *Salmon* v0.8.1 (Patro et al., 2017) was used to align and quantify the reads to the Ensembl Metazoa v40 transcriptome (Cunningham et al., 2019), using paired-end mode and default settings. All files had a mapped reads rate of at least 81.86 % and on average 86.19 % (sd = 11.08, n = 36) and scored similarly for metrics of quality control compared to each other, for example; QC-content, adapter sequence content, per sequence quality scores (see supplementary Table S2.1 for mapping rates). This indicates no biasing factor that might impact the further analysis of the data. The quantified reads were imported into *R* v4.0.0 using the R-package *tximport* and differential gene expression analysis was performed by *DESeq2* v1.28.1 using loglikelihood-ratio tests comparing a model including time, treatment and their interaction to a model with only time (Love et al., 2014; Soneson et al., 2016). We corrected for false discovery rates by shrinking the p-value and calculating q-values using a 0.1 p-value cut-off using the package *qvalues* v2.20.0 in *R* (Storey et al., 2020).

Protein expression analysis

The spectra quantity and quality of the Thermo-Fisher raw LC-MS^2 files were visually inspected using *seeMS*, part of the software suite *proteowizard* v3 (Chambers et al., 2012). The files were converted to Mascot Generic Files (mgf) and mzML formats for further analysis by *SearchGUI* v4.1.3 by *MSconvert* (*proteowizard* v3), using peak-picking, i.e. centroid mode. Post-Translation-Modifications (PTMs) were identified on a subset of the mzML files, files from samples 6, 7, 10, 33, and 34, using *MetaMorpheus* v0.0.320 (Solntsev et al., 2018) (see supplementary Table S2.2 for results). Due to high Citrullination R and deamination on Q and N, these PTMs were included as search parameters in a subsequent search with *msgf+*. All samples spectra files were matched to the Ensembl Metazoa v40 (Cunningham et al., 2019) proteome using *SearchGUI* v4.1.3 (Barsnes & Vaudel, 2018) with Oxidation (M), Deamination (N, Q), Citrullination (R) and the fixed modification Carbamidomethyl (C) selected. Other settings used were: trypsin digestion, allowing for two missed cleavages, a precursor (MS1) mass tolerance of 10 ppm and a fragment (MS2) mass tolerance of 0.5 Dalton. We used a reverse decoy database and a standard contaminant database, the common Repository of Adventitious Proteins (cRAP) (Mellacheruvu et al., 2013) and the search-engine *msgf+* (Kim & Pevzner, 2014). We chose *SearchGUI* for its implementation on the *msgf+* search-engine. In a previous study, this relatively novel search engine tool has been proven to outperform other methods matching more raw spectra to peptides, i.e. Peptide-Spectral-Matches (PSMs) (Levitsky et al., 2018) (see supplementary Table S2.1 for identification rates and the supplementary information for LC-MS^2 quality control metrics). Using *PeptideShaker* v2.2.1 (Vaudel et al., 2015), the search results were summarized into a PSM default report file and, subsequently peptide intensities were calculated using *moFF* v2.0.3 on the useGalaxy server v2.0.3 (Afgan et al., 2016). The resulting peptide intensities were read into *R* v4.0.0 using the R-package *MSqRob* v0.7.6 (Goeminne et al., 2020). The pipeline that executes *SearchGUI*, *PeptideShaker* and *moFF* on the European useGalaxy server has been described previously (Mehta et al., 2020). Peptides belonging to decoy or contaminants were removed. Peptides with over 50 % missing values were removed and peptides with less than 50 % missing values were substituted by the K-Nearest-Neighbor (KNN)-algorithm to allow for the subsequent calculation of log2fold changes and performing loglikelihood ratio tests using the R-package *Msnbase v2.14.2* (Gatto & Lilley, 2012). The peptide intensities were normalized using a cyclic-loess and

quantile-robust transformation using *limma v3.44.3* in R (Ritchie et al., 2015). The resulting peptide intensities were combined into proteins using the median polish method (Gatto & Lilley, 2012) and the smallest unique protein subset was selected for by R-package *MSqRob v0.7.6*. Differential protein abundance analysis was done by using loglikelihood-ratio tests comparing a model including time, treatment and their interaction to a model with only time. We corrected for false discovery rates by calculating q-values using the package *qvalues v2.20.0* in *R* (Storey et al., 2020) using a p-value cut-off of 0.1.

Correlation of the transcript-protein-abundances per gene

Log2fold changes (LFC) of transcript and protein abundance were calculated by *DESeq2 v1.28.1* and *limma v3.44.3*, respectively, by creating a condition factor, e.g. "t1_control", "t1_imidacloprid", "t2_control", "t2_imidacloprid", etc. and creating contrasts between the imidacloprid and control conditions for each timepoint (t1, t2, etc.). These methods were chosen because LFC values for RNA counts had to be shrunk using an empirical Bayesian criterion, which is integrated in both *DESeq2* and *limma*. To correct for the greater range of variation in LFC values for the relative transcript counts compared to the relative peptide intensities, the LFC values of the genes found in both the transcriptome and the proteome were standardized separately per gene and platform, i.e. the mean was subtracted from the LFC value and subsequently divided by their standard deviation. In order to determine the correlation per time-lag between the transcript and protein abundances from the same gene, the cross-correlation-function (CCF) was calculated from the scaled LFC values for a transcript and protein from the same gene, i.e. per Transcript-Protein-Pair (TPP), in base *R v4.0.0*. The CCF of two vectors is the correlation per shift in index or time-lag. The CCF at lag 0 is identical to Pearson's correlation between two continuous variables. In this work, we considered 6 measures of similarity between the transcript and protein scaled LFC vectors: no time-lag and 5 delayed time-lags. Following the rationale that translation follows transcription from the same gene, only TPPs with a positive CCF values were considered, i.e. TPPs with log2-LFC transcript expression values positively correlating with protein log2-LFC values, which indicates that shifts in transcript abundances that preceded protein levels. Each CCF value expresses the similarity between two vectors at a timepoint. Note that two scaled LFC vectors with flat-lined expression, i.e. no differential expression, have no CCF, as it cannot be calculated. Also, the CCF is not designed

to determine causality, it only provides a measure of correlation per time-lag (Dean & Dunsmuir, 2016). Each TPP with a CCF value above the 95 % confidence interval was identified as significantly correlated. The number of significant TPPs were compared to 10,000 randomized datasets by randomizing the rows of the transcript and protein LFC values independently. For each significant TPP, the time-delay with maximum positive correlation between transcript and protein scaled LFC values was calculated.

Functional annotation analysis and clustering

The differentially expressed genes (DEGs) and proteins (DEPs), and significantly correlated TPPs were clustered using the DIANA algorithm in the R-package *DEGreport* v1.24.1 (Pantano, 2020) with a minimal cluster size of 15 genes. Functional gene annotation was obtained from Gene Ontology (GO) through the R-package *biomart* v2.44.4 (Durinck et al., 2009) and the Kyoto Encyclopedia of Genes and Genomes (KEGG) by mapping the Ensembl Metazoa proteome to the reference proteome via GHOSTZ in the online webservice KAAS (Moriya et al., 2007) with the algorithm bi-directional best hit and selecting *F. candida* as target organism.

Two Gene Set Enrichment Analyses (GSEAs) were performed with the R-package *goseq* v1.40.0 (Young et al., 2010), using DEGs and DEPs as the "foreground" with the default Wallenius-method. Enrichment of functional annotations in these three foregrounds was carried out comparing them to two "backgrounds": 1. the transcriptome (DEGs), and 2. the proteome (DEPs). The transcriptome included all genes found in the *DESeq2* result table without any missing values, i.e. genes with sufficient counts. The proteome was defined as all genes with proteins found in the "smallest unique subset" defined by *MsqRob*, see the section "protein expression analysis". Both reads and peptides are assigned more readily to genes with longer transcript or peptide sequences. Therefore, to prevent this selection bias in comparing the foreground and background, the transcript sequence lengths for DEGs, the protein sequence lengths for DEPs, and the transcript sequence lengths for significantly correlated TPPs were used to train *goseq* "probability weighting function". For both GSEAs, GO and KEGG terms were deemed significantly enriched if their over-representation p-value was below 0.05, more than one of its members was found in the foreground, i.e. DEGs and DEPs, and their under-representation

p-value was not equal to 1. The latter two arguments prevented the selection of Gene Set Enrichment (GSE) terms with a small number of genes. Per GSE term, the fraction of its members found in the foreground per cluster was calculated.

Results and Discussion

Combined analyses of transcriptomic and proteomic data can facilitate the identification of the response cascade after toxic exposure, which can inform AOP development. However, it is unclear if responses can be observed in the transcriptome and proteome simultaneously or whether the response is time lagged between the layers of biological organization. To address this issue, we have analyzed time-resolved transcriptomic and proteomic data of the springtail *F. candida* after exposure to the neonicotinoid imidacloprid. From this data, we aimed to (1) identify the time point with the most distinctive differential expression pattern, representing the most opportune timepoint for AOP or biomarker development, (2) identify pathways and ontologies affected by imidacloprid exposure and temporal patterns therein, and (3) determine if there was a time-delay in differential transcript and protein expression patterns to streamline their combined analysis.

Transcriptomic response

We detected 20603 expressed genes in the full transcriptome dataset, representing 72% of the 28734 genes in the genome of *F. candida*. Imidacloprid exposure resulted in 360 Differentially Expressed Genes (DEGs) at one or more time points compared to the control samples from the same time points. These DEGs were clustered based on similarity in their gene expression patterns over time, resulting in 5 clusters with a distinct expression pattern and varying in size from 19 (cluster R4) to 166 genes (cluster R5) (Figure 2.1 and supplementary Table S2.3). A remaining group of 73 DEGs was left unclustered. Remarkably, we observed that the 48h timepoint marked a distinctive position in the expression patterns for the majority of the clusters. For three out of five clusters (R1, R2, R5) the 48h timepoint displayed the most prominent differentiation between the two treatments, as indicated by non-overlapping quantiles of the boxplots in Figure 2.1. Cluster R1 demonstrated a gradual increase in gene-expression over time, whereas cluster R2 showed continuous enhanced gene-expression under imidacloprid exposure.

The expression of cluster R5 is upregulated compared to control conditions at timepoints 12h to 24h and timepoints 60h and 72h, with a sudden reversal at timepoint 48h. Because clusters R1, R2 and R5 combined represent roughly 60 % of all DEGs, we conclude that the largest change in the transcriptomic response of *F. candida* to imidacloprid occurred at the 48h timepoint. For the largest cluster R5, however, the strong differentiation at 48h can be mostly attributed to a sudden upregulation of gene expression in the control condition, rather than in exposed animals. This prominent transcriptomic shift cannot be a consequence of developmental processes occurring at a particular age as the springtails were not age-synchronized per 12 hours but ranged between 21 and 24 days old. Rather, we speculate that the shift in gene expression is a consequence of transferring the springtails to LUFA2.2 soil, after being reared on Paris plaster before the onset of exposure. Our data suggest that this response is inhibited or delayed by exposure to imidacloprid. Cluster R5 may, therefore, represent genes for which imidacloprid exposure constraints the response of *F. candida* to soil transfer. Remarkedly, previous studies measuring the gene expression of *F. candida* have also focused on this timepoint as many types of stress cause large shifts in gene-expression after 48h exposure (M. E. de Boer et al., 2009, 2011; T. E. de Boer et al., 2010; Nota et al., 2009; Sillapawattana & Schäffer, 2017). The power of our time-resolved design is that we can distinguish this category of genes from those with an alternative temporal expression pattern, and use this information to refine biomarker discovery and AOP development. Altogether, the 48h timepoint, appears to be most relevant to understand which molecular functions mediate imidacloprid toxicity

Functional annotation analyses of the DEGs can provide insights into the mechanisms of toxicity of neonicotinoids, and can help identify KEs for AOP refinement. Gene set enrichment analyses (GSEA) performed on the complete set of DEGs identified enrichment of 26 Gene Ontologies (GO) and 14 Kyoto Encyclopedia of Genes and Genomes (KEGG) pathways, hereafter collectively referred to as Gene Set Enrichment (GSE)-terms (see supplementary Table S2.3). Many of the GSE terms were related to neuronal signal transduction or neuron degradation. For example, cluster R1 was enriched for genes involved in mediating signal transduction over the synaptic cleft, including various subunits of the neonicotinoid target receptor nAChR, and the GABA-$_A$ receptor subunit β,

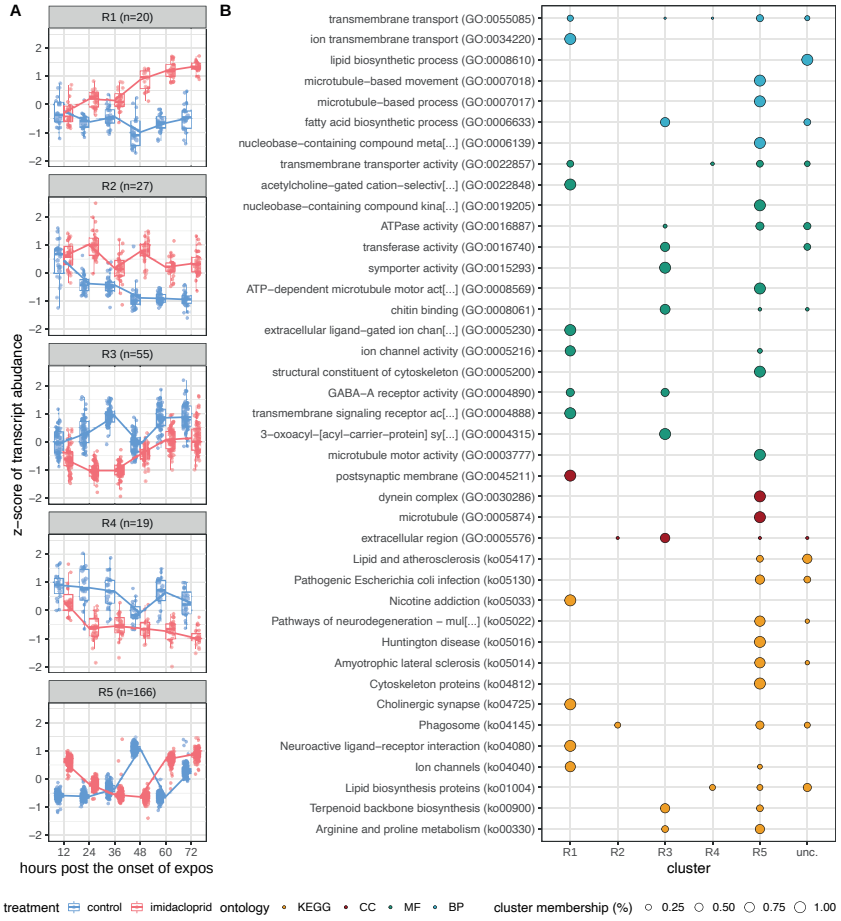

Figure 2.1: Clustering of time-resolved transcription abundance patterns (A) and associated molecular gene functions (B) after exposure to imidacloprid of *Folsomia candida*. Response of differentially expressed transcripts (DEGs, n=360), collection A, divided into various clusters with similar response to imidacloprid exposure (red) compared to control conditions (blue). Every dot on the panels of collection A is a z-score transformed transcript abundance (y-axis). The z-score transformation is not used to either determine whether the transcript is differential-expressed, only for the clustering of the patterns and for visualization. Boxplots indicate the spread of the transcript abundance per cluster for each condition per 12-hour timepoint from 12 hours to 72 hours post exposure (x-axis), lines connect the medians of each box-plot. The titles of each panel show the cluster name and the number of its gene members. The shared molecular function of the entire DEG list, as determined by a Gene Set Enrichment Analysis (GSEA), is shown in collection B. The cluster names are shown on the x-axis of the panels with on the y-axis the GSE terms with their description. Dot size shows the percentage of genes in the clusters annotated with that GSE term. The color of each dot is per ontology, i.e. Kyoto Encyclopedia of Genes and Genomes (KEGG) in orange, Gene Ontology (GO) Cellular Component (CC) in red, GO Molecular Function (MF) in green, GO Biological Process (BP) in blue.

indicated by associated GSE terms such as GO:0019205, GO:0004890, and ko04725 (see Figure 2.1 and Table S2.2). Cluster R2 was enriched for genes related to the extracellular region (GO:0005576), and cluster R5 had a range of associated GSE terms, which have also been related to the human disorder Amyotrophic Lateral Sclerosis (ALS) (ko05014). For example, in ALS in humans, microtubule (GO:0007017, GO:0007018, GO:0003777, GO:0005874) and dynein (GO:0030286) based transport is disrupted, both impeding synaptic vesicle trafficking (Redler & Dokholyan, 2012). Although nAChR over-excitation is not directly involved in ALS, dysregulation of nAchR neuronal signaling can cause comparable symptoms to ALS as seen in humans poisoned with organophosphate insecticides acting on ACh neurotransmission (Binukumar & Gill, 2010). Our results also align well with the transcriptomic response of water fleas (*Daphnia magna*) to imidacloprid exposure, which showed ontologies and pathways related to neuron degradation, such as GABA synthesis, synaptic vesicle trafficking and Parkinson's and Alzheimer's disease (Pfaff et al., 2021). Although no sequential order of responses can be inferred from our transcriptomic data alone, as shifts in gene expression occur almost simultaneously, the order in which molecular functions occur during human disorder ALS can provide a probable sequence for AOP refinement (see Figure S2.1 for ALS sequential order and Figure 2.2 for the improved putative AOP for nAchR overexcitation). The AOP for nAchR overexcitation contained only few (sub)cellular KEs up to now (Figure 2.2). With our transcriptomic analysis this AOP can be supplemented with multiple KEs (see purple tiles in Figure 2.2). Also, our data indicate that the putative AOP is applicable to a larger taxonomic group than what was known before, now including honey bee, bumble bee, water fleas and *Folsomia candida*, see literature references below the tiles.

Similar to the transcriptomic response, the proteomic response may provide putative biomarkers and KEs for AOP refinement. In total, we identified 4400 expressed proteins, of which 219 were identified as Differentially Expressed Proteins (DEPs) under imidacloprid exposure. Clustering of all DEPs based on similarity in expression patterns over time and treatment resulted in 7 clusters of DEPs, varying in size from 17 (cluster P1) to 23 genes (cluster P2). A remaining group of DEPs (n=82) was left unclustered (Figure 2.3 and supplementary Table S2.3). A larger percentage of DEPs was left unclustered (37 %) compared to the DEGs (20 %). A possible reason for this is that protein intensities are less variable compared to transcript counts.

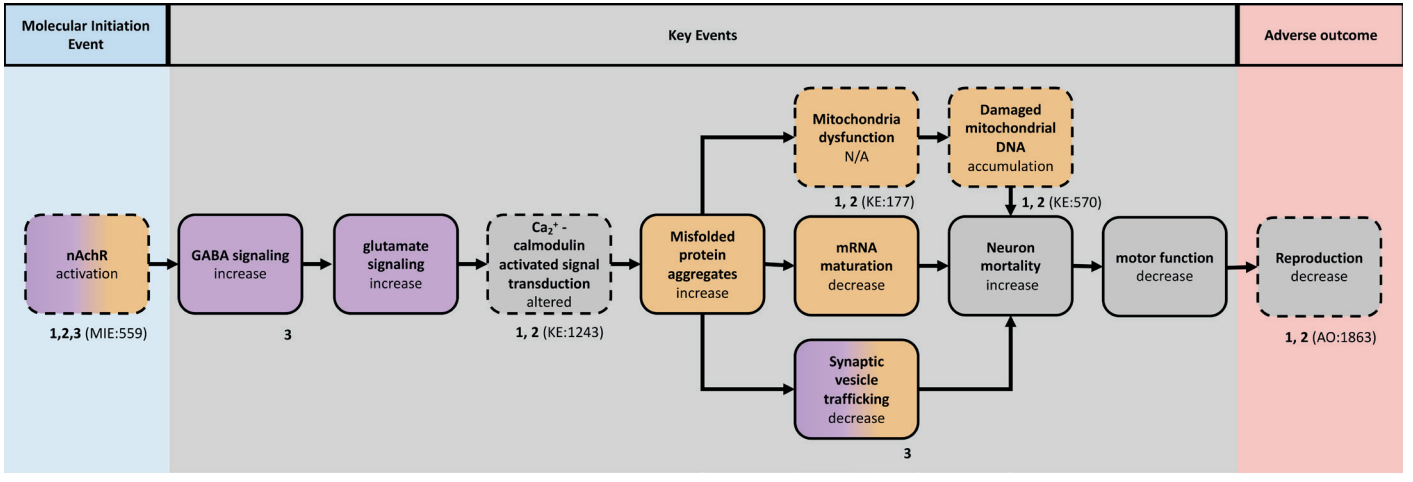

Figure 2.2: Adverse Outcome Pathway (AOP) for nicotinic Acetylcholine Receptor (nAChR) activation as the Molecular Initiation Event (MIE) and reduced reproduction as its Adverse Outcome (AO). Various Key Events (KEs) connect the MIE to the AO and are connected by Key Event Relationships (KER) shown as solid arrows between the text tiles. The titles of each KE are written in bold with the effect's direction written in non-bold letters below the titles. Only a limited set of words are allowed to describe the effect direction of the KE (OECD, 2018). Key Events have to be necessary and relevant for the progression from MIE to AO in a pathway. As per the OECD guidelines, each AOP is linear and hence the figure represents three parallel pathways that share the same MIE, AO and some KEs (OECD, 2018). Tiles shading is altered based on the result that lends support for the inclusion of the KE into the AOP; purple indicates support from our transcriptomic analysis, orange our proteomic analysis, and orange and purple gradient shading indicates support from both. Grey shading indicates that the KE was derived from KEGG map05014 and not supported by our transcriptome or proteome analysis, see Figure S2.1. Dashed outlines indicate KEs that were already present in the AOP for nAchR activation (MIE 559) and the event ID is written below the tiles in parenthesis (LaLone et al., 2017). Novel KE additions have solid tile outlines. When KEs are supported from previous findings this work is referenced with the numbers 1-3 below the tiles in bold: [1] LaLone et al. (2017); [2] Camp & Lehmann (2021); and [3] Pfaff et al. (2021)).

Proteomic response

This lower variability of DEPs makes is difficult to identify clusters with clearly distinct patterns, which could result in higher number of clusters with few clustered proteins (Kaufman & Rousseeuw, 1990). As we had set a minimum cluster size of n=15, DEPs from small clusters are labelled as unclustered. All clusters had their most differential protein expression at 48h post onset of exposure, as indicated by non-overlapping box-plots in Figure 2.3. Depending on the cluster, protein abundances were either increased (P1, P2, P4, and P7) or decreased (P3, P5, and P6) in the imidacloprid exposure compared to control conditions at this timepoint. Therefore, the results corresponded well with the transcriptomic response, in which changes in gene-expression were also most pronounced at the 48h timepoint. These results indicate that 48h is also is the most opportune timepoint for biomarker and AOP refinement based on protein expression.

The GSEA of the DEPs identified 10 GO-terms and 15 KEGG pathways (see supplementary Table S2.3). Many of the GSE terms associated with DEPs could also be linked to neuron degradation. For instance, the terms chaperone binding (GO:0051087), mitophagy (ko04137) and the many ribosome associated GSEs (GO:0006412, GO:0003735, GO:0015935, GO:0005840, ko03010 and ko03011) suggest an impeded turn-over of ribosomes, mitochondria and proteins, which is known to play a role in neurodegeneration (Chua et al., 2021) (Figure 2.3). Other GSE terms suggest an enrichment of genes involved in motor-neuron signaling leading to cardio-muscular contraction (ko05410, ko05414, and ko04216). The imidacloprid target receptor nAChR was clustered with DEPs implicated in cardio-muscular contraction, which were upregulated throughout the time series and, therefore, upregulated by imidacloprid exposure. There is, with one exception, no overlap in GSE terms between the proteome and transcriptome data, which suggests that imidacloprid exposure did not affect the exact same pathways and ontologies in both modalities. Despite this limited overlap, both sets of data support the putative AOP for nAChR activation, although the transcriptomic response corresponds mostly to early KEs and the proteomic response to KEs later in the putative AOP (Figure 2.2). Both omics datasets provide support to the KE “synaptic vesicle trafficking”. The proteomic response provides empirical support to both KEs that were previously identified in honey bees, and the newly added KEs derived from molecular insights on ALS in humans, which supports our approach to refine the AOP for nAChR activation.

Figure 2.3: Clustering of time-resolved protein abundance patterns (A) and associated molecular gene functions (B) after exposure to imidacloprid of *Folsomia candida*. Response of differentially expressed proteins (DEPs, n=219), collection A, divided into various clusters with similar response to imidacloprid exposure (red) compared to control conditions (blue). Every dot on the panels of collection A is a z-score transformed transcript abundance (y-axis). The z-score transformation is not used to either determine whether the protein is differential-expressed, only for the clustering of the patterns and for visualization. Boxplots indicate the spread of the protein abundance per cluster for each condition per 12-hour timepoint from 12 hours to 72 hours post exposure (x-axis), lines connect the medians of each box-plot. The titles of each panel show the cluster name and the number of its gene members. The shared molecular function of the entire DEP list, as determined by a Gene Set Enrichment Analysis (GSEA), is shown in collection B. The cluster names are shown on the x-axis of the panels with on the y-axis the GSE terms with their description. Dot size shows the percentage of genes in the clusters annotated with that GSE term. The color of each dot is per ontology, i.e. Kyoto Encyclopedia of Genes and Genomes (KEGG) in orange, Gene Ontology (GO) Cellular Component (CC) in red, GO Molecular Function (MF) in green, GO Biological Process (BP) in blue.

Correlation and time-lag in gene transcript and protein abundance.

Our results have demonstrated that each omics dataset can provide insights into the molecular mechanisms that mediate toxicity at a singular layer of biological organization. It is generally recommended to combine various omics data for the purpose of AOP development and KE identification (Canzler et al., 2020; Leung, 2018). However, it is unclear if responses in two omics data types occur simultaneously or if they are delayed in time. To warrant their combined analysis for AOP development, we aimed to quantify the correlation between our two omics datasets and to determine if a time-delay exists between transcript and protein abundances.

Nearly all proteins (4364 out of 4400) identified in the proteome of *F. candida* also had a transcript in the transcriptome (n=20603). From this overlap, 269 Transcript-Protein-Pairs (TPPs) had significantly correlated temporal patterns of transcript and protein expression (see supplementary Table S2.3). The number of significant TPPs is much larger than expected from random abundances ($p<0.001$ in 10,000 random bootstraps of the data set, see Figure 2.4A), and is considerably higher than the overlap of DEGs and DEPs (n=5, Figure 2.4D). This suggests a significant correlation between the transcriptome and the proteome, even though the shifts in transcript and protein expression in response to imidacloprid exposure themselves may not be statistically significant. From the 269 significantly correlated TPPs, 15 genes overlapped with either DEGs, DEPs, and two genes overlapped with both DEGs and DEPs. These genes encode two subunits of the target receptor nAChR, Fcan01_17957 and Fcan01_01431. This result suggests that both transcript and protein expression patterns of the target receptor could be used as biomarkers to indicate neonicotinoid exposure.

Analyses of the temporal correlation patterns of the TPPs indicated the strongest correlation when no time-lag was assumed between the transcript and protein expression patterns for the majority of the significant TPPs (Figure 2.4B). Moreover, significantly correlated TPPs overall had a shorter time-lag compared to the background, i.e. non-significant TPPs. The temporal correlation patterns of the TPPs clustered into 7 clusters, varying in size from 19 (cluster C1 and C5) to 30 genes (cluster C7) (see supplementary Table S2.3). The percentage unclustered TPPs was relatively high with 39 %, which is comparable to the number of

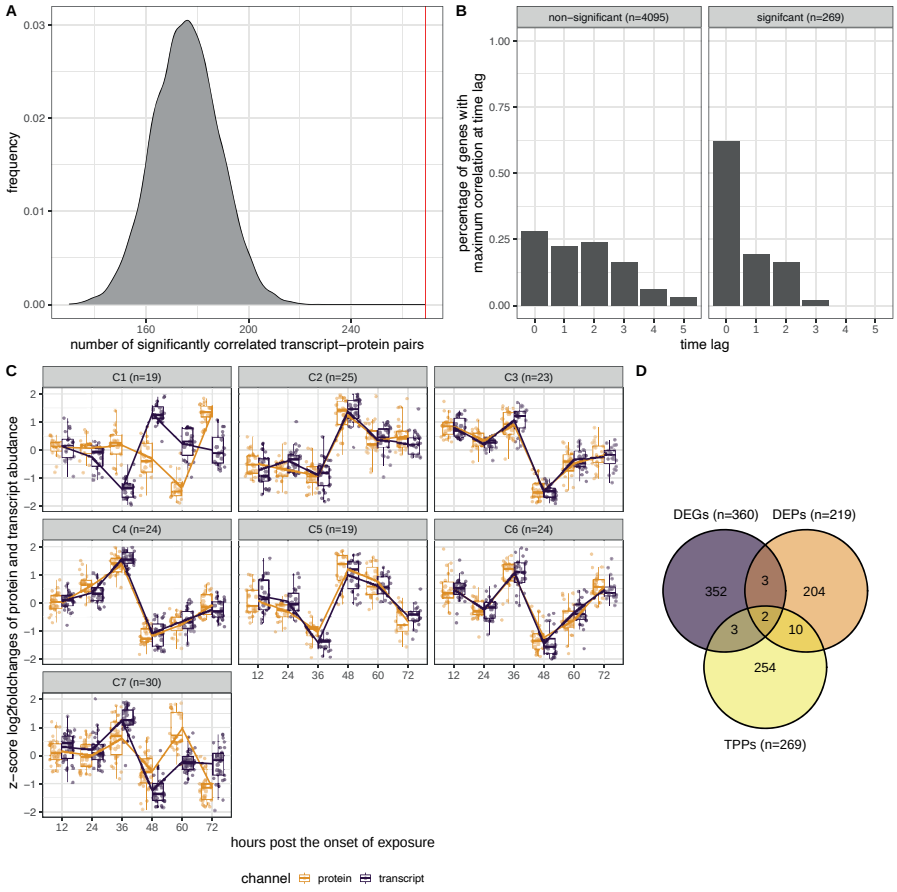

Figure 2.4: Temporal correlation of differentially expressed transcripts (DEGs) and proteins (DEPs) after imidacloprid exposure in *Folsomia candida*. The number of significantly correlated transcript-protein-pairs (TPPs) is higher compared to 10,000 randomized draws (panel A) and significant TPPs have their highest correlation at shorter time-lags compared to non-significantly correlated TPPs (panel B). Clustering of time-resolved relative abundance patterns of correlated TPPs (A), the numerical overlap of genes in the differentially expressed transcripts (DEGs), proteins (DEPs) and TPP lists (B). In panel A, the number of significantly correlated TPPs (n=269, red vertical line) is compared to a frequency distribution representing significantly correlated TPPs when the data is randomized 10,000 times. In panel B, each bar indicates the percentage of TPPs with their highest-correlation, i.e. maximum correlation, with that time-lag for non-significant (left panel) or significant (right panel) TPPs. A TPP is deemed significantly correlated at a threshold of 5 %. In panel A, the dots on the panels are z-score transformed log2fold-changes of imidacloprid over control condition abundances of either transcripts (purple) or proteins (orange). Boxplots indicate the spread of relative abundances per cluster for each modality per 12-hour timepoint from 12 hours to 72 hours post exposure, lines connect the medians of each box-plot per cluster and modality. The titles of each panel show the clusters name and the number of TPP members.

unclustered DEPs (37 %) and may again be linked to a low variability of the LFC temporal patterns. The patterns indicate that the majority of clusters, i.e. 6 out of 7, had no visible time-lag between expression patterns of the transcript and protein (see Figure 2.3). Only cluster C1 displayed a time-lag of two timepoints, i.e. 24 hours. Combined, these observations indicate a limited time lag between transcript and protein expression after imidacloprid exposure in *F. candida*, when tested with 12-hour time-intervals. This finding seems to contradict the conclusions of Simões et al. (2019), who observed a time-lag of 2-3 days between transcript and protein abundances in *F. candida* exposed to a fungicide formulation with the active substance chlorothalonil. However, transcript and protein samples in that study were taken at 2, 4, 7 or 10 days after onset of exposure, which largely exceeds the time frame we studied. This hampers a direct comparison of the two findings. However, as shifts in gene expression can occur in the order of minutes and protein regulation in the order of hours after toxicant exposure, one might argue that smaller time frames of 12h, as used in our study, provide a better resolution to the correlation of these dynamic transcript and protein responses.

Previous studies have suggested staggered data collection or modelling approaches to facilitate multi-omics data analysis (Canzler et al., 2020; Garcia-Reyero & Perkins, 2011). Although these analyses may be necessary to study multi-omics expression patterns over a test duration of a few hours, our findings suggest this is not necessary when multi-omics data is obtained over a test duration of multiple days.

Conclusion

By combining time-resolved transcriptomic and proteomic data on the response to pesticide exposure in the soil invertebrate *F. candida*, our study has provided valuable insights that support AOP development and biomarker discovery. Both the transcriptome and the proteome analysis identified GSE terms associated with imidacloprid exposure that support the existing AOP on nAChR activation and refine it by identifying novel KEs (Figure 2.2). Moreover, we here provide evidence that transcriptomic and proteomic data obtained from the same timepoint can be combined, which is an important requirement to assess AOP applicability and robustness. The largest shift in both transcript and protein expression after imidacloprid exposure was observed at the 48h timepoint, indicating this as the most opportune moment for biomarker and AOP development. These findings

contribute to the application of the AOP framework as a tool for Environmental Risk Assessment of neonicotinoid polluted soils or compounds with similar Modes of Actions, which may play an important role in providing rapid and cost-effective tools for pesticide monitoring programs.

Statements and declarations

Declaration of interests

☒ The authors declare that they have no known competing financial interests or personal relationships that could have appeared to influence the work reported in this paper.

☐ The authors declare the following financial interests/personal relationships which may be considered as potential competing interests:

CRediT author statement

Ruben Bakker – Conceptualization, Methodology, Formal analysis, Investigation, Data Curation, Writing - Original Draft: **Dick Roelofs** – Conceptualization, Funding acquisition, Project administration, supervision, Writing - Review & Editing: **Tjeerd Dijkstra** – Conceptualization, Funding acquisition, Project administration, supervision, Writing - Review & Editing: **Jacintha Ellers** – Supervision, Funding acquisition, Project administration, supervision, Writing - Review & Editing: **Cornelis A.M. van Gestel** – Conceptualization, Funding acquisition, Project administration, Supervision, Writing - Review & Editing: **Katja M. Hoedjes** – Supervision, Writing - Review & Editing.

Acknowledgements

The authors wish to extend their gratitude to Janine Mariën and Rudo Verweij for their help and guidance in carrying out the experiments as part of this work. The authors also thank Yuliya Shapovalova for her insight into the statistics used throughout the work.

Chapter 2: supplementary information

S2.1. Quality control of the soil spiking

The imidacloprid concentration in control and test soil was confirmed by Groen Agro Control, Delfgauw, the Netherlands, following certified analytical methods and with a detection limit of 0.01 mg kg^{-1} dry soil. No imidacloprid was detected in the control soil. The recovery of imidacloprid in the spiked soil at the onset of the exposure was 80 % or 0.20 mg kg^{-1} dry soil (from the desired 0.25 mg kg^{-1}), and falls within the EC_{20} estimate reducing *F. candida* juvenile reproduction by 20 % (Bakker et al., 2022). Therefore, the imidacloprid exposure is referred to as the EC_{20} throughout this work.

S2.2 LC-MS^2 quality control metrics

Visual inspection of the Thermo Fisher raw files did not indicate the LC-MS^2 runs had ended prematurely or that the peptides were not sufficiently separated by the LC-column. However, some had low overall intensity, e.g. sample 8, or high intensity, e.g. sample 25. However, this variation is accounted for at further stages of the analysis.

The calibration of MetaMorpheus indicated that 10 ppm and a fragment (MS/MS) mass tolerance of 0.5 Dalton were the right search settings for all LC-MS^2 files. These parameters were used for readjusting the other search software.

The Global Post-Translational Modification Discovery (GPTMD) search of MetaMorpheus showed that Acetylation on N-terminus, Oxidation on M and deanimation on N, Q and R were the most commonly found Post Translational Modifications (PTMs), see Table S2.2. The top 5 PTMs found represented over 68 % of all PTMs in the dataset. Other search software, i.e. MaxQuant and SearchGUI, settings were adjusted to accommodate these PTMs in the search parameters. Due to a lack of PTMs that could not be accounted for with the other software, we conclude that PTMs could not hamper the further analysis of the LC-MS^2 data.

The PSM ID rate, i.e. the fraction of all MS/MS spectra that could be assigned to a peptide, was on average 11.08 % (sd = 1.71, n=36) for MSGF+, see Table S2.1. This PSM ID rate was 60 % times higher compared to the PSM ID rates of Andromeda (6.96 %, sd = 1.53, n=36) and 50 % higher than the PSM ID rates for MetaMorpheus

(7.36 %, sd 1.4). Therefore, the search engine MS-GF+ outperformed the other search engines. One reason could be the automated readjusting of search parameters and PSM scoring of the MS-GF+ algorithm (Kim & Pevzner, 2014). The PSM ID rates in our study were lower than observed in other studies, for example the PSM rate from single tissue human or model organism isolates is expected to be between 20 to 40 % (Bielow et al., 2016). This may be explained by the fact that we did not isolate proteins from a single tissue and used a less standard model organism compared to humans, fruit flies or zebrafishes. From the comparative analysis between the three search engines, we conclude that Andromeda and MetaMorpheus did not perform well on our data, possibly because these search engines could not readjust their settings to accommodate the type of data used in this work. As the MS-GF+ search engine performed best in terms of PSM ID rates, we used this method for further analysis.

S2.3 KEGG pathway color coding (figure S2.1)

For coloring in the KEGG pathways, the Log2-Fold-Change (LFC) values of KEGG gene identifiers associated to the DEGs were selected and had a color assigned to them in hexa-color-code per chosen timepoint based on their quantile (25^{th} percentile distribution): quantile one (Q1) was colored blue, #0000ee, Q2 light blue "#3399ff", Q3 pink "#ff6699", Q4 red "#ff0000". Therefore, genes with high expression values in the imidacloprid exposure were assigned a red color and genes with high expression values in the control conditions a blue color. The colors were uploaded to the KEGG mapper - color webtool, www.genome.jp/kegg/mapper/color.html, and colored map05014 png was downloaded. The colored KEGG map served as the basis of a putative AOP, which was constructed following the AOP User's handbook (OECD, 2018).

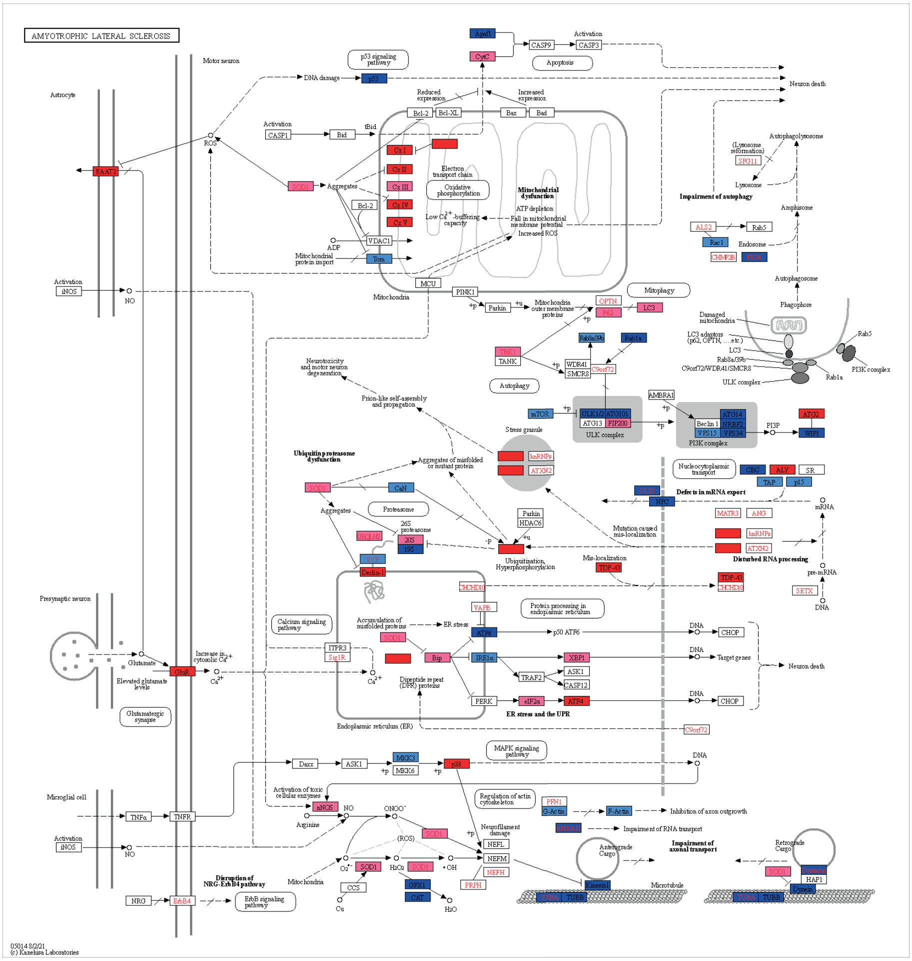

Figure S2.1: The Kyoto Encyclopedia of Genes and Genomes (KEGG) pathway map05014 representing the human disorder Amyotrophic Lateral Sclerosis (ALS) colored with Differentially Expressed Genes (DEGs) found after 48 hours exposure as part of a time-series assay comparing the gene-expression of *Folsomia candida* exposed to imidacloprid at a concentration corresponding with the EC_{20} for effects on reproduction. Each tile represents a gene, its abbreviations written in the tile. The shading of the tiles represents whether the DEG was expressed higher in the imidacloprid exposure (red or pink), or under control conditions (blue or light blue). Expression was ordered by their quantiles and colored as follows: Q1: blue; Q2, light blue; Q3, pink; Q4, red. Abbreviations in red lettering are genes whose malfunction or altered expression is associated to human ALS disorder. All dots represent metabolites, enzymatic (by-)products and biomolecules with arrows connecting these molecules and genes to represent activations or expression. Arrows with blunt tips represent repression or inhibition. Dotted arrows suggest indirect linkage of events. Arrows crossed by dashes represent missed linkage due to mutation or malfunction.

Table S2.1: Mapping rate of RNAseq reads and identification rate of MS/MS spectra. Transcriptomic (RNAseq) and proteomic (LC-MS^2) data obtained from *Folsomia candida* exposed to imidacloprid or control conditions. Sampling was done every 12 hours for a total of 72 hours after the onset of exposure. Here the RNAseq mapping rate (%), which was done using *Salmon* v0.8.1, and the MS/MS-spectra identification rate (%), which was done using *msgf+*, are shown.

sample	hours	condition	RNAseq mapping rate (%)	MS/MS id rate (%)
1	12	control	87.00	11.5
2	12	control	88.22	9.81
3	12	control	86.24	11.86
4	12	imidacloprid	84.99	9.46
5	12	imidacloprid	86.50	11.52
6	12	imidacloprid	83.79	13.15
7	24	control	81.86	12.45
8	24	control	87.72	11.31
9	24	control	87.63	13.13
10	24	imidacloprid	86.75	12.34
11	24	imidacloprid	87.86	12.42
12	24	imidacloprid	84.79	10.36
13	36	control	85.83	10.13
14	36	control	86.92	10.95
15	36	control	86.65	11.28
16	36	imidacloprid	87.79	12.2
17	36	imidacloprid	84.16	8.77
18	36	imidacloprid	88.01	11.38
19	48	control	89.15	10.86
20	48	control	83.44	9.25
21	48	control	90.69	10.47
22	48	imidacloprid	87.91	10.9
23	48	imidacloprid	89.02	13.5
24	48	imidacloprid	86.80	12.06
25	60	control	85.13	8.22
26	60	control	85.75	11.63
27	60	control	83.61	11.82
28	60	imidacloprid	83.94	10.46
29	60	imidacloprid	84.18	11.99
30	60	imidacloprid	87.22	11.61
31	72	control	85.05	12.42
32	72	control	87.95	6.54
33	72	control	87.00	11.68
34	72	imidacloprid	84.00	12.55
35	72	imidacloprid	84.60	12.98
36	72	imidacloprid	84.80	5.98

Table S2.2: the top 5 Post Translation Modification (PTM) found by Global Post-Translational Modification Discovery (GPTMD) module in the software *MetaMorpheus*. Each top PTM is also shown as a percentage of the total modifications found in the data. Data obtained from *Folsomia candida*, for every 12 hours for a total of 72 hours, exposed to imidacloprid or control conditions.

Modifications	Count (n)	Percentage (%) of total PTMs found
Deamination on Q	1240	25
Deamination on N	1043	21
Citrullination on R	615	13
Hydroxylation on P	264	5
Hydroxylation on N	156	3
Total top 5 PTMs	3318	68
Total PTMs all data	4870	100

Table S2.3: Gene Set Enrichment report for differentially expressed genes (DEGs) and proteins (DEPs), and a list of significantly correlated Transcript Protein Pairs (TPPs). Transcriptomic and proteomic data had been obtained from *Folsomia candida* exposed to imidacloprid or under control conditions. Sampling occurred every 12 hours for a total of 72 hours for both conditions as detailed in the methods section. Lists of DEGs, DEPs and TPPs are provided in three separate sheets ("DEG report", "DEP report", and "TPP report", respectively). For each gene the following information is provided: the Ensembl gene identifiers of these groups, according to Ensembl Metazoa (Cunningham et al., 2019), log-likelihood estimate, p-value and q-value of the model comparisons, the gene's description, associated Gene Set Enrichment terms, and clustering results. Gene Set Enrichment Analysis (GSEA) of DEGs and DEPs were done and the outcomes are presented in two separate sheets ("GSEA DEGs" and "GSEA DEPs", respectively), which show the over- and under representation of GSE terms in the DEGs and DEPs compared to the overall transcriptome and proteome, respectively. The column "numDEInCat" shows the number of differentially expressed (DE) genes or protein in that GSE term. The number of genes or proteins in the transcriptome or proteome, respectively, with that GSE term annotation is found in the column "numInCat". The last two columns provide a description of the GSE term and the ontology or database the GSE term can be found in.

Table S2.3 can be found in the associated Excel sheets.

Follow the link:

https://docs.google.com/spreadsheets/d/1VWpIujM5iuJO-xfXQJxHmLQb96hazSLz/edit?usp=sharing&ouid=109773965507433810260&rtpof=true&sd=true

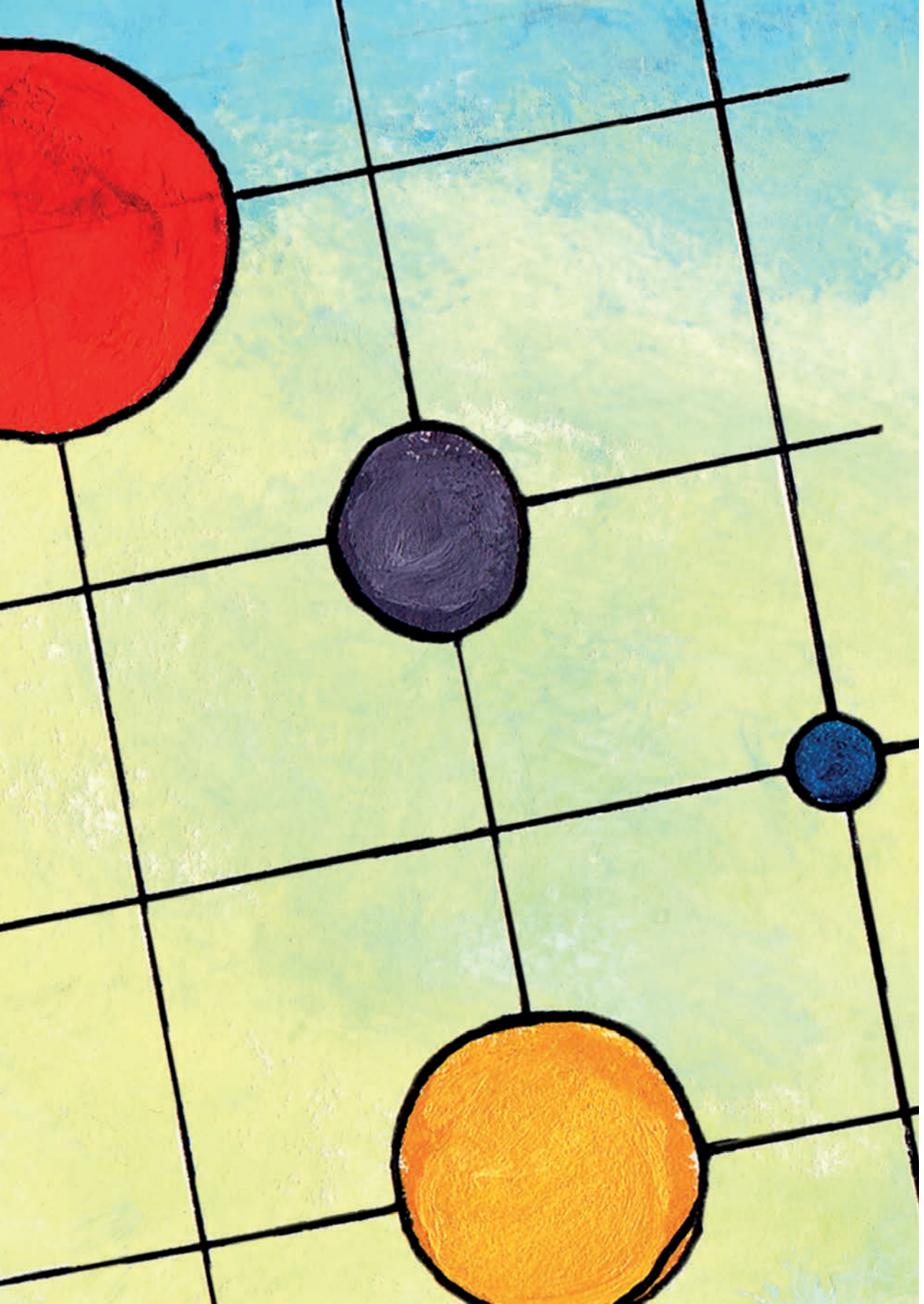

Chapter 3

A Gaussian processes approach facilitates the identification of robust biomarkers for exposure to complex pesticide mixtures

Ruben Bakker[1], Yuliya Shapovola[2], Tjeerd Dijkstra[3*], Tom Heskes[2], Cornelis A.M. van Gestel[1], Katja Hoedjes[1]

[1]Vrije Universiteit Amsterdam, Faculty of Science, Amsterdam Institute for Life and Environment (A-LIFE), De Boelelaan 1085, 1081 HV Amsterdam, The Netherlands
[2]Radboud Universiteit Nijmegen, Houtlaan 4, 6525 XZ Nijmegen, The Netherlands
[3]University Clinic, Department for Women's Health, Calwerstraße 7, 72076 Tübingen, Germany
*Corresponding author
E-mail contact: tjeerd.dijkstra@uni-tuebingen.de

Manuscript in preparation.

Complex pesticide mixtures are found in many agricultural soils, contributing to a global decline in invertebrate populations. Traditional chemical monitoring of pesticide mixtures underestimates their environmental risk as these methods underestimate pesticide (synergistic) interaction effects and cannot determine their bioavailable fraction in the soil. Characteristic gene-expression patterns could be used as biomarkers to determine the type of soil pollution present and its intensity even under varying mixture compositions. However, current differential gene expression methods are ill-suited for biomarker discovery from mixture exposure transcriptomic data due to (1) high variability of gene expression, (2) nonlinear concentration-response relationships, (3) and genetic interaction effects. In this study, we obtained transcriptomic data from the springtail *Folsomia candida* under two binary mixture exposures in a grid design and finely resolved for stress intensity. The mixtures either had the same or different presumed mechanisms of toxic action, combining two neonicotinoids insecticides, imidacloprid and clothianidin, or imidacloprid and the azole fungicide cyproconazole, respectively. We analyzed the data using a custom-made statistical framework based on Gaussian Processes (GP) models to meet the three common challenges of mixture toxicity transcriptomic data, and analyzed the two datasets in conjunction without the need for batch effect correction. The identified candidate biomarkers were validated by exposing springtails to soil spiked with imidacloprid and cyproconazole. Our findings demonstrate the efficacy of GP models to analyze mixture exposure transcriptomic data, which has potential applications far beyond ecotoxicology, such as in pharmacology and other fields of biology.

Keywords: transcriptomics, ecotoxicogenomics, neonicotinoids, springtails, differential gene expression analysis

Introduction

Intensive pesticide application contributes to the decline of non-target invertebrates worldwide. Non-target invertebrates are essential to sustainable agricultural practices such as pollination, predation of pest species, or nutrient cycling (FAO, ITPS, GSBI, 2020). Traditionally, pesticide regulation and risk assessment are based on standardized tests that determine the Effect Concentrations (EC) at which a pesticide reduces phenotypic end-points of model organisms, such as reproduction or survival. These ECs ultimately inform risk assessors on the environmentally safe concentration limits of pesticides. However it is difficult to extrapolate the ECs obtained in single pesticide toxicity tests to field-relevant conditions as, most importantly, pesticide mixtures pollute most agricultural soils (Pelosi et al., 2021; Silva et al., 2019). Determining the toxicity of pesticide mixtures using standardized phenotypic toxicity tests is practically impossible because their (synergistic) interaction effects are mainly unknown, soil properties influence pesticide bioavailability, and all possible combinations of pesticide mixtures are innumerable (Gunstone et al., 2021; van Gestel, 2012). Besides the inaccuracy of extrapolating the results of standardized toxicity tests to field-relevant conditions, another problem is the enforcement costs. Monitoring programs currently require the chemical assessment of the concentration of a myriad of pesticides and other pollutants, which is a highly laborious and expensive process that commonly underestimates the cumulative toxicity of mixtures of environmental pollutants (Escher et al., 2020). Therefore, the current environmental risk assessment lacks accurate metrics for the toxicity and composition of complex pesticide mixtures. New metrics to identify the type of pesticide exposure and its toxicity are urgently needed to guide pesticide abatement efforts and prevent a further decline of non-target invertebrate species.

Supplementing phenotypic toxicity tests with bioanalytical tools, such as gene-expression biomarkers, can more accurately monitor complex pollution mixtures (Escher et al., 2020; Fontanetti et al., 2011). In this framework model organisms are exposed to environmental soil samples in a testing facility. Then, a panel of gene-expression biomarkers surveys the soil for pollution (G. Chen et al., 2014; Lionetto et al., 2019). When pollution is detected, soil samples are submitted to a higher tier and more costly testing, such as bioassays and chemical analysis of the soil. Informed by the results of the biomarker panel, risk assessors can focus their efforts on the most

concerning samples allowing them to expand monitoring programs while reducing costs. Biomarkers, in this manner, support an ongoing shift in environmental risk assessment to enforce not the environmental concentration of pollutants but their harmful effects on non-target organisms (Escher et al., 2020). The springtail *Folsomia candida* would be ideal for this purpose as it can reproduce asexually, is easily reared, and its genome has been annotated and sequenced, which facilitates gene expression studies (Faddeeva-Vakhrusheva et al., 2017; Fountain & Hopkin, 2005). *F. candida* belongs to the Collembola, a species-rich family of soil invertebrates that contribute to nutrient cycling and the spread and maintenance of the microbiome (Cragg & Bardgett, 2001; Rusek, 1998). Moreover, *F. candida* is considered representative of the susceptibility to pesticides of other springtail species and it is, therefore, considered an important soil ecotoxicological model (de Lima e Silva et al., 2017, 2021).

Because the molecular effects of pollutants, e.g., pesticides, are diverse, multiple biomarkers are required for their assessment (Lionetto et al., 2019). However, multiple biomarkers per pesticide would result in a panel with an unpractical number of biomarkers. For the successful implementation of biomarkers as a bioanalytical tool, first, a set of genes affected by exposure to a specific class of pesticide must be identified. Second, genes with nonspecific responses to the pesticide type and those part of the universal stress response must be filtered from this set. The remaining characteristic gene-expression patterns are the pesticide's toxicogenomic fingerprint. The toxicogenomic fingerprint can then form the basis for biomarker development. To this end, defining the specificity of gene-expression patterns under exposure to multiple pesticides is essential. Mixture exposure toxicity data is inherently highly variable and contains nonlinear and interaction effects that act on the concentration-response relationships (Altenburger et al., 2012). Routinely parametric models used by popular software, such as edgeR and DESeq2, are ill suited to analyze such variable, non-linear relationships, which constraints differential gene expression analysis (DGEA) for identifying toxicogenomic fingerprints under mixture exposure (Love et al., 2014; Robinson et al., 2009).

Parametric models rely on the assumption of fixed gene expression concentration-response relationships, which makes them unsuitable for analyzing mixture transcriptomic data in three ways. First, parametric models perform poorly on

nonlinear concentration-response relationships (Ren & Kuan, 2020). Second, parametric models deal poorly with uncertainty caused by high data variability and require various correction methods or estimation techniques (Love et al., 2014; Reeb & Steibel, 2013). Third, parametric models have fixed shapes of the concentration-response relationships (Ewald et al., 2021; Larras et al., 2018). For example, current DGEA methods categorize the concentration-response relationships as a bell-shape, U-shape, or S-curve. Mixture exposures over a broad range of intensities will inevitably result in numerous shapes of the concentration-response relationships, due to the interaction effects of the multiple compounds. Fixed-shaped models require a vast number of additional parameters to permit these surfaces. Besides the computational costs of adding more parameters to the models and selecting those that fit best, it would also render the p-value ranking of genes impossible, as p-values from fixed-shaped models with different levels of parametrization are incomparable. In brief, DGEA methods used for analyzing mixture transcriptomic data should account for: (1) nonlinear concentration-response relationships of gene expression, (2) have to quantify uncertainty in the data accurately, (3) and be parameter-free.

Gaussian process (GP) models allow for non-parametric and non-stationary, i.e., rapid changes, modeling of concentration-response relationships. GP models can fit complex nonlinear patterns in a robust Bayesian probabilistic framework and thus provide reliable prioritization of the differentially expressed genes across complex concentration-response surfaces. Additionally, they can accurately quantify the high degree of uncertainty caused by variability typical for transcriptomic data. GP models, therefore, address all three challenges associated with DGEA of complex mixture exposure data. Previously, GP models have been applied to DGEA (Kalaitzis & Lawrence, 2011), drug-drug interaction modeling (Shapovalova et al., 2022), and pharmacological responses and biomarkers development (Wang et al., 2020), but to date not yet for mixture toxicity data. Besides the advantages mentioned above, our approach can consider that various experiment can have the same chemical compound and treat the single experimental data of the same chemical compound jointly across all the experiments. In this study, we extend current approaches for GP modeling to analyze transcriptomic data obtained under mixture of exposures and over a range of stress intensities by various pesticides.

Neonicotinoids are the most commonly used insecticides and are highly toxic to non-target invertebrates. They overstimulate the neuronal signal over the

nicotinic acetylcholine receptor (nAChR). They are commonly found alongside azole fungicides, which are known to synergize with neonicotinoids by inhibiting their primary route of detoxification, the biotransformation pathway (Glavan & Bozic, 2013; Raimets et al., 2017; Sgolastra et al., 2017). Here, we used GP models to identify toxicogenomic fingerprints of *F. candida* to the broader neonicotinoid insecticide class even under interaction effects with an azole fungicide, cyproconazole. We selected two binary mixtures of either two neonicotinoids, imidacloprid and clothianidin, or imidacloprid and cyproconazole (an azole fungicide). First, we quantified the interaction toxicity effects of the mixtures on *F. candida* reproduction by Hand GP models (Shapovalova et al., 2022). By studying the interaction effects on mixture toxicity to reproduction, we demonstrate that the pesticide exposure caused genetic interaction effects as non-additive toxicity stems from molecular interaction effects and, hence, gene expression. Next, we sought to identify robust signatures of differential gene expression of exposure to neonicotinoids and cyproconazole. For this, we generated *F. candida* transcriptomic data under the two binary mixtures and analyzed both datasets with GP models.

Materials and methods

Soil preparation.

Imidacloprid, ≥ 98 % purity, was provided by Bayer (Monheim, Germany). Clothianidin and cyproconazole, both ≥ 98 % purity, were bought from Merck (Amsterdam, The Netherlands) and Thermo Fisher Scientific (Landsmeer, The Netherlands), respectively. LUFA2.2 test soil (Speyer, Germany) was used for the binary mixture toxicity tests, transcriptomics exposures, and the gene expression survey with spiked soils. LUFA2.2 is a natural, sandy soil with a total organic carbon content of 2.1 %, Water-Holding-Capacity (WHC) of 46.5 %, and a soil pH of 5.5 % (0.01 M $CaCl_2$); as determined by the supplier.

For all exposures, imidacloprid and clothianidin were dissolved in ultra-pure water and left to stir at 300 rpm overnight, and covered in aluminum foil. Cyproconazole was dissolved in acetone and this mixture was used to spike 10% of the sample test soil per condition. The soil and acetone mixture was mixed every half hour for two hours or three times. After that, the acetone was left to evaporate entirely, overnight, covered in aluminum in a fume hood. For the binary mixture of imidacloprid and

cyproconazole, all conditions had 10 % of the test soil treated with acetone as described above. For the binary mixture of imidacloprid and clothianidin, no pre-treatment with acetone was carried out. Then, where applicable, all dry test soil, including acetone pre-treated soil, was mixed thoroughly with a demineralized water mixture containing the desired amount of imidacloprid and clothianidin equal to 50 % of the Water Holding Capacity (WHC) or 22 % of the test soil total dry weight. Soils were left overnight before starting exposures.

For springtail reproduction toxicity tests of the binary mixtures, the following concentrations were chosen: imidacloprid, 0, 0.1, 0.2, 0.4, 0.8, 1.6 mg kg^{-1} dry soil, with either: clothianidin, 0, 0.05, 0.1, 0.2, 0.4,0.8 mg kg^{-1} dry soil, or: cyproconazole 0, 62.5, 125, 250, 500, 1000 mg kg^{-1} dry soil. The concentrations represent ¼, ½, 1, 2, and 4 Toxic Unit (TU equals to the Effect Concentration reducing juvenile counts by 50 %, i.e., EC_{50}). The effect concentrations were determined in an earlier study (Bakker et al., 2022, *under review*). For the 1:0, 0:1, and 1:1 TU:TU conditions, 5 replicates were used, and for the other conditions 3 replicates, resulting in 140 samples, see Figure 3.1.

For transcriptomic exposures, the concentrations chosen for the neonicotinoid mixture were: imidacloprid: 0.00, 0.08, 0.16, 0.24, 0.32 and 0.40 mg kg^{-1} dry soil combined with 0, 0.048, 0.096, 0.144, 0.192, 0.240 mg of clothianidin kg^{-1} dry soil. For the imidacloprid-cyproconazole mixture, the same concentrations of imidacloprid were chosen, and 0, 50, 100, 150, 200, and 250 mg of cyproconazole kg^{-1} dry soil. Concentrations of all pesticides were equal to 0, ⅕, ⅖, ⅗, ⅘, and 1 TU. Only the conditions 1:0, 0:1, and 1:1 (TU:TU) were used for the highest exposures. All other concentrations were combined in a full factorial design, resulting in 50 conditions and 168 samples over the two experiments, see Figure 3.1.

For the gene-expression survey on spiked soils, the following concentrations were chosen: 0, 0.1, 0.2, 0.4 mg imidacloprid kg^{-1} dry soil and 0, 10, 40 mg cyproconazole kg^{-1} dry soil. The imidacloprid concentrations were roughly equal to the Effect Concentration (EC), reducing juvenile counts by 1 %, 10 %, and 50 %, respectively, EC_1, EC_{10}, and EC_{50} (Bakker et al. 2022, *under review*).

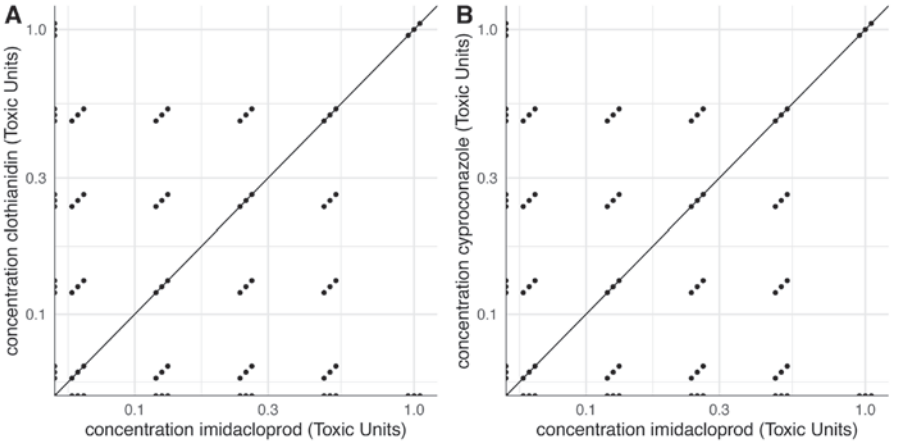

Figure 3.1: a schematic overview of the experimental design to obtain transcriptomic data from the springtail *Folsomia candida* under the exposure to mixtures of either imidacloprid and clothianidin (A) or imidacloprid and cyproconazole (B) in LUFA2.2. In both exposures, the concentrations are in Toxic Units; each Toxic Unit is equal to the Effect Concentration of that pesticide, reducing juvenile counts by 50 % (EC_{50}). Dots on the panels represent a sample at each condition and are separated by arbitrary distances to visualize the number of samples. The solid black line depicts a 1:1 ratio of toxicity exposure based on Toxic Units.

Toxicity tests, transcriptomic exposure, and gene-expression survey.

In all tests, springtails *Folsomia candida* (Berlin strain), aged 22-24 days old, were obtained from inhouse cultures maintained for over 30 years at the Amsterdam Institute for Life and Environment (A-LIFE) at the Vrije Universiteit Amsterdam. For the springtail reproduction toxicity tests on binary mixtures, transcriptomic exposures (RNA-sequencing), and gene-expression surveys (qPCR), a pool of 10, 80, and 40 *F. candida*, respectively, were exposed to 30 grams of moist test soil. The duration of the binary mixture toxicity test was 21 days, while it was 48 hours for the transcriptomic exposure and gene-expression survey. The latter exposure duration was chosen because previous findings have indicated this time point as the most opportune moment for biomarker development for neonicotinoid exposure in *F. candida* (Bakker et al. *in preparation*). At the end of all tests, the soil was decanted in plastic beakers, waterlogged, stirred, and left to rest for 5 minutes to let all animals surface. For the toxicity tests, the samples were photographed by a Nikon Coolpix P510, and the adult and juvenile *F. candida* on the pictures were counted with *Fiji* (version *Image-J 1.52v*) using the *Cell Counter* plugin (Kurt de Vos, version from 2010). For transcriptomic and gene-expression surveys, the

springtails were scooped off the surface by a fine mesh, transferred by an aspirator to 1.5 ml reaction tubes, snap-frozen in liquid nitrogen, and stored at -80 °C.

For the exposures to obtain transcriptomic data, samples were homogenized using a pestle while frozen. Following the manufacturer's instructions, RNA was isolated using a TRIzol-based method (Invitrogen) and 500 µL as a starting volume. The first precipitation step with isopropanol (1:1 V:V) was extended from 10 minutes at room temperature to overnight at -20 °C to increase RNA yield. After RNA isolation and wash, a DNse was carried out using a DNse-I kit from Promega (Leiden, The Netherlands), following the manufacturer's instructions. The DNse was removed by phenol-chloroform wash and washed three times in a 75 % ethanol RNAse-free water mixture. After the last wash step, all water was removed by pipet, and the remaining ethanol and water were left to evaporate entirely. The RNA was resuspended in ultra-pure RNAse-free water. RNA integrity was monitored by separating RNA on a 1% agarose gel electrophoresis and, subsequently, a 2100 Bioanalyzer (Agilent, Amstelveen, The Netherlands) following the manufacturer's instructions. RNA concentration was determined on a nanodrop (Thermo Fisher Scientific, Aalsmeer, The Netherlands) and a Qubit (BioRad, Veenendaal, the Netherlands). Per sample, 1 µg of RNA was used for RNAseq library preparation, and 150bp paired-end sequencing was done on a NovaSeq600 (Illumina, Eindhoven, The Netherlands) with a sequencing depth of 10 million reads per sample by Macrogen (Amsterdam, The Netherlands).

For the gene-expression survey on spiked soil, the RNA was isolated using an RNA-isolation kit (Promega), following the instructions of the manufacturer. RNA integrity and quantity were determined by 1 % agarose gel-electrophoresis and nanodrop (Thermo Fisher Scientific). Roughly 500 ng of RNA was transcribed into cDNA using an MML-V reverse transcriptase kit (Promega). Per 7 samples, one sample had the reverse transcriptase omitted to generate no-template controls. All samples were measured in a Cyber-Green reaction mix on a CFX Connect Real-Time PCR Detection System (BIO-RAD, USA) and in the presence of no-template controls and samples containing only the reaction mix (blanks). The primer selection was based on this work and earlier findings investigating the transcriptomic response of *F. candida* to imidacloprid exposure (Bakker et al., 2022, *under review*). The primer sets for neonicotinoid exposure were: *nicotinic Acetylcholine Receptor subunit alpha1* (*nAchR*), the target receptor of neonicotinoids; *Sodium-coupled*

MonoCarboxylate Transporter 1 (*SMCT*), involved in the transport of nicotine like and other monocarboxylate compounds over the cell membrane; *ARRestin Domain-containing protein 3* (*ARRD*), involved with the transport and activation of many transmembrane receptors. The primer sets for cyproconazole exposure were: *Cytochrome P450 3A56* (*CYP*), a phase-I biotransformation enzyme, *ABC-transporter 1* (*ABC*), a phase II biotransformation enzyme, and *sphingomyelin phosphodiesterase* (*SMPD*), sphingomyelins are involved in stress signaling. The reference genes, also known as housekeeping genes, were *tyrosine 3-monooxygenase* (*YWHAZ*) and *Eukaryotic Transcription Initiation Factor 1A* (*ETIF*). The primer sets *nAchR*, *SMCT*, *GluCl*, *YWHAZ,* and *ETIF* were previously designed in other studies in our lab (Bakker et al., 2022; M. E. de Boer et al., 2009). All other primers were designed, as part of this work, using the NCBI Primer BLAST tool (Ye et al., 2012). See Table 3.2 for a full description of the primers.

Binary mixture toxicity tests

We used the HandGP model (Shapovalova et al., 2022) for the analysis of interaction effects between imidacloprid and clothianidin, or imidacloprid and cyproconazole. The HandGP model is based on fitting a Gaussian process surface to the dose-response data and overall dose combinations. Once the dose-response surface is estimated, Hand principles are applied to construct a non-interaction surface. Subsequently, the observed and non-interaction surfaces are compared to predict synergistic/antagonistic effects.

For consistency check, we also analyze the data using the MuSyC model, which is based on a parametric model over the whole dose-response surface and thus the closest parametric alternative to the HandGP approach (Shapovalova et al., 2022; Wooten et al., 2021). The MuSyC model estimates 12 parameters, five of which indicate interaction effects. In particular, parameter β indicates synergistic efficacy (how much the effect changes at large doses), parameters $\alpha 12$ and $\alpha 21$ indicate the change in the effective dose, and parameters $\gamma 12$ and $\gamma 21$ indicate the change in the Hill slope. There is no interaction according to the MuSyC model if $\beta=0$ and $\alpha 12 = \alpha 21 = \gamma 12 = \gamma 21=1$.

Transcriptomic data analysis

Before and after removing the adapter sequences of the reads, *Fastqc v0.11.9* reports were generated per fastaq file using the software *GNU parallel* (Tange, 2011) and combined in a single report using *MultiQC v1.10.1* (Ewels et al., 2016). The trimming of adapter sequences was carried out by *trimgalore,* a wrapper around *cutadapt v0.6.7* (Martin, 2011). The *MultiQC*-reports were used to ensure that all reads had similar qualities: e.g.; QC-content, sequence length, duplications, and that trimming of adapter sequences affected all files similarly. Reads were mapped to *F. candida* Ensembl Metazoa transcriptome v49 (Cunningham et al., 2019) using *Salmon v1.4.0* (Patro et al., 2017). Quantified reads were read into R using the R-package *tximport v1.16.1*, and the unnormalized counts were compiled into a data frame by R-package *DESeq2 v1.28.1* (Love et al., 2014; Soneson et al., 2016).

Comparing General Linear Models and Gaussian Process models fit

For a fair comparison between the Generalized Linear Model (GLM) approach and Gaussian Process (GP) model, the transcriptomic data from exposure 1, imidacloprid and clothianidin, and 2, imidacloprid and cyproconazole, were analyzed separately. This resulted in four sets of differentially expressed genes (DEGs), one set per exposure per method. Both General Linear Models (GLMs), by *R*(-package) *DESeq2 v1.28.1*, and Gaussian Process (GP) models, by *Python*(-library) *GPflow v2.0.0*, considered the influence of exposure to imidacloprid, clothianidin, and their interaction effect compared to a model that contained white noise. For DEGs under cyproconazole exposure, two models were compared, either including the effects of imidacloprid, cyproconazole, and their interaction effects with a model that only considered the influence of imidacloprid. Model comparison was by loglikelihood-ratio tests, as implemented by *R-DESeq2* or *Python-Scipy v1.4.1.* The DEG sets of both methods were ranked on their p-value. The DEGs of exposures 1 and 2 were compared between the methods by correlating their p-values step-wise per 10 % using Spearman's correlation in *Python-Scipy*, starting at DEGs with low p-values.

The kernel fit allowing a nonlinear and nonstationary fit of the GP models was compared to a linear kernel. The elected kernels were Matern32 and Linear implemented in *GPflow*. For a discussion on the structure of the additive GP

models see Section 3.1. GP model fit was visualized for on the scaled raw reads of genes with gene identifier Fcan01_00630 by *Python-matplotlip v.3.1.2*.

A GP model was fitted using *Python-GPflow* with kernel Matern32, first on the normalized reads of gene Fcan01_00630 from exposures 1 and 2 separately and, then, jointly. The GP model equation was MX, see Table 3.1. The GP model fit was visualized using *Python-matplotlip*.

Gaussian additive models for differential gene expression

We modelled the responses y_1 and y_2 -- gene expression in experiments 1 and 2, respectively - through a Gaussian process additive model (de Matthews et al., 2017; Duvenaud, 2014). Both experiments contained imidacloprid (x_0), but the second pesticide in the mixtures varied. In the context of the experimental section, x_0 represents a concentration of imidacloprid, x_1 a concentration of clothianidin, and x_3 a concentration of cyproconazole. In principle, this approach can easily be used for an arbitrary number of toxicants, e.g., pesticides, in a mixture and for an arbitrary number of exposures. The nonlinear dependence between responses y_1 and y_2 and the concentration of chemical compounds can be modeled through a Gaussian process (GP) regression:

$$y_1 = f_0(x_0) + \varepsilon \qquad y_2 = f_0(x_0) + \varepsilon \qquad \text{(Eq 3.1)}$$

where $f_0(x_0) \sim GP(0, K(x_0,x_0'))$ is a Gaussian process with zero mean and covariance matrix $K(x_0,x_0')$ defined by a kernel function $k^0_{\theta 0}(x_0,x_0')$, ε is an ii^d Gaussian noise with zero mean and variance σ_ε. Since gene expression data can have rapid changes when exposed to chemical compounds we choose $k^0_{\theta 0}(x_0,x_0')$ to be Matern32 kernel (de Matthews et al., 2017). Further, in experiment 1 the mixture contained a chemical compound denoted by x_1 and in experiment 2 a chemical compound denoted by x_2. To model the dependence of responses y1 and y_2 on x_0 and x_1 and x_0 and x_2, respectively we constructed the following models

$$y_1 = f_0(x_0) + f_1(x_1) + \varepsilon \qquad y_2 = f_0(x_0) + f_2(x_2) + \varepsilon \qquad \text{(Eq 3.2)}$$

where $f_1(x_1) \sim GP(0, K(x_1,x_1'))$ and $f_2(x_2) \sim GP(0, K(x_2,x_2'))$ are Gaussian processes with zero mean and covariance matrices defined by kernel functions $k^1_{\theta 1}(x_1,x_1')$ and $k^2_{\theta 2}(x_2,x_2')$.

Finally, to model possible interactions between chemical compounds in these experiments we modelled the responses y_1 and y_2 as

$$y_1 = f_0(x_0) + f_1(x_1) + f_{01}(x_0,x_1) + \varepsilon \qquad y_2 = f_0(x_0) + f_2(x_2) + f_{02}(x_0,x_2) + \varepsilon \qquad \text{(Eq 3.3)}$$

where $f_{01}(x_0, x_1) \sim GP(0, K(x_0, x_0', x_1, x_1'))$ and $f_{02}(x_0, x_2) \sim GP(0, K(x_0, x_0', x_2, x_2'))$ are Gaussian processes with zero means and covariance matrices defined by kernel functions $k^{01}{}_{\theta 1}(x_0, x_0', x_1, x_1')$ and $k^{02}{}_{\theta 2}(x_2, x_2', x_2, x_2')$.

Further, we analyzed these two experiments jointly. This is in particular due to both of them containing the same compound x_0 – imidacloprid. We assumed that due to biological variation the measurement noise $f_0(x_0)$ should be the same in both experiments. Overall, there are 11 possible models, summarized in Table 3.1, which represent dependence of the response variables y_1 and y_2 on different concentrations of chemical compounds and reflecting different non-linear relations between gene expression and the concentration of the chemical compounds.

Table 3.1: the equations of the Gaussian Additive (GP) models used in Differential Gene Expression Analysis (DGEA). The models considered the influence of imidacloprid (f_0), clothianidin (f_1), cyproconazole (f_2), or their interaction ($f_{01,}$ f_{02}) on scaled gene expression in *Folsomia candida* exposed in LUFA 2.2 soil, and the noise in the data (ε). The covariance matrix defined by kernel functions is shown for data under exposure to imidacloprid (x_0), clothianidin (x_1) or cyproconazole (x_2). The gene expression data was obtained from two exposures of imidacloprid with clothianidin (y_1; Experiment 1) or cyproconazole (y_2; Experiment 2). The models were fitted to these data jointly.

Model	Experiment 1	Experiment 2
M_1	$y_1 = f_0(x_0) + e$	$y_2 = f_0(x_0) + e$
M_2	$y_1 = f_0(x_0) + e$	$y_2 = f_0(x_0) + f_2(x_2) + e$
M_3	$y_1 = f_0(x_0) + f_1(x_1) + e$	$y_2 = f_0(x_0) + e$
M_4	$y_1 = f_0(x_0) + f_1(x_1) + e$	$y_2 = f_0(x_0) + f_2(x_2) + e$
M_5	$y_1 = f_0(x_0) + f_1(x_1) + f_{01}(x_0,x_1) + e$	$y_2 = f_0(x_0) + e$
M_6	$y_1 = f_0(x_0) + f_{01}(x_0,x_1) + e$	$y_2 = f_0(x_0) + e$
M_7	$y_1 = f_0(x_0) + e$	$y_2 = f_0(x_0) + f_{02}(x_0,x_2) + e$
M_8	$y_1 = f_0(x_0) + e$	$y_2 = f_0(x_0) + f_2(x_2) + f_{02}(x_0,x_2) + e$
M_9	$y_1 = f_0(x_0) + f_1(x_1) + f_{01}(x_0,x_1) + e$	$y_2 = f_0(x_0) + f_2(x_2) + f_{02}(x_0,x_2) + e$
M_{10}	$y_1 = f_0(x_0) + f_1(x_1) + f_{01}(x_0,x_1) + e$	$y_2 = f_0(x_0) + f_2(x_2) + e$
M_{11}	$y_1 = f_0(x_0) + f_1(x_1) + e$	$y_2 = f_0(x_0) + f_2(x_2) + f_{02}(x_0,x_2) + e$

Models from Table 3.1 were built and fitted jointly for experiments 1 and 2 using *python-GPflow* (de Matthews et al., 2017). Once the models were optimized, we performed likelihood-ratio tests to identify the best fitting model. As a result, genes responsive to a single chemical or mixtures of the chemical compounds (in an additive or interactive sense) were identified.

Differential gene expression analysis and Gene Set Enrichment Assays

Obtained gene expression data for all pesticide exposures was analyzed simultaneously with a custom Gaussian process (GP) additive model. The model was constructed in such a way that both experiments were analyzed simultaneously. Different additive components (individual pesticides and/or their interaction) were included in the model sequentially, and the models were compared with log-likelihood-ratio-tests, identifying genes responsive to individual pesticides or their interaction. More details on the GP additive model can be found in the Supplementary material. Results were obtained at 10% significance level.

Two gene set enrichment analyses (GSEA) were carried out for all differentially expressed gene (DEG) lists, either those genes affected by (1) imidacloprid and clothianidin or their interaction effect, or genes affected by (2) cyproconazole or cyproconazole and imidacloprid interaction effects. The GSEA was carried out with the R-package *goseq v1.40.0*. Gene Ontology (GO) terms were obtained through the R-package *biomart v2.44.4.* and Kyoto Encyclopedia for Genes and Genomes (KEGG) pathway annotation was obtained as previously described in Bakker et al. (*in preparation*). The bias correction of *goseq* was set to the transcript length (Coding DNA Sequence – CDS - length). A GSE term was deemed significant when the over-representation p-value was lower than 10 % and more than one gene from the DEG list found in the GSE term. The latter criteria were applied to prevent small GSE terms from becoming significantly enriched.

After GSEA, the over representation of each GSE term in the interaction DEGs was determined. To this end, the proportion of genes under the interaction per GSE term was compared by a Fisher exact test in base *R v4.0.0*. The p-values were -log10 transformed and a 0.1 p-value was used as a cut-off to indicate enrichment. GSE terms without no gene members under the pesticide interaction were omitted from the analysis.

Gene expression survey for biomarker validation on spiked soil.

For the gene-expression survey on spiked soil, the RNA was isolated using an RNA-isolation kit (Promega), following the instructions of the manufacturer. RNA integrity and quantity were determined by 1 % agarose gel-electrophoresis and nanodrop (Thermo Fisher Scientific). Roughly 500 ng of RNA was transcribed into cDNA using MML-V reverse transcriptase kit (Promega). Per 7 samples, one sample had the reverse transcriptase omitted to generate no-template controls. All samples were measured in a Cyber-Green reaction mix on a CFX Connect Real Time PCR Detection System (BIO-RAD, USA) and in the presence of no-template controls and samples containing only the reaction mix (blanks). The primer selection was based on this work and earlier findings investigating the transcriptomic response of *F. candida* to imidacloprid exposure (Bakker et al., *under review*, 2022). The primer sets for neonicotinoid exposure were: *nicotinic Acetylcholine Receptor subunit alpha1* (*nAchR*), the target receptor of neonicotinoids; *Sodium-coupled MonoCarboxylate Transporter 1* (*SMCT*), involved in the transport of nicotine like and other monocarboxylate compounds over the cell membrane; *Glutamate-gated Chloride channel* (*GluCl*); *Glutamate Receptor Ionotropic Delta-1* (*GRID1*), both involved in the cholinergic synapse neuro-transmission mediated by glutamate; *ARRestin Domain-containing protein 3* (*ARRD*), involved with the transport and activation of many transmembrane receptors. The primer sets for cyproconazole exposure were: *CYtochrome P450 3A56* (*CYP*), a phase-I biotransformation enzyme; *UDP-Glucuronosyltransferase 2B9* (*UDPG*), a phase-II biotransformation enzymes, *ABC-transporter 1* (*ABC*), a phase III biotransformation enzyme, and *sphingomyelin phosphodiesterase* (*SMPD*), sphingomyelin are involved in stress signaling. The reference genes, also known as housekeeping genes, were *tyrosine 3-monooxygenase* (*YWHAZ*) and *Eukaryotic Transcription Initiation Factor 1A* (*ETIF*). The primer sets *nAchR*, *SMCT*, *GluCl*, *YWHAZ* and *ETIF* were previously designed in our lab (Bakker et al., 2022; M. E. de Boer et al., 2009; T. E. de Boer et al., 2010). All other primers were designed, as part of this work, using the NCBI Primer BLAST tool (Ye et al., 2012). See Table 3.2 for a full description of the primers.

The expression values were obtained from the CFX Connect Real Time PCR Detection System accompanying software (BIO-RAD, USA). These expression values were log2-transformed to generate expression values for adherence to homogeneity. For each primer set, a generalized additive model (GAM) was fitted over the log2-transformed expression values using the R-package *mgcv v1.8.40*.

Two models were compared using likelihood-ratio tests considering a model including neonicotinoid without cyproconazole and a model including both, as previously described in (Bakker et al., 2022, *under review*)

Two models were fitted to determine biomarker reliability in indicating toxic exposure of either imidacloprid and cyproconazole even under mutual exposure.

$$E = g^{-1}(\beta_0 + \sum_{j=1}^{k_1} \beta_1 s_j(X_j)) \quad \text{(Eq. 3.4)}$$

$$E = g^{-1}(\beta_0 + \sum_{j=1}^{k_1} \beta_j s_j(x_j) + \sum_{p=1}^{k_2} \beta_p s_p(X_p)) \quad \text{(Eq. 3.5)}$$

in which E is the expected value of the log2-normalised expression values, g^{-1} the inverse linkage function, 0 the intercept, j and p the coefficients for neonicotinoid (j) and cyproconazole exposure (p), s_j and s_p smooth terms for neonicotinoid (j) and cyproconazole exposure (p) with k the basis size, respectively.

Basis size (k_x) for the neonicotinoid smooth term (k_1) was set to four and for the cyproconazole smooth term (k_2) it was set to three, i.e. the maximum size for this experimental design. Gaussian error distribution of the residuals was assumed, thin plate regression splines and restricted maximum likelihood (REML) were used to fit the models. Models were compared using an F-test of their fits and the alternative model was accepted when $p \leq 0.1$. Adherence of homogeneity of residuals was visually checked by histogram frequency plot and quantile-quantile plots.

Results and discussion

Binary mixture toxicity on springtail reproduction

Reliable gene expression biomarkers should be able to indicate the stress intensity and pesticide type, even when an organism is exposed to a mixture or chemicals with interacting effects on toxicity to the phenotype. Non-additive toxicity, i.e., interaction effects, of pesticide mixtures on the phenotype stems from molecular interaction effects and, thus, gene expression. Therefore, we here tested the effects of two binary pesticide mixtures on the reproduction of *F. candida*: (1) the neonicotinoid pesticides imidacloprid and clothianidin, and (2) imidacloprid and the fungicide cyproconazole. We analyzed the phenotypic data with recently developed Hand GP models (Shapovalova et al., 2022) to assess mixture interaction effects, such as synergism or antagonism, on springtail reproduction.

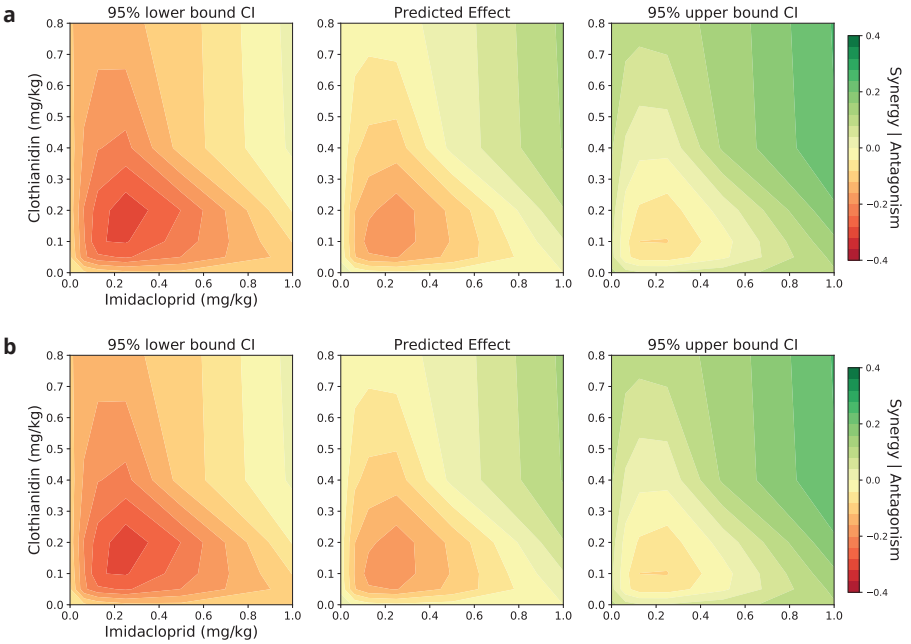

Figure 3.2: The Hand Gaussian Process (GP) was used to model toxicity interaction effects of imidacloprid in combination with either (a) clothianidin or (b) cyproconazole on springtail reproduction. The middle panels show the additive (yellow), synergistic (green) or antagonistic (red) effects of the pesticide mixtures on the reproduction of *Folsomia candida*. The intensities of the pesticide toxicity interaction effects are indicated by the hue of the colors with darker colors indicating stronger interaction effects. The lower bound and upper bound 95 % Confidence Interval (CI) of the Hand GP interaction effect estimates are shown in the panels on the right and left in both a and b rows. Pesticide concentrations are in mg kg^{-1} dry soil.

These analyses showed concentration-dependent additive and interaction effects of the binary pesticide mixtures on springtail reproduction. The neonicotinoids imidacloprid and clothianidin showed antagonistic effects at low to medium concentrations and synergistic effects at high concentrations of both compounds, as indicated by red and green shaded areas in Figure 3.2a, respectively. The mixture toxicity of imidacloprid and cyproconazole was antagonistic at low- to medium-concentrations of cyproconazole, whereas no synergistic interaction was observed (Figure 3.2b). At high concentrations of cyproconazole, i.e., above 400 mg kg^{-1} dry soil, imidacloprid and cyproconazole toxicity was additive, as indicated by a yellow shaded area in Figure 3.2b. Under all concentrations of imidacloprid, toxicity to springtail reproduction was antagonistic between imidacloprid and cyproconazole (red shaded areas in Figure 3.2b). A high degree of uncertainty

regarding the combined effects of both pesticide mixtures was observed at high concentrations, as illustrated by the wide confidence intervals in Figures 3.1a and b. We, therefore, validated the hand GP model results by comparison with the results of the conventional MuSyc model (Wooten et al., 2021), which gave comparative results (see Table S3.1).

Interestingly, both binary pesticide mixtures induced antagonistic effects at low to medium concentrations, suggesting that both pesticide mixtures had differential mechanisms of toxic action. For the neonicotinoids, we expected additive effects because imidacloprid and clothianidin have the same mechanism of action (overstimulating the nicotinic acetylcholine receptors) and have comparable toxicity to *F. candida* reproduction (de Lima e Silva et al., 2020). Moreover, imidacloprid and clothianidin are commonly reported to have additive toxic effects on the reproduction of other invertebrates (Taillebois & Thany, 2022). Our results highlight that even at low concentrations, interaction effects between neonicotinoids can occur and, therefore, filtering for genes affected by their interaction effects is a crucial step to develop biomarkers that can reliably indicate the broader neonicotinoid family.

Neonicotinoids can synergize with other pollutants by inhibiting cytochrome P450 enzymes (CYPs) in *F. candida* (Bakker et al., 2022). These enzymes are the primary route of pesticide detoxification in invertebrates (Hawkins et al., 2019; van Straalen & Roelofs, 2011). In particular, azole fungicides, such as cyproconazole, tend to synergize with neonicotinoids by probable inhibition of CYP enzymes in various bee species (Feyereisen, 2018; Glavan & Bozic, 2013; Raimets et al., 2017; Sgolastra et al., 2017). Here, however, we observed antagonistic, and not synergistic, effects for the mixture of imidacloprid and cyproconazole. There are two possible explanations. First, other neonicotinoids than imidacloprid are more prone to interaction effects by CYP inhibitions due to faster detoxification and, hence, CYP inhibition synergized with these neonicotinoids more than with imidacloprid (Beadle et al., 2019; Manjon et al., 2018), or the formation of more toxic metabolites of imidacloprid by CYP enzymes decreases, not increases, when CYP enzymes are inhibited (Suchail et al., 2004). Even though these results did not fully match our expectations, it is clear that imidacloprid and cyproconazole interact with each other, and analyzing the transcriptomic response to mixtures of these pesticides, therefore, also allows us to filter out genes that are involved in

the interaction effect. At the same time, analyzing contrasting types of pesticides allows us to distinguish between genes indicative of specific pesticides or those playing a role in a nonspecific stress response.

Performance of Gaussian Process modelling approaches in differential gene expression analysis

Conventional differential gene expression analysis (DGEA) methods are ill-suited in their application to transcriptomic data obtained under mixture exposure as they rely on parametric models. Here, we focus on two limitations of parametric models when applied to this type of transcriptomic data. First, parametric models are deficient in analyzing complex nonlinear concentration-response relationships. Second, parametric models have predefined concentration-response relationships. When the shape of the concentration-response relationship is defined in one dataset, this fit cannot be applied to another dataset. Results obtained from two experimentally distinct datasets cannot be analyzed in conjunction without batch-effect correction. We compared the performance of General Linear Models (GLMs) as implemented by conventional DGEA software, the popular R-package DESeq2, with our custom-made Gaussian Process (GP) modelling approach. These approaches implement parametric and non-parametric models, respectively.

To allow a fair comparison, we treated the transcriptomic data from both mixture exposures separately and compared models with the same consideration of the influence of the pesticides on gene expression. First, we determined genes affected by imidacloprid and clothianidin, by comparing models considering the influence of imidacloprid, clothianidin, and their interaction effect on gene expression and a model only consisting of noise estimation. To identify genes affected by cyproconazole, we compared a model considering imidacloprid, cyproconazole, and their interaction effect, with a model that only considered the influence of imidacloprid on gene expression. The model comparison yielded two sets of differentially expressed genes (DEGs). DEGs that are affected by neonicotinoids or their interaction effect, and DEGs that are affected by cyproconazole. Henceforth, we will refer to these DEG sets as the results of experiments 1 and 2. Figure 3.3 suggests that especially for the top 10-20% of differentially expressed genes the p-value results obtained with the simplified GP approach and DESeq2 are significantly correlated. Thus, overall the two approaches provided comparable results.

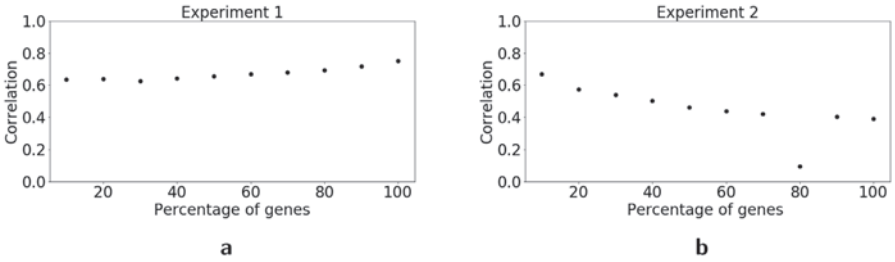

Figure 3.3: Spearman's correlation between gene rankings on the basis of parameter-free or parametrized model comparisons for differentially expressed genes in the springtail *Folsomia candida*. The parameter-free models were implemented by our custom-made statistical framework using Gaussian Process (GP) and parametrized Generalized Linear Models (GLMs) as implemented in the DESeq2 R-package. Data was obtained from springtails exposed to imidacloprid in mixtures with either clothianidin (a) or cyproconazole (b). Both GP and GLM model comparisons ranked genes based on the effects of imidacloprid, clothianidin and their interaction effect (a) or of imidacloprid, cyproconazole and their interaction effect (b) on gene expression. This resulted in two sets of differentially expressed gene (DEGs), one for each experiment. Correlations between the gene ranking of the models was determined by sliding-window, correlating the ranks of DEGs by incorporating a larger percentage of DEGs at each step. Incorporation started at highly ranked genes and continued by incorporating lower ranked genes.

Further, we illustrate the importance of nonlinear and nonstationary assumptions in differential gene expression analysis. For that, we provide an illustrative example of a GP model fit under two assumptions: 1) gene expression can be nonlinear and nonstationary, where non-stationarity implies that gene expression can have rapid changes when exposed to a certain effect concentration, 2) gene expression can be described by a linear function. For the GP model with nonlinear and nonstationary assumptions, a Matern32 kernel was assumed, while for a GP model which assumes a linear relationship between concentration and gene expression, a linear and stationary kernel was assumed. Figure 3.4 provides an illustrative example for a *Bacillopeptidase F* gene (Fcan01_00630) in experiments 1 and 2 with the nonlinear and linear GP models. Figure 3.4a shows that a GP model with a nonlinear assumption has a nonlinear pattern, and gene expression level increased at higher concentrations of imidacloprid. This is also confirmed by a p-value of 0.038 when the GP model with neonicotinoid terms and GP noise models are compared. Figure 3.4b illustrates a fit with a linear kernel which allows only for a linear relationship between gene expression and concentration. While we observed an increasing trend in the gene expression, it was not statistically significant compared to the noise model. Thus, a GP model with Matern32 kernel has the potential to capture relationships that would be ignored with a linear model.

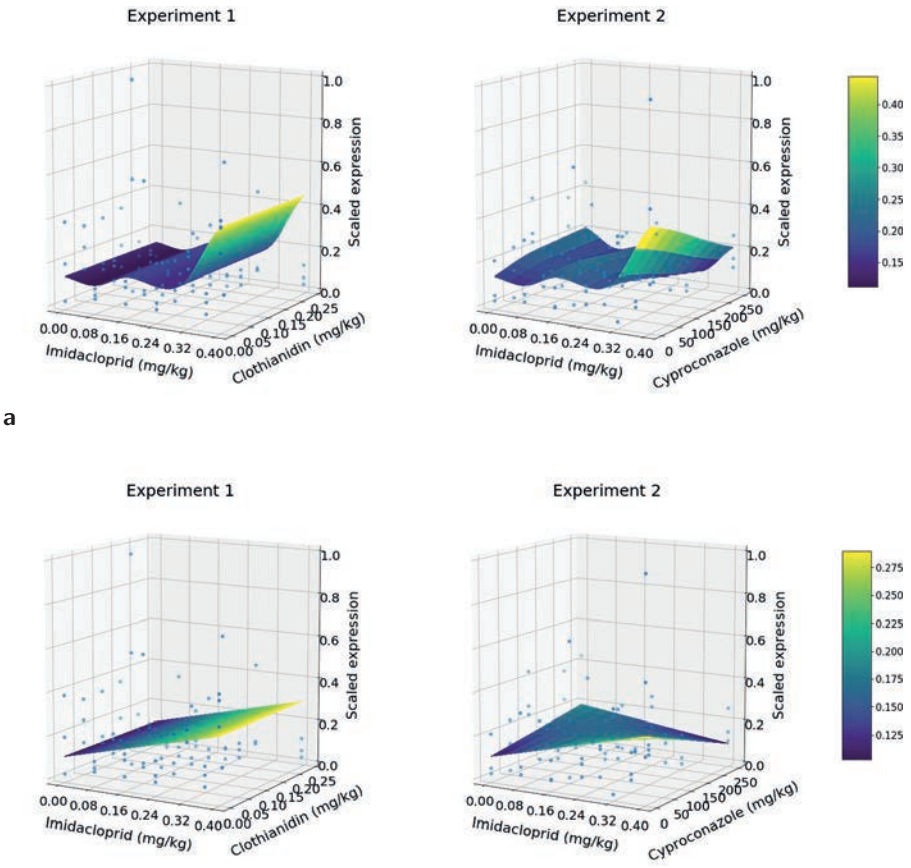

Figure 3.4: Gaussian process (GP) model fit assuming two kernels with differential assumptions, modelling the gene expression of *Bacillopeptidase F* gene (Fcan01_00630) in the springtail *Folsomia candida* in experiments 1 (left panels) or 2 (right panels). The experiments involved exposure of the springtails to imidacloprid in mixtures with either clothianidin (experiment 1) or cyproconazole (experiment 2). In panels **a**, the GP model assumed a Matern32 kernel that allows for nonlinearity and nonstationary, i.e., rapid changes in the data, and fit of the concentration-response surface. In panels **b**, the GP model assumed a linear kernel that did not permit nonlinear and nonstationary fits of the concentration-response relationship. A GP model assuming a linear kernel models acts like parametric Generalized Linear Models conventionally used in methods for Differential Gene Expression Analysis. Gene expression was scaled to lie between 0 and 1 in both experiments jointly. The blue dots on the panels depict scaled gene expression values. The color of the fit-surfaces changes according to the modelled scaled gene expression, ranging from low (dark blue) to medium (yellow) scaled gene expression values.

Finally, we provide an illustrative example which compares independent and joint analyses of the two exposures on the same gene *Bacillopeptidase F*

(Fcan01_00630). For this comparison, we fitted two Gaussian processes models to single imidacloprid exposure data with Matern32 kernel and a joint model with the same kernel assumption. Figures 3.5a and b illustrate independent model fits, and Figure 3.5c is a joint analysis of the data from both exposures. For experiment 1, the gene was identified as differentially expressed, with a p-value of 0.00018 compared to the noise model, but it was not in experiment 2, with a p-value 0.85 compared to the noise model. When the genes from both experiments were combined, the gene was identified as differentially expressed with a p-value of 0.015 compared to the noise model. This demonstrates the importance of the joint analysis when one toxic compound is shared in two (or more) experiments. Overall, if experiments 1 and 2 were analyzed independently, at a 5% significance level, 4801 and 1318 genes were identified as differentially expressed in experiments 1 and 2, respectively, which resulted in 3483 genes with inconsistent results. At 15%, this number increased to 5151. Thus, inconsistency is relatively high when the experiments are treated independently.

Differential Gene Expression Analysis and Gene Set Enrichment

Transcriptomic data obtained under mixture exposure had nonlinear concentration-response relationships, a high variability of gene expression patterns, and displayed genetic interaction effects. We generated transcriptomic data of the springtail *F. candida* after exposure to the aforementioned binary pesticide mixtures for a wide range of stress intensities with a fine-scale resolution. We extended a GP model statistical framework to allow its application to transcriptomic data obtained from two mixture experiments and analyzed this data jointly. With this approach, we were able to distinguish differentially expressed genes (DEGs) with responses to either neonicotinoids or cyproconazole from those with interaction effects. From these lists of DEGs, we selected candidate biomarkers based on their molecular functions with known close association to the mechanisms of toxic action of these pesticides. With this step, we filtered out DEGs that were part of the presumed non-specific or universal stress response.

We compared 11 models with the log-likelihood ratio test, see Table 3.1. We selected neonicotinoid DEGs by comparing the models containing: 1) only dependence on imidacloprid (i.e., model 1 or M1), 2) additive components of imidacloprid and clothianidin (M3), 3) additive components and interaction terms of imidacloprid

and clothianidin (M5), and 4) imidacloprid and the interaction term for imidacloprid and clothianidin (M6). Similarly, for DEGs affected by cyproconazole, the models contained: 1) only dependence on imidacloprid (M1), 2) additive components of imidacloprid and cyproconazole (M2), 3) additive components and the interaction term of imidacloprid and cyproconazole (M8), and 4) imidacloprid and the interaction term for imidacloprid and cyproconazole (M7). We excluded genes affected by the interaction effects of the neonicotinoids or cyproconazole for biomarker discovery, including 142 and 122 DEGs, respectively. DEGs affected by the additive effects of neonicotinoid exposure (n=2049) and by cyproconazole (n=1058) were all considered candidate biomarkers.

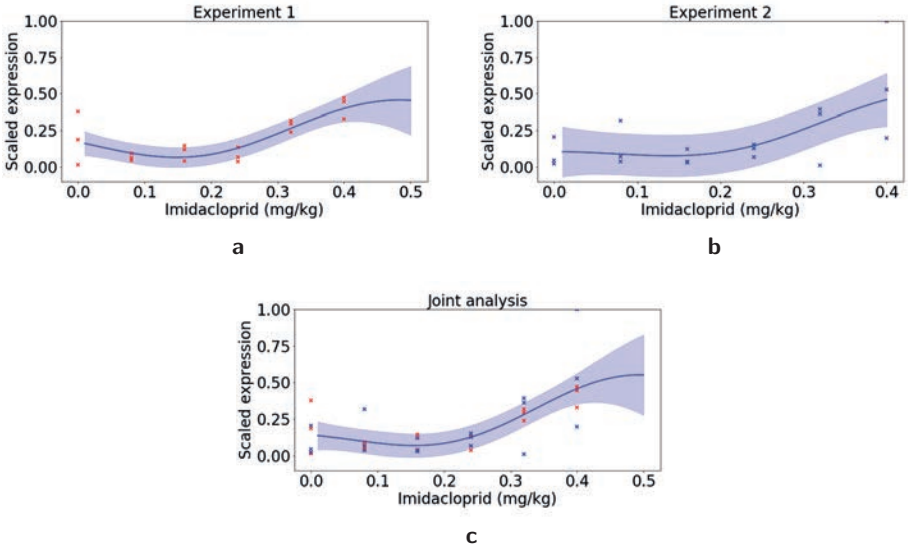

Figure 3.5: Visualization comparing Gaussian process (GP) fits that model the effects of imidacloprid on scaled gene expression of the springtail *Folsomia candida* in two experiments separately (a and b) and jointly (c). The exposures were in a grid-design and consisted of imidacloprid with either clothianidin (experiment 1) or cyproconazole (experiment 2). Gene expression was scaled from 0 to 1 for both experiments jointly. Then, models were fitted to the gene expression data of experiments 1 and 2 separately (**a** and **b**) or jointly (**c**). The panels show the fit of the GP models only for the imidacloprid exposure data in the absence of other pesticides or control condition. The GP model fits are solid blue lines and its confidence intervals are blue shaded areas around the model fit. The scaled gene expression values are depicted by red or blue crosses for data derived from experiments 1 or 2, respectively.

Gene Set Enrichment (GSE) Analysis of the DEGs for neonicotinoid exposure indicated significant enrichment of 37 Gene Ontology (GO) and Kyoto

Encyclopedia of Genes and Genomes (KEGG) categories, hereafter referred to as GSE terms (Figure S3.1A). Among the enriched GSE terms were those associated with neurotransmission, for example, GO:0007267, GO:0055085, GO:0022857, GO:0005576, and GO:0005615. We used these GSE terms to select putative biomarkers because neurotransmission-associated genes have previously been identified as reliable indicators of neonicotinoid exposure in *F. candida* (Bakker et al., *under review*, 2022). For neonicotinoids, we selected three putative biomarkers; i.e., *nAchR*, *SMCT*, and *ARRD,* based on previous findings and as their associated GSE terms related to neurotransmission (Anand et al., 2018; Bakker et al., *under review*, 2022), see Table 3.2.

Among the DEGs indicative for the response to cyproconazole, we observed significant enrichment of 36 GSE terms (Figure S3.1B). The majority of these GSE terms were associated with biotransformation, the direct detoxification pathway for organic compounds. Another noteworthy GSE term was the sphingolipid signaling pathway (k004071) and metabolism (ko00600) relating to a stress signaling pathway, which we did not observe in the GSE analysis of DEGs for neonicotinoid exposure. We selected DEGs categorized within the GSE terms linked to CYP metabolism (GO:0055114, G0:0016614, GO:0016705, GO:0016788, ko00980, and ko00982), ABC transporters (ko02010), and sphingolipid signaling (k004071 and ko00600) for biomarker selection. For cyproconazole exposure, we selected three candidate biomarkers on the bases of these GSE terms; i.e, *ABC*, *CYP*, and *SMPD*, see Table 3.2.

Validation of candidate biomarkers on spiked soil

We assessed the reliability of six putative gene-expression biomarkers for either neonicotinoids or cyproconazole, see Table 3.1. To this end, we exposed the springtail *F. candida* to imidacloprid and cyproconazole in spiked LUFA2.2 soil to determine the reliability of the biomarkers in indicating either pesticide in combination or absence of the other pesticide. The influence of single and mutual exposure to imidacloprid and cyproconazole on biomarker expression was determined by Generalized Additive Models (GAMs), as previously described (Bakker et al., *under review*, 2022). Loglikelihood-ratio tests were used to determine the influence of imidacloprid or cyproconazole on biomarker expression, referred to as GAM smooth terms hereafter.

The expression of all neonicotinoid biomarkers, *nAchR*, *SMCT*, and *ARRD*, increased with the concentration of imidacloprid compared to the control conditions as indicated by the fit of the GAMs, see Figure 3.6. The expression of the three-neonicotinoid biomarker was significantly influenced by imidacloprid exposure as indicated by the imidacloprid GAM term p-values ($p<0.01$), see Figure 3.6A. Importantly, cyproconazole exposure did not influence the expression of either of the three neonicotinoid biomarkers as indicated by the overlapping confidence intervals of the GAM fits and non-significant p-value of the cyproconazole GAM term ($p>0.1$), see Figure 3.6A. Therefore, all neonicotinoid biomarkers responded in a concentration-dependent manner to imidacloprid exposure and not to the mutual exposure with cyproconazole.

Two out of three cyproconazole candidate biomarkers, ABC and CYP, increased in expression in response to cyproconazole exposure, but not by imidacloprid exposure, as indicated by the flat fit of the GAMs, the p-values of the cyproconazole smooth terms ($p<0.05$), and their separated confidence intervals for each level of cyproconazole exposure, see Figure 3.6B. In particular, the highest concentration of cyproconazole increased biomarker gene expression compared to no cyproconazole exposure, as indicated by the GAM fits see Figure 3.6. The results indicate that these two biomarkers, both associated with biotransformation, i.e., *ABC* and *CYP*, signal cyproconazole exposure even in animals mutually exposed to imidacloprid. For the third cyproconazole candidate biomarker, *SMPD,* we did not observe changes in its expression in response to either pesticide, which contradicts the results from the transcriptome analysis. The GAM smooth terms of both imidacloprid or cyproconazole were non-significant for *SMPD* ($p>0.1$)*,* and the GAM fit remained flat (see Figure 3.6).

In summary, our results confirm that the candidate biomarkers *ARRD*, *nAchR*, *SMCT*, *CYP*, and *ABC*, responded only to their intended pesticide even under mutual exposure. These biomarkers also indicated the intensity of the exposure. These outcomes validate that application for GP models in DGEA and, subsequent, biomarker discovery. As we have chosen biomarkers on the basis of their GSE terms, this step proofed insightful in identifying robust biomarkers.

Table 3.1: Summary of the primer sets used in quantitative PCR to determine the effects on the gene expression of *Folsomia candida* of exposures in LUFA 2.2 soil spiked with the neonicotinoid imidacloprid or the azole fungicide cyproconazole. Given are the primer direction (F: forward or R: reverse), the primers' target gene id' according to Ensembl metazoa v50, the gene description, the abbreviated gene name, the primer oligo sequence and its cDNA amplification efficiency per cycle as a percentage.

gene id	description	name	direction	oligo sequence	efficiency (%)
Fcan01_06830	*tyrosine 3-monooxygenase*	*YWHAZ*	F	CCTACAAAAACGTCGTCGGTG	101.2
			R	TGTTGCTTTCGTTCGAACC	
Fcan01_13627	*eukaryotic transcription initiation factor 1A*	*ETIF*	F	TGATTCTGGAGATCTTCGCGAG	94.9
			R	ACAGTGCAAAGGATTTCCCGA	
Fcan01_01431	*nicotinic acetylcholine receptor subunit alpha 1*	*nAchR*	F	CGTGGACCAGGACAGAGAAA	85.6
			R	TTGCAGACCCCCATAGTCTG	
Fcan01_08638	*sodium-coupled monocarboxylate transporter*	*SMCT*	F	ATGGTTTGGGTCGTTTCGTG	90.6
			R	CGGTTGTCCGTATTCGCTTG	
Fcan01_13564	*Arrestin domain-containing protein 3*	*ARRD*	F	ACTACTTTGTCCACTTGCTCGT	82.6
			R	TTCGTTCCCAGAGTGATGGG	
Fcan01_20262	*Cytochrome P450 3A56*	*CYP*	F	CATTGACGCCTACAGCAAGG	87
			R	GTTGTCTCCCTTCATAAACTCCG	
Fcan01_17454	*Sphingomyelin phosphodiesterase*	*SMPD*	F	GATCGACATGTACGCGGAAAA	95.6
			R	TCTTTCGCCATCGCAATCTTC	
Fcan01_18435	*ABC-transporter 1*	*ABC*	F	AGGGAAGACGTGACGCTAAA	85.5
			R	GACGGTTTCGTACCCATTCG	

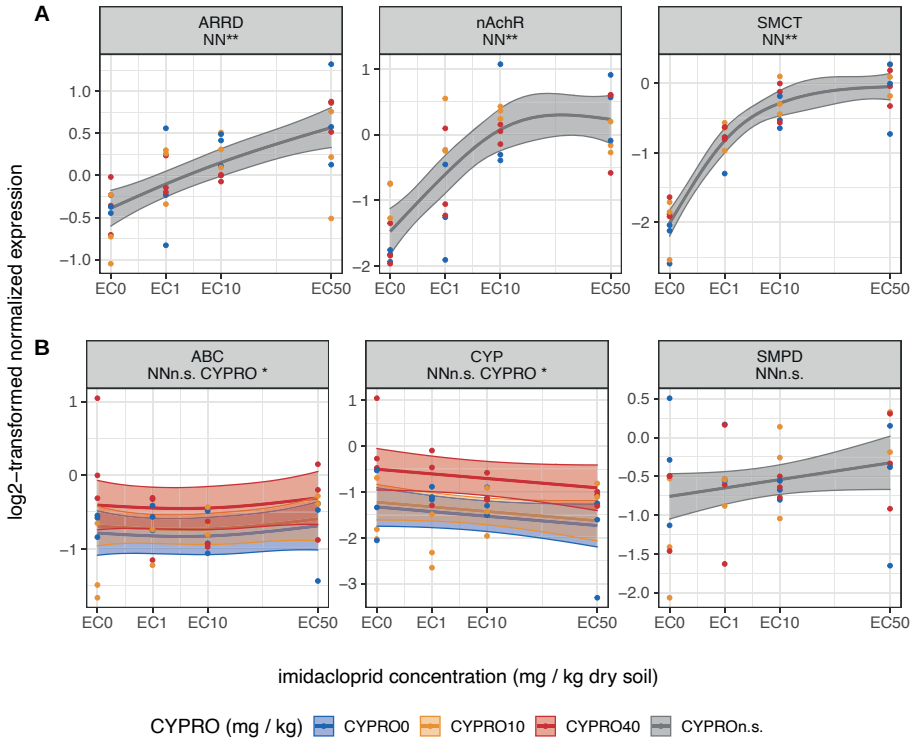

Figure 3.6: Expression patterns of candidate pesticide biomarkers for (A) neonicotinoid and (B) cyproconazole exposure in the springtail *Folsomia candida*. Springtails were exposed for 48h to a mixture of the two pesticides at a range of concentrations in spiked soils. The concentrations of imidacloprid applied were Effect Concentrations (ECs) roughly equal to 0, 1, 10 to 50% reduction in juvenile counts (x-axis). The cyproconazole ("CYPRO") concentrations were 0, 10, and 40 mg kg^{-1} dry soil. Each panel represents the normalized expression pattern of one gene: *arrestin domain containing protein 3* (*ARRD*), *nicotinic Acetylcholine Receptor subunit alpha1* (*nAchR*), *sodium-coupled monocarboxylate transporter 1* (*SMCT*), *ABC-transporter 1* (*ABC*), *cytochrome P450 3A56* (*CYP*) and *sphingomyelin phosphodiesterase* (*SMPD*). Below the names are the significance levels of the generalized additive models (GAMs), smooth terms of neonicotinoid (NN) and cyproconazole (CYPRO). Significance levels of the smooth terms are depicted by the following symbols: p>0.1 "N.S", p<= 0.1 ".", p<= 0.05 "*", p<=0.01 "**". GAM mean functions are shown in solid lines, the 95 % confidence intervals are shown as outlined transparent bands and dots depict the log2-transformed normalized expression values. Each concentration of CYPRO exposure is shown as a separate color, i.e. blue (0), orange (10) and red (40). Mean function and confidence interval outlined bands are shown in grey when the influence of CYPRO was not included in the GAM model fit, due to not being significant.

A roadmap for biomarker discovery in mixture exposure transcriptomic data

Most non-target invertebrates are exposed to complex mixtures of pesticides. Gene expression biomarkers can supplement current environmental risk assessment methods to monitor these pesticide mixtures. Identifying gene expression patterns characteristic for the class of pesticide even under genetic interaction effects with other pesticide is essential for biomarker discovery. However, current differential gene expression analysis (DGEA) methods used in biomarker discovery are ill-suited for mixture transcriptomic data due to their dependency on parametric models. Mixture exposure transcriptomic data suffer from three aspects; i.e., nonlinear concentration-response relationships, genetic interaction effects, and high data variability of the gene expression patterns. We demonstrated that GP models successfully identified differentially expressed genes (DEGs) in transcriptomic data containing all three aspects. By identifying the DEGs on the bases of their molecular functions, we identified reliable biomarkers for neonicotinoid and cyproconazole exposure. This work can be used as a roadmap for biomarker discovery and is not limited to pesticide research. The GP models can be used in DGEA in pharmacology or multiple stressors in any branch of biology.

Acknowledgements

The authors thank Janine Mariën, Riet Vooijs and Rudo Verweij for their assistance and guidance in the laboratory. Moreover, the authors wish to extend their gratitude to the users committee Dutch Research Council (NWO) domain Applied and Engineering Sciences (TTW) (Project number 15494)

Chapter 3: supplementary information

Table S3.1: indicates the results for the interaction effects analysis with the MuSyC model of experiments exposing *Folsomia candida* to imidacloprid and clothianidin (Experiment 1) or imidacloprid and cyproconazole (Experiment 2), both single and in mixtures. The model analyzed data for mixture interaction effects of the pesticides in springtail reproduction after 21 days exposure in LUFA 2.2 soil. The following parameter values indicate no interaction if β=0 and $\alpha 12 = \alpha 21 = \gamma 12 = \gamma 21 = 1$. In experiment 1, the model indicates synergy due to the change in Hill slope coefficient as $\gamma 21 > 1$; in experiment 2, the model indicates additivity, i.e., no interaction. Overall, the estimates in both models contain a lot of uncertainty about the predicted effect, which is expected as at low- and mid-range concentrations, the measurements had high variance.

	Experiment 1 imidacloprid and clothianidin				Experiment 2 imidacloprid and cyproconazole			
Change in	**Estimate**	**CI 95% lower**	**CI 95% upper**	**Effect**	**Estimate**	**CI 95% lower**	**CI 95% upper**	**Effect**
β synergistic efficacy	-0.21	-0.4	0.1	≈0	-1.40	-0.90	0.06	≈1
α_{12} effective dose	3.25	0.02	955878.77	≈1	0.50	0.0	54.2	≈1
α_{21} effective dose	3.42	0.04	80.27	≈1	0.24	0.0	1.1	≈1
γ_{12} Hill slope coefficient	0.14	0.0	8.63	≈1	0.96	0.95	1.03	≈1
γ_{21} Hill slope coefficient	16.4	9.04	40.99	**>1**	5.49	0.0	50.7	≈1

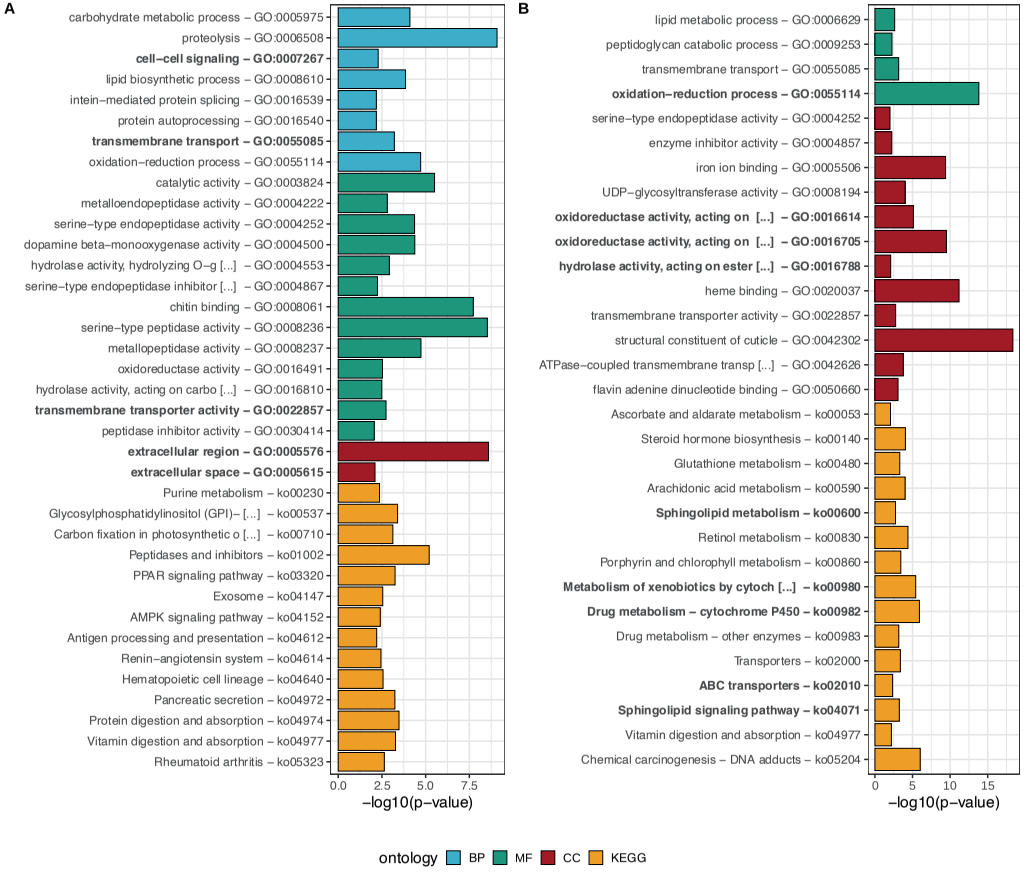

Figure S3.1: The Gene Set Enrichment Analysis (GSEA) results measuring the GSE terms in *Folsomia candida* affected by imidacloprid and clothianidin (A) or cyproconazole (B) exposures compared to all genes found in the transcriptomic data. The y-axis labels are the abbreviated descriptions of each GSE term followed by a dash (-) and the GSE term number. The bold font GSE terms served in the selection of candidate biomarkers. The bar color varies per ontology or database as Gene Ontology Biological Process (BP), Gene Ontology Molecular Functions (MF), Gene Ontology Cellular Compartment (CC), or Kyoto Encyclopedia for Genes and Genomes (KEGG), in blue, green, red and orange, respectively.

Chapter 4

Biomarker development for neonicotinoid exposure in soil under interaction with the synergist piperonyl butoxide in *Folsomia candida*

Ruben Bakker[1*], Astrid Ekelmans[1], Liyan Xie[1], Riet Vooijs[1], Dick Roelofs[1,2], Jacintha Ellers[1], Katja M. Hoedjes[1], Cornelis A.M. van Gestel[1]

[1] Amsterdam Institute for Life and Environment (A-LIFE), Faculty of Science,
Vrije Universiteit Amsterdam, De Boelelaan 1085, 1081 HV Amsterdam, The Netherlands
[2] Keygene N.V., Agro Business Park 90, Wageningen, 6708 PW, The Netherlands
* corresponding author
Corresponding e-mail: r.r.bakker@vu.nl

Published in: *Environmental Science and Pollution Research* (2022), 1-17
DOI: 10.1007/s11356-022-21362-z

Pesticide toxicity is typically assessed by exposing model organisms to individual compounds and measuring effects on survival and reproduction. These tests are time-consuming, labor-intensive and do not accurately capture the effect of pesticide mixtures. Moreover, it is unfeasible to screen the nearly infinite combinations of mixtures for synergistic effects on model organisms. Therefore, reliable molecular indicators of pesticide exposure have to be identified, i.e. biomarkers. These biomarkers can form the basis of rapid and economical screening procedures to assess the toxicity of pesticides even under synergistic interaction with other pollutants. In this study, we screened the expression patterns of eight genes for suitability as a biomarker for neonicotinoid exposure in the soil ecotoxicological model *Folsomia candida* (springtails). Springtails were exposed to the neonicotinoids imidacloprid and thiacloprid either alone or with various levels of piperonyl butoxide (PBO), which inhibits cytochrome P450 enzymes (CYPs): a common point of synergistic interaction between neonicotinoid and other pesticides. First, we confirmed PBO as a potency enhancer for neonicotinoid toxicity to springtail fecundity, and then used it as a tool to confirm biomarker robustness. We identified two genes that are reliably indicative for neonicotinoid exposure even under metabolic inhibition of CYPs by PBO, *nicotinic acetylcholine receptor subunit alpha 1* (*nAchR*) and *sodium-coupled monocarboxylate transporter* (*SMCT*). These results can form the basis for developing high-throughput screening procedures for neonicotinoid exposure in varying mixture compositions.

Key words: springtails; imidacloprid; thiacloprid; quantitative real-time PCR; piperonyl butoxide

Introduction

Neonicotinoids are the most commonly used insecticides globally of the past three decades (Borsuah et al., 2020), but are harmful to non-target organisms like pollinators (Goulson, 2013; Pisa et al., 2014) and soil invertebrates (de Lima e Silva et al., 2017, 2020, 2021). As a consequence, ecosystem services crucial for sustainable agriculture, such as nutrient cycling, pest control and pollination, are under threat by the use of neonicotinoid insecticides (EASAC, 2015; FAO, ITPS, GSBI, 2020; Gunstone et al., 2021).

Current environmental risk assessment (ERA) and policy regarding pesticides is based on phenotypic toxicity tests that measure effects on the survival and reproduction of model organisms after exposure to individual pesticides. Extrapolation of these findings to ecotoxicological effects in the field is difficult as most agricultural soils are polluted by pesticide mixtures (Pelosi et al., 2021; Silva et al., 2019), and the synergistic interactions between pesticides within mixtures is a major knowledge gap (Gunstone et al., 2021). Furthermore, the predicted effect concentrations derived from these phenotypic tests can only be used in ERA after measuring the exposure concentration of the pollutants in soil, a laborious and costly procedure. On the contrary, gene expression responses can be used to determine the type of pollution even under varying mixture composition (Fontanetti et al., 2011; Shi et al., 2017). Determining the effects of the near infinite number of possible soil pollution mixtures on the gene expression of model organisms is unfeasible. Therefore, reliable genetic responses, i.e. biomarkers, have to be identified that remain indicative for a group of soil pollutants even under synergistic interaction with other pollutants. Gene expression biomarkers, in turn, can be used in biomonitoring; a cost-effective tool to screen for samples that, in case of detecting a potential risk, may be subjected to subsequent chemical analysis to identify the chemical(s) of concern. In this way, gene-expression assays may provide ERA with more accurate metrics of adverse effects by pesticides than traditional toxicity tests.

The selection of candidate gene expression patterns requires an understanding of the molecular mediators behind pesticide toxicity in a relevant non-target model organism. Most studies on the molecular mechanisms that mediate neonicotinoid toxicity in invertebrates have been carried out in honey bees. However, the honey bee is not an ideal representative for non-target soil invertebrates because it does not live

in the soil, its genome is limited in its detoxification capacity (Claudianos et al., 2006), and it has an unusual life history due to its social lifestyle (Gradish et al., 2019). *Folsomia candida* is a more suitable representative for non-target soil invertebrates because (1) it belongs to the springtails (Collembola), which is one of the most prevalent non-target invertebrate groups (Rusek, 1998), and a key component of the soil food web by promoting nutrient cycling (FAO, ITPS, GSBI, 2020); (2) *F. candida* is well established as a soil ecotoxicological model species since the 1960s (van Gestel, 2012); (3) its genome has been sequenced and annotated facilitating the development of molecular tools for studying its genomic responses to pollution (Faddeeva-Vakhrusheva et al., 2017), and (4) *F. candida* is representative for the sensitivity to neonicotinoids of other springtail species (de Lima e Silva et al., 2021). Together, these aspects make *F. candida* an ideal candidate for the development of biomarker assays for the monitoring of pesticide exposure in soil.

For the successful applications of neonicotinoid biomonitoring, gene-expression patterns have to be identified that are indicative for the exposure to a variety of neonicotinoids and remain to do so even under synergistic interaction with other pollutants. Neonicotinoids are commonly subdivided in two groups, depending on the inclusion of either nitro- or cyano-moieties into their chemical structure (Buszewski et al., 2019). Although both groups share the same mode-of-action, the nitro-substituted neonicotinoids are more toxic than the cyano-substituted ones to the fecundity and survival of various springtail species (de Lima e Silva et al., 2017, 2020, 2021). In the honey bee, the differential toxicity of the two groups of neonicotinoids has been attributed to an increased detoxification rate of the cyano-substituted ones by CYP enzymes (Iwasa et al., 2004; Manjon et al., 2018). Moreover, CYP inhibition has also been proposed to trigger synergistic interactions between neonicotinoids and other pesticides such as triazole fungicides (Feyereisen, 2018; Glavan & Bozic, 2013; Raimets et al., 2017; Sgolastra et al., 2017). Finally, various studies on the genomic response of *F. candida* to various pollutants have identified CYP genes as biomarkers for a variety of chemicals (G. Chen et al., 2014; M. E. de Boer et al., 2009; Nota et al., 2009; Roelofs et al., 2012). Based on these findings, CYPs have emerged as promising biomarkers for the toxicity of neonicotinoid exposure. Yet, it remains to be confirmed if expression patterns of CYP genes provide a reliable indication for the toxicity of both cyano- and nitro-substituted neonicotinoids, as well as for synergistic interaction with other pesticides. This also needs to be confirmed still for other biomarkers identified for neonicotinoid

exposure in the honey bee (Christen et al., 2016; Fent et al., 2020; Manjon et al., 2018). Given the central role of CYPs in mediating differential effects of the two major classes of the neonicotinoid family and their role in mediating synergy, we propose inhibition of CYPs could serve as "stress-test" to assess biomarker robustness. For this we applied piperonyl butoxide (PBO), which is a CYP inhibitor that forms a metabolite-inhibitory complex with CYPs and thereby prevents the binding of other substrates (Hodgson & Levi, 1999). By choosing PBO over toxicants, we can ensure that observed effects on biomarker gene-expression are the result CYP inhibition, rather than, other synergistic interactions.

The integration of multiple biomarkers into a panel for biomonitoring and ERA is highly recommended, because the range of effects soil pollution has on organisms is diverse (Lionetto et al., 2019). The aim of this study was to assess the suitability of candidate genes to construct a panel of biomarkers for the assessment of soil polluted with neonicotinoids. For this we considered three criteria: (1) the panel should indicate exposure of both nitro- and cyano-substituted neonicotinoids, (2) the response of the panel should relate in a concentration-dependent manner with the adverse fitness effect of neonicotinoid exposure on *F. candida*, and (3) the expression patterns of biomarkers in the panel should be reliable under synergistic interaction caused by CYP inhibition by PBO. To represent the two major classes of neonicotinoids we selected imidacloprid and thiacloprid, as representatives of nitro- and cyano-substituted neonicotinoids, respectively. First, we determined the effect of PBO on the fecundity of springtails and its potency-enhancing effects when combined with thiacloprid and imidacloprid. Then, we screened the expression of eight candidate biomarker genes at various PBO and neonicotinoid concentrations using RT-qPCR. These were derived from previous studies on the genomic response of *F. candida* to various pollution types, which have identified gene expression patterns that may have potential to be applied as biomarkers (M. E. de Boer et al., 2009; Nota et al., 2009; Qiao et al., 2015; Roelofs et al., 2012).

Materials and methods

Test animals

Folsomia candida culture has been maintained by the A-LIFE section Ecology & Evolution of the Vrije Universiteit Amsterdam for > 20 years. The culture is kept in the dark at 16 ± 1 °C and 75 % relative air humidity (RH). The culture was reared

in 1000 ml polypropylene containers with approximately 2 cm deep substrate of moistened activated charcoal and Paris plaster, at a 1:8 ratio, and continuously fed *ad libitum* with instant baker's yeast (Algist Bruggeman N.V., Ghent, Belgium). To obtain age-synchronized individuals, batches of approximately 30 adults were sampled from the culture and placed in 125 ml translucent polypropylene containers filled with a 2 cm deep layer of the aforementioned substrate and covered with perforated lids to allow air flow. These were kept at 20 ± 1 °C, 75 % RH and a 16:8 light-to-dark regime for about 48 hours to allow egg laying. After this period, the adults were removed and the substrate frequently moistened with demineralized water up to the point of saturation until the eggs hatched, about 10 days after egg-laying. The age-synchronized juveniles were fed with baker's yeast and the substrate was moistened three times a week.

Chemicals and test soil

Thiacloprid and imidacloprid, both 98 % pure, were provided by Bayer CropScience, Monheim, Germany. Piperonyl butoxide (PBO; 90 % pure) was obtained from Sigma-Aldrich, the Netherlands. All tests were carried out in natural LUFA 2.2 soil, Lufa Speyer, Germany. Soil attributes as determined by the supplier were: total organic carbon content 2.1%, water-holding-capacity (WHC) 46.5% (w/w), and soil pH 5.5 (0.01 M $CaCl_2$).

To spike the soil with thiacloprid or imidacloprid, stock solutions in demineralized-water were thoroughly mixed in with dry soil to reach a moisture content of 22 % of its dry weight, corresponding with 50 % of its WHC. Thiacloprid was first dissolved in acetone amounting to approximately 3 % of the stock solution volume before adding ultra-pure water. Imidacloprid was directly dissolved in ultra-pure water. Before use, stock solutions of both test chemicals were left overnight and stirred at 300 rounds per minute, at room temperature and covered with aluminum foil.

For PBO treatments, 15 grams or 10 % of the dry soil per treatment was placed into 100 ml glass jars wrapped with aluminum foil. The soil was submerged in a PBO-acetone solution and stirred every half hour for two hours, after which it was left overnight in the fume hood to allow complete evaporation of the acetone. Then, the remaining soil for a treatment was added, mixed, moistened to 50 % of its WHC and again mixed thoroughly. In all tests, acetone controls were included as well as water controls that were not pretreated with acetone. All other treatments

had 10 % of their dry soil undergoing acetone pretreatment as described above.

Soils were prepared one day before the springtails were added. The concentration ranges used for single exposure to PBO were 0, 100, 200, 400, 600, 800 and 1000 mg kg^{-1} dry soil. For mutual exposure with neonicotinoids: PBO 0, 1 and 10 mg kg^{-1} dry soil was combined with thiacloprid at 0, 0.25, 0.5, 1, 2, 4, 8 and 16 mg kg^{-1} dry soil or imidacloprid at 0, 0.05, 0.1, 0.2, 0.4, 0.8, 1.6 mg kg^{-1} dry soil. For the gene expression assays, soil was spiked at 0, 10 and 100 mg PBO kg^{-1} dry soil (all concentrations << EC_1), and combined with either 0, 0.1, 0.2 and 0.4 mg imidacloprid kg^{-1} dry soil or 0, 0.5, 1 and 2 mg thiacloprid kg^{-1} dry soil. The neonicotinoid concentrations for the gene-expression assays were chosen to represent EC_1, EC_{10} and EC_{50} values for reproduction effects of imidacloprid and thiacloprid from previous studies and fall within the proposed application concentrations of neonicotinoids (de Lima e Silva et al., 2017, 2020, 2021).

To determine the accuracy of soil spiking, 3-5 grams of soil were sampled and stored at -20 °C immediately after moistening and mixing and at the end of the toxicity tests. A selection of four samples taken before and one taken at the end of the toxicity test were analyzed by Groen Agro Control, Delfgauw, the Netherlands, following certified analytical methods. Detection limit was 0.01 mg kg^{-1} dry soil.

Toxicity tests

Toxicity tests followed OECD guideline 232 for collembolan reproduction testing in soil (OECD, 2016) with the exception that the age of the animals was 21-23 days instead of 11-13 days after hatching and the test duration was reduced from 28 to 21 days.

Ten age-synchronized animals were added together with roughly the same number of grains of baker's yeast to each 100 ml glass test jar containing approximately 30 g moist test soil. Every week the water content of the soil was maintained using demineralized water and yeast was added when depleted. Toxicity tests were conducted at 20 ± 1 °C, 75 % RH, and a 16:8 light-dark regime. The tests were terminated by waterlogging the content of each jar and decanting it into 300 ml polypropylene beakers. Jars were rinsed to ensure all its content was collected in the beakers. The beakers were then stirred and left to rest for at least 5 minutes to allow all animals to float to the surface. Then the surface was photographed

by a Nikon Coolpix P510, and the adult and juvenile *F. candida* on the pictures were counted with Image J-based software Fiji (version Image.J 1.52p) using the Cell Counter plugin (Kurt de Vos, version from 2010).

Gene expression analysis

Thirty age-synchronized springtails, i.e. 21–23 days after hatching, were exposed to soils spiked as described above. No food was added. After 48 hours, the jars' content was waterlogged. The springtails were scooped from the water surface into separate containers using a fine mesh sieve and transferred into 1.5 ml reaction tubes using an aspirator. The reaction tubes were snap frozen with liquid nitrogen and stored at -80 °C. RNA was extracted with the SV Total RNA extraction kit (Promega, USA), following the manufacturer's guidelines. Purity and quantity of Total RNA was assessed by spectrophotometric measurements using a Nanodrop (Thermo-Fisher). The quality was checked on a 1 % agarose gel containing 0.5 % ethidium bromide. Approximately 500 ng of RNA was reverse transcribed into cDNA using Promega MML-V reverse transcriptase kit, following the manufacturer's instructions. To verify DNA contamination, a no cDNA sample was prepared for one out of seven samples by omitting reverse transcriptase from the reactions. Quantitative PCR (qPCR) analysis was performed on a CFX Connect Real Time PCR Detection System (BIO-RAD, USA), using BIO-RAD 96 well plates and Cyber Green mix. The selected genes consisted of: (1) Three *Cytochrome P450 monooxygenases* (CYPs) that are affected by PBO enzymatic inhibition: *CYP3A13* and *CYP6e2*, which are involved in biotransformation of xenobiotics, and the CYP *methyl farnesoate epoxidase* (*FE*), which is involved in the maturation of juvenile hormone III, (2) Markers for the action of neonicotinoids on neural signaling: *nicotinic acetylcholine receptor-subunit alpha1* (*nAchR*), which is the direct target of neonicotinoid activation, and *sodium-coupled monocarboxylate transporter 1* (*SMCT*) involved in the transmembrane transport of monocarboxylates such as nicotinate, and (3) Adverse effect indicators: *heat shock protein 70* (*HSP70*), a general stress response protein; *isopenicillin N synthase* (*IPNS*), which catalyzes the formation of isopenicillin and response to stress; and a marker for fecundity: *vitellogenin-1* (*VIT*), which is required for egg yolk formation and transport. Primer sequences are listed in Table S4.1 with reference annotations according to Ensembl Metazoa version 50 (Cunningham et al., 2019). The primers of SMCT and nAchR were designed using the tool Primer Blast (Ye et al., 2012). The other primers were taken from previous studies (M. E. de Boer et al., 2009; Roelofs

et al., 2012). All samples were run in comparison to two reference genes, i.e. *tyrosine 3-monooxygenase* (*YWHAZ*) and *eukaryotic transcription initiation factor 1A* (*ETIF*), and a no template and a no cDNA measurement. All measurements were performed in duplicate and measurements were rejected and repeated when they differed by half a threshold cycle (Ct). In case the measurements of either reference gene differed by half a threshold cycle (Ct), measurements for all primer sets were repeated for that sample.

Data analysis

Data analysis was performed in *R* 4.0.0 (R Core Team, 2019). Graphics were generated via *ggplot2* (Wickham, 2016). Concentration-response curves were fitted using the R-package *drc* (Ritz et al., 2015) following the three-parameter logistic dose-response model. The EC_{50} values for the toxicity of imidacloprid and thiacloprid for the various levels of PBO exposure were compared using a likelihood ratio test.

The relative potencies, expressed as the ratio of ECx values at different PBO levels, were also calculated by the *drc* package in R as described in Ritz et al., (2006), with the 95 % confidence intervals estimated using the delta method (Beckman & Weisberg, 1987) to determine deviation from 1.

General Additive Models (GAMs) were fitted over the log2-transformed gene expression values and analyzed using the R-package *mgcv* (Wood, 2011). Two models were fitted. The null model only took into consideration the influence of neonicotinoid exposure (equation 4.1), the full model did include the influence of neonicotinoid and PBO exposure (equation 4.2).

$$E = g^{-1}(\beta_0 + \sum_{j=1}^{k_1} \beta_1 s_j(X_j)) \qquad \text{(Eq. 4.1)}$$

$$E = g^{-1}(\beta_0 + \sum_{j=1}^{k_1} \beta_j s_j(x_j) + \sum_{p=1}^{k_2} \beta_p s_p(X_p)) \qquad \text{(Eq. 4.2)}$$

in which E is the expected value of the log2-normalized expression values, g^{-1} the inverse linkage function, β_0 the intercept, β_j and β_p the coefficients for neonicotinoid (j) and PBO exposure (p), s_j and s_p smooth terms for neonicotinoid (j) and PBO exposure (p), and k the basis size.

Error was assumed normally distributed by selecting Gaussian-family models and the smooth terms were estimated by restricted maximum likelihood (REML).

The basis size (k) of the smooth terms (s) was set to maximum, i.e. to four for s_j, the neonicotinoid smooth term (k1), and three for s_p, the PBO smooth term (k2) (equations 1 and 2). Model fit was checked via numerous metrics. Residuals were inspected visually to see adherence to homogeneity using quantile-quantile plots and a histogram frequency plot of the residuals. The three models were compared using an F-test (Table S4.2). Full model was accepted when the p-value was lower than 0.1. The p-values per smooth term were determined at default by *mgcv* via F-tests.

Results

Soil concentrations

Chemical concentrations were measured in test soils spiked at concentrations around the EC_{50} for the toxicity of imidacloprid (0.4 mg kg^{-1} dry soil) and thiacloprid (1 mg kg^{-1} dry soil). The measured concentration of imidacloprid was on average 45 % higher than the nominal one, and concentrations at the beginning and end of the exposure period were similar. The measured concentration of thiacloprid was 1.3 % lower than the nominal one, and decreased to 31 % of its original concentration at the end of the 21-day test period. Across both neonicotinoid exposures, PBO was detected at concentrations between 66 and 119 % of the nominal ones. PBO degraded to about 57 % of its original concentration at the end of the exposures (Table S4.3). All effect values are based on nominal concentrations.

Effects of neonicotinoids and PBO on springtail fecundity

All controls, including the ones treated with acetone or with 1 and 10 mg PBO kg^{-1} dry soil, met the validity criteria set out by the OECD guideline 232, which are >80 % adult survival, >100 juveniles and a variation in juvenile numbers <30 % (Table S4.4). In the 1 mg kg^{-1} PBO reference group of the thiacloprid test, the coefficient of variance of juvenile numbers was slightly above the limit with 34 % (Table S4.4). To facilitate visual comparison of the concentration-response curves, all juvenile counts are shown as a percentage of the respective reference group mean.

PBO and the neonicotinoids did not cause sufficient mortality at the highest test concentrations to enable calculating LC_{50} values. PBO reduced the number of juveniles by 1% (EC_1) at 288 mg kg^{-1} dry soil, and had an EC_{10} of 424 and an EC_{50} of 602 mg PBO kg^{-1} dry soil (Figure S4.1).

EC_1, EC_{10} and EC_{50} values for the effects on imidacloprid on juvenile numbers were 0.11, 0.21 and 0.37 mg kg^{-1} dry soil, respectively (Table 4.1). The concentration-response curves showed higher juvenile counts for the treatment of 0 mg PBO kg^{-1} dry soil, and intermediate effects for 1 mg PBO kg^{-1} dry soil. The lowest juvenile counts were observed for 10 mg PBO kg^{-1} dry soil, see Figure 4.1A. The relative potency of imidacloprid at 10 mg PBO kg^{-1} dry soil was significantly increased compared to 0 mg PBO kg^{-1} dry soil between the 19 and 51 % relative potencies: see Figure 4.1B. The likelihood ratio test showed that PBO did not significantly affect the EC_{50} of imidacloprid (df_3, LR = 5.88, p = 0.12, Loglikelihood Ratio test).

Table 4.1: Toxicity of piperonyl butoxide (PBO) and its effect on the toxicity of imidacloprid and thiacloprid to *Folsomia candida* after 21 days exposure in LUFA 2.2 soil. EC_1, EC_{10} and EC_{50} are effective concentrations reducing juvenile numbers by 1, 10 and 50 % compared to the control, respectively. Values in parenthesis are 95% confidence intervals calculated using the delta method.

Exposure	PBO (mg kg^{-1} dry soil)	EC_1 (mg kg^{-1} dry soil)	EC_{10} (mg kg^{-1} dry soil)	EC_{50} (mg kg^{-1} dry soil)
PBO	*NA*	288 (160-418)	424 (324-524)	602 (544-660)
Thiacloprid	0	0.14 (-0.1-0.38)	0.40 (0.02-0.78)	1.0 (0.70-1.4)
	1	0.53 (0.26-0.81)	0.88 (0.62-1.1)	1.4 (1.2-1.6)
	10	0.03 (-0.01-0.06)	0.14 (0.03-0.25)	0.63 (0.40-0.87)
Imidacloprid	0	0.11 (0.05-0.17)	0.21 (0.15-0.27)	0.37 (0.33-0.41)
	1	0.06 (0.03-0.10)	0.16 (0.11-0.20)	0.36 (0.31-0.40)
	10	0.04 (0.01-0.07)	0.12 (0.07-0.16)	0.30 (0.25-0.35)

Thiacloprid affected springtail reproduction with EC_1, EC_{10} and EC_{50} values of 0.14, 0.40 and 1.0 mg kg^{-1} dry soil, respectively (Table 4.1). The concentration-response curves (Figure 4.1C), and EC_x values (Figure 4.1D) show an increase in the potency of thiacloprid at 10 mg PBO kg^{-1} dry soil and a reduced potency at 1 mg PBO kg^{-1} dry soil. The effect of PBO on the EC_{50} was significant (df_3, LR = 19.34, p = 0.0002, Loglikelihood Ratio test). The influence of PBO on the potency of thiacloprid was in particular pronounced at low concentrations, i.e. between 0 and 0.5 mg thiacloprid kg^{-1} dry soil.

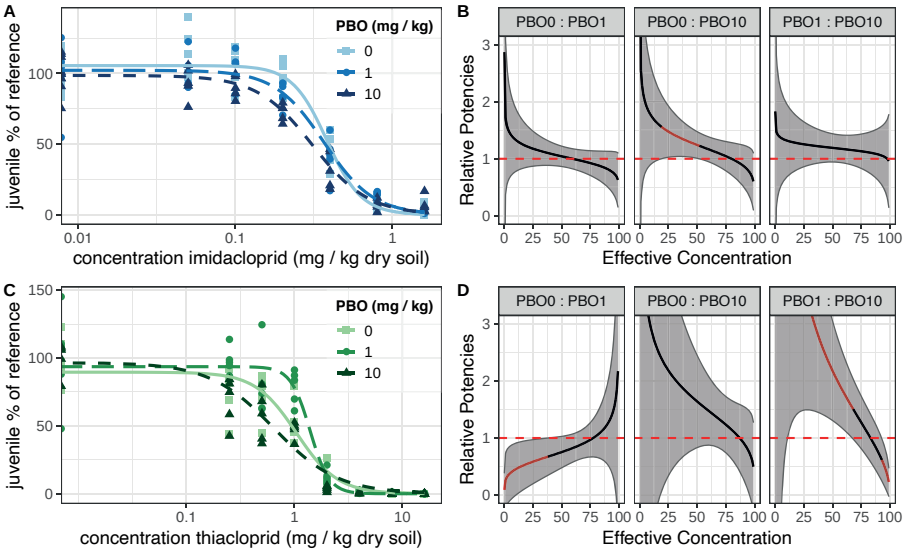

Figure 4.1: The effect of piperonylbutoxide (PBO) on the toxicity of the neonicotinoids imidacloprid (A, B) and thiacloprid (C, D) to the fecundity of the springtail *Folsomia candida* after 21 days exposure in LUFA 2.2 soil. Panels A and C show the fit to the data of the three-parameter concentration-response model for exposures to imidacloprid (panel A; blue) and thiacloprid (panel C; green) at various levels of PBO: solid lines and squares for 0 mg kg^{-1} dry soil, long-dashed lines and circles for 1 mg PBO kg^{-1} dry soil, and short-dashed lines and triangles for 10 mg PBO kg^{-1} dry soil. In panels A and C, the numbers of juveniles produced by the springtails are shown as a percentage of the reference group means. Panels B and D show the relative potencies of the neonicotinoids comparing the PBO regimes as indicated in the portrait headers. Solid black lines follow the relative potencies, and 95 % confidence intervals calculated using the delta method are shown in grey bands outlined with grey lines. When the relative potencies deviated from equal potencies, i.e. the confidence interval not overlapping with 1 Toxic Unit, lines are shown in red indicating a significant effect of PBO addition on the toxicity of the neonicotinoid. The dashed red line indicates equal potency.

The direct comparison of the effect of PBO on the potency of imidacloprid and thiacloprid was hampered by the rather large variation in juvenile numbers in the reference groups of the thiacloprid tests. We assume it is coincidental and probably due to high variability in the control responses which is common in *F. candida* toxicity tests (Crouau & Cazes, 2003). Therefore, we compared models constrained and unconstrained in their EC_{50}-values and calculated relative potencies between PBO exposure levels. This allows determining differential toxicity of compounds even when the control groups are dissimilar (Ritz et al., 2006, 2015).

Effects of neonicotinoids and PBO on biomarker gene expression

Imidacloprid suppressed the expression of all three CYPs (*CYP6e2*, *CYP3A13*, and *FE*), but did not exert significant effects on *HSP70* and *VIT* expression (Figure 4.2). *IPNS* was upregulated by imidacloprid; although the pattern did not relate linearly with an increase of neonicotinoid exposure but rather reflected the variation within the data at the highest imidacloprid concentration (0.4 mg kg^{-1} dry soil), see Figure S4.2. Imidacloprid strongly upregulated the expression of *nAchR* and *SMCT* in a concentration-dependent manner (Figure 4.2). For *SMCT*, we observed a concentration-dependent upregulation by imidacloprid until a concentration of 0.2 mg kg^{-1} dry soil, where after gene regulation remained at the same level.

Thiacloprid did not influence the expression of *CYP6e2*, *CYP3A13*, *IPNS* and *HSP70* (Figure 4.3). *FE* expression was inhibited by thiacloprid exposure until 1 mg kg^{-1} soil and subsequently expression returned to control expression levels. *VIT* was upregulated by thiacloprid. Thiacloprid strongly upregulated the expression of *nAchR* and *SMCT* in a concentration-dependent manner, up to concentrations of 1 and 2 mg thiacloprid kg^{-1} dry soil after which gene expression levels remained at the same level.

PBO exposure strongly enhanced the expression of all CYPs when co-exposed with both neonicotinoids (Figures 4.2 and 4.3). For all CYPs, the effect of PBO on gene expression was greater than the influence of the neonicotinoids, as determined by the significance levels of the GAM smooth term coefficients; Figures 4.2 and 4.3. *VIT* was upregulated by PBO in a concentration-dependent manner under co-exposure of both neonicotinoids. *HSP70* and *SMCT* were upregulated by PBO under mutual exposure with thiacloprid (Figure 4.3). For *HSP70*, upregulation occurred at the highest concentration of PBO (10 mg kg^{-1} dry soil). PBO did not influence *HSP70* and *SMCT* under mutual exposure with imidacloprid. *nAchR* was down-regulated by PBO under mutual exposure with imidacloprid in particular at the highest concentration of PBO at 10 mg kg^{-1} dry soil (Figure 4.1). *nAchR* was not affected by PBO exposure under mutual exposure with thiacloprid (Figure 4.2).

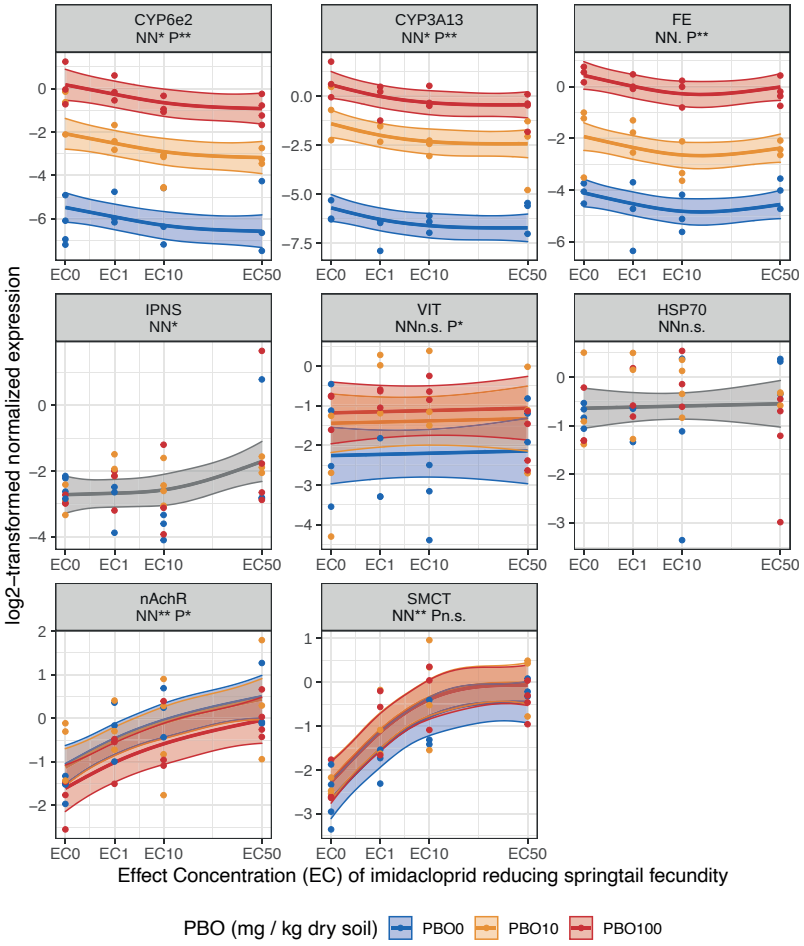

Figure 4.2: The influence of piperonylbutoxide (PBO) on the effect of imidacloprid on the gene expression of the springtail *Folsomia candida* exposed for 48 hours in LUFA 2.2 soil. Imidacloprid concentrations are depicted as reference groups without imidacloprid, EC_0, and the effect concentrations (EC) reducing the number of juveniles by 1, 10 and 50 %, i.e. EC_1, EC_{10} and EC_{50}. Each panel represents the results of one gene, the names listed in the portrait headers are abbreviations for: cytochrome P450 monooxygenases (CYP) 3A13, CYP6e2, methyl farnesoate epoxidase (FE), Heat Shock Protein 70 (HSP70), isopenicillin N synthase (IPNS), vitellogenin-1 (VIT), nicotinic acetylcholine receptor-subunit alpha1 (nAchR), and sodium-coupled monocarboxylate transporter 1 (SMCT). Below the names are the significance levels of the general additive model (GAM) smooth terms of neonicotinoid (NN) and PBO (P), depicted by the following symbols: p>0.1 "N.S", p<= 0.1 ".", p<= 0.05 "*", p<=0.01 "**". GAM mean functions are shown in solid lines, 95 % confidence intervals as outlined transparent bands and dots depict the log2-transformed normalized expression values. PBO exposure levels are shown in blue, orange and red for 0, 10 and 100 mg PBO kg^{-1} dry soil. Mean function and confidence interval outlined bands are shown in grey when the influence of PBO was not included in the GAM model fit.

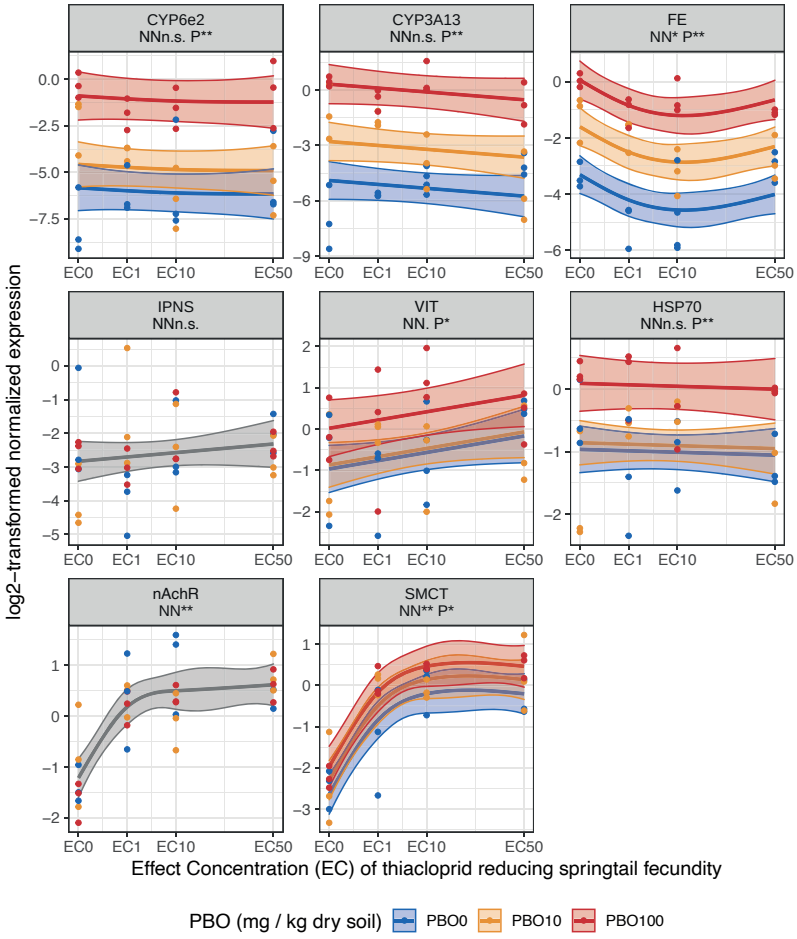

Figure 4.3: The influence of piperonylbutoxide (PBO) on the effect of thiacloprid on the gene expression of the springtail *Folsomia candida* exposed for 48 hours in LUFA 2.2 soil. Thiacloprid concentrations are depicted as reference groups without thiacloprid, EC_0, and the effect concentrations (EC) reducing the number of juveniles by 1, 10 and 50 %, i.e. EC_1, EC_{10} and EC_{50}. Each panel represents the results of one gene, the names listed in the portrait headers are abbreviations for: *cytochrome P450 monooxygenases* (CYP) 3A13, CYP6e2, *methyl farnesoate epoxidase* (FE), *Heat Shock Protein 70* (HSP70)*, isopenicillin N synthase* (IPNS), *vitellogenin-1* (VIT), *nicotinic acetylcholine receptor-subunit alpha1* (nAchR), and *sodium-coupled monocarboxylate transporter 1* (SMCT). Below the names are the significance levels of the general additive model (GAM) smooth terms of neonicotinoid (NN) and PBO (P), depicted by the following symbols: p>0.1 "N.S", p<= 0.1 ".", p<= 0.05 "*", p<=0.01 "**". GAM mean functions are shown in solid lines, the 95 % confidence intervals are shown as outlined transparent bands and dots depict the log2-transformed normalized expression values. PBO exposure levels are shown in blue, orange and red for 0, 10 and 100 mg PBO kg^{-1} dry soil. Mean function and confidence interval outlined bands are shown in grey when the influence of PBO was not included in the GAM model fit.

Discussion

Cytochrome P450 enzymes (CYP) are important mediators of differential toxicity between nitro- and cyano-substituted neonicotinoids in bees (Beadle et al., 2019; Iwasa et al., 2004; Manjon et al., 2018) and form a probable point of molecular synergistic interaction between neonicotinoids and triazole fungicides (Feyereisen, 2018; Glavan & Bozic, 2013; Raimets et al., 2017; Sgolastra et al., 2017). Therefore, we proposed the use of PBO as a "stress-test" to assess the reliability of biomarkers in indicating the exposure of the two major neonicotinoid classes, i.e. nitro- and cyano-substituted, in *F. candida*. To this end, we screened various genes to verify whether collectively their expression adhered to three criteria: (1) indicate exposure of both nitro- and cyano-substituted neonicotinoids, (2) in a concentration-dependent manner relate with the adverse effects of neonicotinoid exposure on *F. candida* fecundity, and (3) be reliable under synergistic interaction by CYP metabolic inhibition.

PBO can be applied as a stress-test for both nitro- and cyano-substituted neonicotinoids In this study, we applied PBO to determine the reliability of biomarkers in indicating the two major classes of neonicotinoids, i.e. nitro- and cyano-substituted, and as a model for synergistic interaction. In other words, we proposed PBO as a "stress-test" for biomarker robustness. The application of PBO in this manner was mainly based on earlier findings in different bee species (Beadle et al., 2019; Iwasa et al., 2004; Manjon et al., 2018). However, the genome of the honey bee has less redundancy in xenobiotic detoxification enzymes compared to other species (Claudianos et al., 2006), while *F. candida* has a genome with a diverse range of xenobiotic detoxification enzymes (Faddeeva-Vakhrusheva et al., 2017). Therefore, we first had to confirm that CYP-mediated metabolism had a comparative influence on neonicotinoid detoxification as in other species and also mediated differential toxicity of nitro- and cyano-substituted neonicotinoids. Our results show that PBO enhances the potency of both nitro- and cyano-substituted neonicotinoids and that this potency-enhancing effect is larger for the cyano-substituted thiacloprid. Our results are, therefore, in line with earlier findings in bees (Beadle et al., 2019; Gomez-Eyles et al., 2009; Manjon et al., 2018) and indicate that CYP detoxification mediates neonicotinoid similarly in *F. candida* compared to previously studied species.

Moreover, we observed that PBO affects neonicotinoid toxicity at concentrations lower than the EC_1 for PBO effects on springtail fecundity, i.e. 288 mg PBO kg^{-1} dry soil. Because PBO enhanced the potency of the neonicotinoids to springtail reproduction far below concentrations at which it becomes toxic itself, we may attribute the potency-enhancing effect of PBO on neonicotinoid toxicity to *F. candida* fecundity to the metabolic inhibition of CYP enzymes by PBO.

Because of these two findings, PBO can serve as a "stress-test" to determine if biomarkers remain reliable indicators of the exposure to two major classes of neonicotinoids even under synergistic interaction by CYP-inhibiting pollutants.

Stability of biomarkers for neonicotinoid exposure

In our study, the three CYP genes did not adhere to any of the three biomarker criteria mentioned above, but mainly responded to the PBO treatment. Fent *et al.* (2020) surveyed the expression of two CYP genes in honey bee brains that were previously identified by Manjon *et al.* (2018) to metabolize imidacloprid and thiacloprid. However, these CYP genes were not differentially expressed at either low or high dosages of thiacloprid after 48 hours exposure. Our results indicate that CYP genes associated with xenobiotic detoxification, i.e. *CYP6e2* and *CYP3A13*, were downregulated after exposure to thiacloprid and showed no significant response to imidacloprid. Based on our findings and those of Fent *et al.* (2020), it is doubtful that CYP genes involved in xenobiotic detoxification, even when involved in neonicotinoid detoxification in *F. candida* would respond to neonicotinoid exposure and could be used as biomarkers under our criteria. Therefore, we conclude that CYP genes are poor candidates to include in a panel of biomarkers for neonicotinoid exposure.

The genes *IPNS*, *VIT* and *HSP70* in *F. candida* that have previously been shown to respond to variety of stress types (M. E. de Boer et al., 2009; Roelofs et al., 2012), and thereby could provide adherence of the biomarker panel to criteria 2, did not relate in a concentration-dependent manner to the adverse effect of neonicotinoids. Only two genes, when considered together, did adhere to all three criteria, *nAchR* and *SMCT*. Because PBO altered the expression of *nAchR* under co-exposure with imidacloprid and of *SMCT* under co-exposure with thiacloprid, we conclude that combined within a biomarker panel they provide a robust indication

for cyano- or nitro-substituted neonicotinoid exposure, also under synergistic interaction of CYP inhibition (criteria 1 and 3).

These results confirm the potential of our approach to identify robust biomarkers for neonicotinoid toxicity, in the context of synergistic interactions with other pollutants. At the same time, the results also demonstrate that the majority of the prominent candidate-biomarkers proposed to date are not suitable. To supplement a biomarker panel that could include *SMCT* and *nAchR*, subsequent studies could aim at using high-throughput screening methods, such as transcriptomics, to identify additional biomarkers that relate concentration-dependently to higher levels of neonicotinoid exposure.

A thorough Environmental Risk Assessment (ERA) of soils requires various lines of information on the physiochemical properties of the soil and the chemical presence, and on the ecological and toxicological impacts of soil pollution (Apitz et al., 2005). Providing support for these lines of evidence can be cumbersome and costly. In particular in case of complex mixtures, chemical analysis of the soil can result in an underassessment of risk because it may not include all, biologically relevant, chemicals and their degradation products (Escher et al., 2020). In addition, chemical analysis usually focuses on total chemical concentrations while risk is related to the biologically available fraction. Gene expression responses are immediate and specific to the type of pollution and can, thereby, provide accurate information on exposure, bioavailability and bioaccumulation of contaminants in organisms even when no effects on phenotypic traits are observed (Lionetto et al., 2019). The ERA of pesticides in the soil is in particular pressing case, because most European agricultural soils are polluted with a mixture of pesticides and their derivates and physiochemical properties of soil can alter the bioavailability and, therefore, exposure of these pesticides' mixtures (Pelosi et al., 2021; Silva et al., 2019; van Gestel, 2012). Gene expression biomarkers can help focusing the efforts of the risk assessors to the most offending samples and inform their further analyses, while providing biologically relevant information on the type, toxicity and exposure of contaminants, single and in mixtures (Escher et al., 2020; Fontanetti et al., 2011; Lionetto et al., 2019; Shi et al., 2017).

Conclusion

For the successful biomonitoring of a variety of neonicotinoids using gene expression, a panel of biomarkers have to be identified that remain robust indicators for the two main classes of neonicotinoids even under synergistic interaction by CYP inhibition. Our study demonstrated that PBO can be used to test the reliability of genetic expression patterns for both major classes of neonicotinoids. Subsequently, we used PBO as a tool to confirm the validity of *SMCT* and *nAchR* as indicators of neonicotinoid exposure even under synergistic interaction by CYP inhibition. The biomarkers can form the basis of rapid and cost-effective tools in biomonitoring of neonicotinoid exposure in soil.

Acknowledgements

We wish to extend our gratitude to Rudo A. Verweij and Janine Mariën for their help in conducting and planning the experimental work presented here. Also, we wish to thank Yuliya Shapovalova for her insights and guidance in the statistics used throughout this work.

Statements and Declarations

Ethical Approval

Not applicable.

Consent to Participate

Not applicable.

Consent to Publish

All authors and participants of the funding consortium have approved publication.

Funding

This research was financed by the Dutch Research Council (NWO) domain Applied and Engineering Sciences (TTW) (Project number 15494).

Competing Interests

The authors have no relevant financial or non-financial interests to disclose.

Availability of data and materials

All data will be made available upon request to the authors. The authors are committed to publish material, such as R-code, and data alongside the publication.

Author contributions

All authors have contributed to the conceptualization of the work. Ruben Bakker has carried out the methodology, the data analysis and wrote the manuscript. Astrid Ekelmans, Liyan Xie and Riet Vooijs carried out the methodology of the work. Dick Roelofs and Cornelis A.M. van Gestel acquired the funding for the project. Katja Hoedjes, Dick Roelofs, Cornelis A.M. van Gestel and Jacintha Ellers carried out the project administration, supervision and helped in the revision, editing and writing of the manuscript.

Chapter 4: supplementary information

Table S4.1: Summary of the primer sets used in quantitative PCR to determine the effects of neonicotinoid or piperonyl butoxide (PBO) exposure on the gene expression of *Folsomia candida* in LUFA 2.2 soil. Given are the name of the primer set used, the primer direction, oligo sequence, the description of the primer set target, the target gene id according to release version 50 (Cunningham et al., 2019) and the efficiency at which the sets amplify the DNA fragments at each cycle shown as percentages.

name	direction	oligo sequence	description	gene id	Efficiency (%)
YWHAZ	Forward	CCTACAAAAACGTCGTCGGTG	*tyrosine 3-monooxygenase*	Fcan01_06830	89.3
	Reverse	TGTTGCTTTCGTTCGAACC			
ETIF	Forward	TGATTCTGGAGATCTTCGCGAG	*eukaryotic transcription initiation factor 1A*	Fcan01_13627	94.9
	Reverse	ACAGTGCAAAGGATTTCCCGA			
CYP 3A13	Forward	TTCCATGCAAGTCATCACATCAG	*Cytochrome P450 monooxidase 3A13*	Fcan01_20588	106.5
	Reverse	CGGAAACACAAAGATTCGTTCTG			
CYP 6a2	Forward	GCGTTAAAAGCGAGGCAAGA	*Cytochrome P450 monooxidase 6a2*	Fcan01_00866	89.3
	Reverse	GCGATATCCACGTTCGAATTGT			
FE	Forward	AGCTTTGGATCCCCTCCAATT	*methyl farnesoate epoxidase*	Fcan01_21605	92.9
	Reverse	CGGTTTTGGTCGTGGCTAAAT			
IPNS	Forward	GACATGTCGGCAAAACTCCTTC	*isopenicillin N synthase*	Fcan01_27072	84.4
	Reverse	GGGTAGCGAATAAGTCGCACTG			
VIT	Forward	CGTGAGACTTGAGTTCGTGCAC	*vitellogenin 1*	Fcan01_15308	100.3
	Reverse	GGACCATTCGTCTGTTGCAAAT			
HSP70	Forward	TTGGTCGACGTAGCTCCACTCT	*Heat shock protein 70*	Fcan01_10020	98.1
	Reverse	TGGGCTTGTTTGCATGGAAT			
nAchR	Forward	CGTGGACCAGGACAGAGAAA	*nicotinic acetylcholine receptor*	Fcan01_01431	85.6
	Reverse	TTGCAGACCCCCATAGTCTG			
SMCT	Forward	ATGGTTTGGGTCGTTTCGTG	*sodium-coupled monocarboxylate transporter*	Fcan01_08638	90.6
	Reverse	CGGTTGTCCGTATTCGCTTG			

Table S4.2: Metrics for model selection of Generalized Additive Models (GAMs) between the null-model (only neonicotinoid smooth term) and full-model (neonicotinoid and piperonyl butoxide (PBO) smooth terms) used to analyze data on the effects of imidacloprid and thiacloprid on gene expression responses of *Folsomia candida* exposed in LUFA 2.2 soil in the absence or presence of different levels of PBO. Selected models are in bold under the "selected model"-column. The full model was accepted when the p-value of the F-test over the model fits was below or equal to 0.1. Abbreviations in the columns are as follows: R^2, the coefficient of determination of the model; AIC, Akaike information criterion; gcv, general cross-validation; residual df, residual degrees of freedom; F, F-value; p, p-value. Names of the target genes listed in the target column are abbreviations for: *cytochrome P450 monooxygenases* (*CYP*) *3A13, CYP6e2*, *methyl farnesoate epoxidase* (*FE*), *Heat Shock Protein 70* (*HSP70*), *isopenicillin N synthase* (*IPNS*), *vitellogenin-1* (*VIT*), *nicotinic acetylcholine receptor-subunit alpha1* (*nAchR*), and *sodium-coupled monocarboxylate transporter 1* (*SMCT*).

neonicotinoid	target	selected model	R^2	AIC	deviation explained	gcv	residual df	F	p
imidacloprid	*CYP6e2*	null	-0.02	188.50	0.01	91.21			
		full	0.59	154.70	0.62	81.77	2.00	28.64	<0.01
	CYP3A13	null	-0.02	182.65	0.01	87.98			
		full	0.56	153.86	0.60	80.65	2.00	23.77	<0.01
	FE	null	-0.03	162.65	0.00	78.68			
		full	0.73	116.61	0.75	64.19	3.23	30.76	<0.01
	IPNS	**null**	0.14	117.20	0.18	57.28			
		full	0.10	120.68	0.19	66.42	1.92	0.17	0.84
	VIT	null	-0.02	128.12	0.00	62.46			
		full	0.11	125.65	0.19	68.44	2.94	2.62	0.07
	HSP70	**null**	-0.03	101.87	0.00	50.11			
		full	0.08	100.61	0.17	57.76	3.12	2.20	0.10
	nAchR	**null**	0.35	95.21	0.38	46.83			
		full	0.39	94.63	0.45	54.76	2.04	2.13	0.13
	SMCT	**null**	0.65	83.38	0.67	41.94			
		full	0.66	84.87	0.70	50.87	2.95	1.20	0.33

neonicotinoid	target	selected model	R^2	AIC	deviation explained	gcv	residual df	F	p
thiacloprid	*CYP6e2*	null	-0.03	181.19	0	87.28			
		full	0.53	155.75	0.57	81.32	2.67	15.76	<0.01
	CYP3A13	null	-0.01	182.38	0.01	88.01			
		full	0.58	151.9	0.61	80	2	25.39	<0.01
	FE	null	0.05	149.28	0.1	72.31			
		full	0.6	119.53	0.64	65.88	2.29	21.33	<0.01
	IPNS	**null**	0	117.31	0.03	57.12			
		full	-0.06	121.17	0.03	66.07	2	0.06	0.94
	VIT	null	0.04	115.29	0.07	56.27			
		full	0.18	112.1	0.26	62.14	2.89	2.9	0.05
	HSP70	null	-0.03	90.59	0	44.5			
		full	0.31	78.02	0.37	46.89	2	9.36	<0.01
	nAchR	**null**	0.61	68.71	0.64	35.37			
		full	0.61	70.83	0.66	44.93	2	0.81	0.45
	SMCT	null	0.68	81.73	0.7	41.49			
		full	0.71	80.11	0.75	49.19	2.01	2.57	0.09

Table S4.3: Nominal and measured concentrations of imidacloprid (IMI), thiacloprid (THIA) and piperonyl butoxide (PBO) in LUFA 2.2 soil, on the day of soil spiking and the end of the exposure, days 0 and 21, respectively. Recovery was calculated as the ratio of measured and nominal concentration and expressed as a percentage. The recovery was not calculated for the samples measured after 21 days exposure, shown as NA (not applicable).

		Neonicotinoid			PBO		
	sampling day	Nominal (mg kg^{-1} dry soil)	Measured (mg kg^{-1} dry soil)	Recovery (%)	Nominal (mg kg^{-1} dry soil)	Measured (mg kg^{-1} dry soil)	Recovery (%)
IMI	0	0	0	0	0	0	0
	0	0.4	0.61	153	0	0	0
	0	0.4	0.62	156	1	0.66	66
	0	0.4	0.50	126	10	8.4	84
	21	0.4	0.53	NA	10	4.56	NA
THIA	0	0	0	0	0	0	0
	0	1	1.03	103	0	0	0
	0	1	0.9	90	1	1.19	119
	0	1	1.03	103	10	10.6	106
	21	1	0.32	NA	10	6.24	NA

Table S4.4: Reference group (control) performance of *Folsomia candida* in toxicity tests with neonicotinoids with piperonyl butoxide (PBO) in LUFA 2.2 soil. Reference groups were exposed to soils only treated with demineralized water, pretreated with acetone or pretreated with acetone and either 1 or 10 mg PBO kg^{-1} dry soil, abbreviated as water, acetone and PBO 1 or PBO 10, respectively. Also added are the validity criteria according to the OECD guideline 232 (OECD, 2016). Only the reference group of the 1 mg PBO kg^{-1} treatment did not adhere to these criteria and therefore is marked in bold.

Compounds	Control type	Mean adult mortality (%)	Mean juvenile count	Coefficient of variance (%)
Imidacloprid and PBO	Water	9	1055	14
	Acetone	17	1085	12
	PBO 1	8	1090	18
	PBO 10	12	1137	12
Thiacloprid and PBO	Water	6	565	20
	Acetone	2	532	17
	PBO 1	14	411	**34**
	PBO 10	12	607	12
PBO	Water	6	877	24
	Acetone	8	781	21
OECD validity criteria		<20	>100	<30

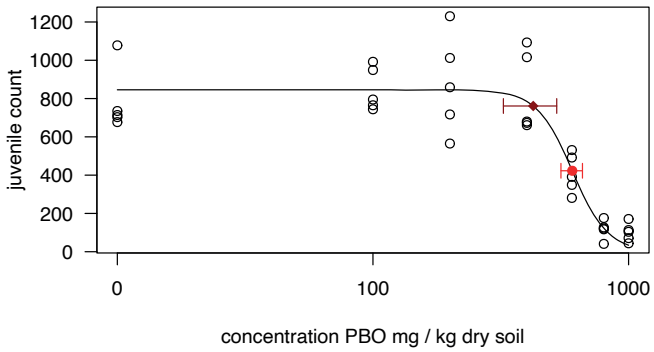

Figure S4.1: The effects of piperonyl butoxide (PBO) on the fecundity of *Folsomia candida* after 21 days exposure in LUFA 2.2 soil. The juvenile counts are shown as circles, the solid line shows the fit of a three-parameter logistic model. Effect concentration (EC) for the reduction in juvenile counts by 10 % and 50 %, EC_{10} and EC_{50}, are shown as a dark red diamond and a red dot, respectively. Whiskers show the 95% confidence interval estimators as obtained using the delta method.

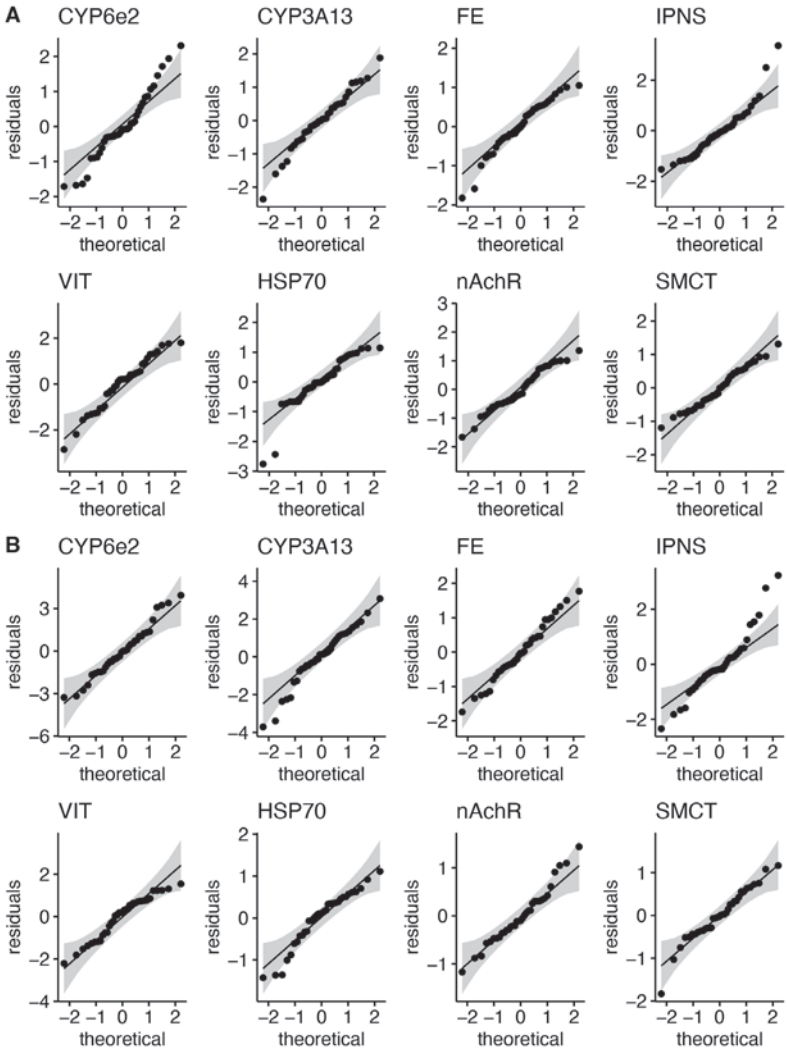

Figure S4.2: Quantile-quantile plots of the residuals compared to their theoretical normal distribution. The residuals are from the Generalized Additive Models (GAMs) fitted on log2-transformed normalized gene expression measured with quantitative PCR (qPCR) on *Folsomia candida* exposed in LUFA2.2 soil to imidacloprid (panel collection A) and thiacloprid (panel collection B) and piperonyl butoxide for 48 hours. Quantile-quantile plots per target gene, their names are above the panels. The names are abbreviations for: *cytochrome P450 monooxygenases* (*CYP*) *3A13*, *CYP6e2*, *methyl farnesoate epoxidase* (*FE*), *Heat Shock Protein 70* (*HSP70*), *isopenicillin N synthase* (*IPNS*), *vitellogenin-1* (*VIT*), *nicotinic acetylcholine receptor-subunit alpha1* (*nAchR*), and *sodium-coupled monocarboxylate transporter 1* (*SMCT*). Residuals are shown as dots on the panels, perfect agreement between the residuals and the normal distribution is shown as solid black lines, 95 % confidence intervals are shown as grey bands.

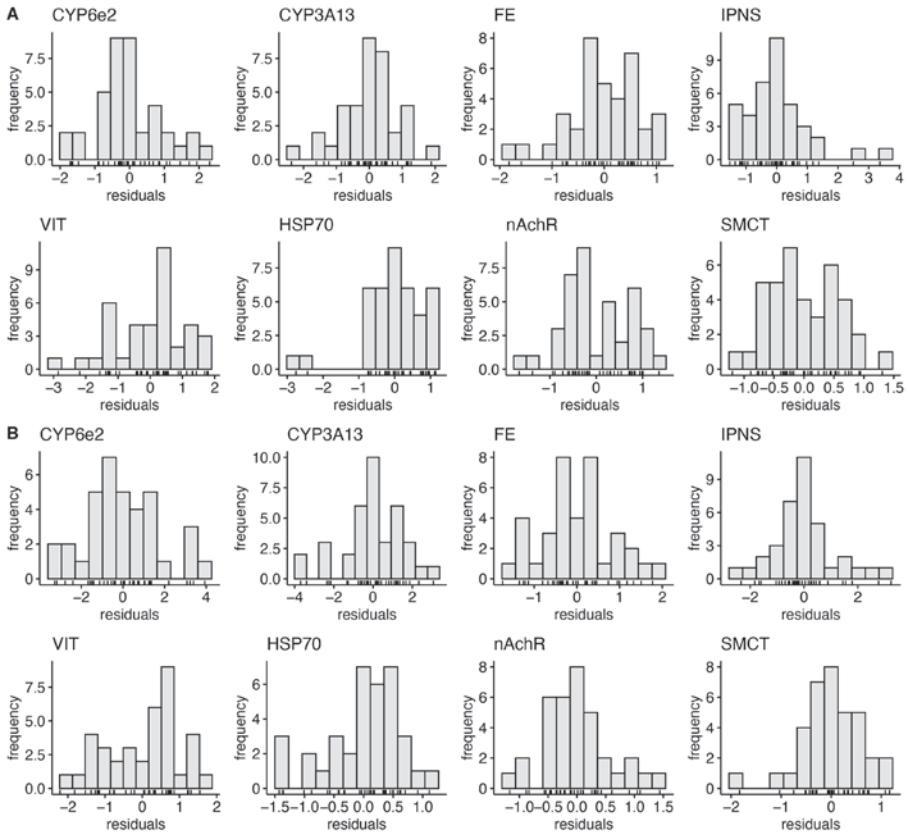

Figure S4.3: Histogram frequency plots of residuals from Generalized Additive Models (GAMs) fitted on log2-transformed normalized expression from quantitative PCR (qPCR) measurements on the gene expression of *Folsomia candida* exposed to imidacloprid (collection of panels A) and thiacloprid (collection of panels B) and piperonyl butoxide in LUFA2.2 soil for 48 hours. Models per target gene as indicated by the name above each panel, which are abbreviations for: *cytochrome P450 monooxygenases* (*CYP*) *3A13*, *CYP6e2*, *methyl farnesoate epoxidase* (*FE*), *Heat Shock Protein 70* (*HSP70*), *isopenicillin N synthase* (*IPNS*), *vitellogenin-1* (*VIT*), *nicotinic acetylcholine receptor-subunit alpha1* (*nAchR*), and *sodium-coupled monocarboxylate transporter 1* (*SMCT*). Frequency of the residual occurrence indicated by height of each bar. Value of the residual shown below the axes labelled with "residuals" using ticks. Bars should center in height around zero and decrease in size equally to both sized when the residuals follow the normal distribution.

Chapter 5

Validation of biomarkers for neonicotinoid exposure in *Folsomia candida* under mutual exposure to diethyl maleate

Ruben Bakker[1*], Liyan Xie[1], Riet Vooijs[1], Dick Roelofs[1,2], Katja M. Hoedjes[1], Cornelis A.M. van Gestel[1]

[1] Amsterdam Institute for Life and Environment (A-LIFE), Faculty of Science,
Vrije Universiteit Amsterdam, De Boelelaan 1085, 1081 HV Amsterdam, The Netherlands
[2] Keygene N.V., Agro Business Park 90, Wageningen, 6708 PW, The Netherlands
* corresponding author
Corresponding e-mail: r.r.bakker@vu.nl

DOI: 10.21203/rs.3.rs-1489709/v1

Neonicotinoid insecticides are harmful to non-target soil invertebrates, which are crucial for sustainable agriculture. Gene expression biomarkers could provide economical and high-throughput metrics of neonicotinoid exposure and toxicity to non-target invertebrates and could help guide remediation efforts or policy enforcement. Gene expression of *Glutathione S-Transferase 3* (*GST3*), which negates oxidative stress, has previously been proposed as a biomarker for the neonicotinoid imidacloprid in the soil ecotoxicological model species *Folsomia candida* (Collembola). It remains unclear, however, how reliably gene expression of neonicotinoid biomarkers, such as *GST3*, can indicate the exposure to the broader neonicotinoid family under varying oxidative stress conditions. In this work, we exposed springtails to two neonicotinoids, thiacloprid and imidacloprid, alongside diethyl maleate (DEM), a known GST metabolic inhibitor that imposes oxidative stress. First, we determined the influence of DEM on neonicotinoid toxicity to springtail fecundity. Second, we surveyed the gene expression of four biomarkers, including *GST3*, under mutual exposure regimes to neonicotinoids and DEM. We observed no effect of DEM on springtail fecundity. Moreover, the expression of *GST3* was only influenced by DEM under mutual exposure with thiacloprid but not with imidacloprid. The results indicate that *GST3* is not a robust indicator of neonicotinoid exposure and that oxidative stress mediates the toxicity of imidacloprid and thiacloprid differentially. Due to influence of DEM on biomarker expression, future research should investigate biomarker reliability under increased oxidative stress conditions as provided by DEM exposure.

Key words: springtails; neonicotinoids; biomarkers; glutathione-S-transferase; diethyl maleate

Introduction

Remediation efforts and policy enforcement for soil pollution are currently based on the chemical screening of soil samples, which is a laborious and expensive process. Moreover, chemical analysis of the soil can only provide evidence for the presence of contaminants and not their toxicity to non-target invertebrates. Gene expression biomarkers can provide metrics indicating the exposure to or the toxicity of soil pollutants, like pesticides, to soil invertebrates even under synergistic interactions in mixtures with other pollutants (Fontanetti et al., 2011; Shi et al., 2017). Additionally, biomarkers could serve as a tool in environmental biomonitoring by serving as an inexpensive and high-throughput screening method of soil samples (Fontanetti et al., 2011).

Neonicotinoids are harmful to non-target invertebrates that are crucial to sustainable agriculture, such as pollinators (Pisa et al., 2014) and soil invertebrates (de Lima e Silva et al., 2017, 2020, 2021). As such, it is essential to have biomarkers available that indicate the exposure to or possible effects of these insecticides in soil. One molecular pathway that may provide a source for candidate biomarkers for neonicotinoid exposure in non-target invertebrates are the genes involved in the biotransformation and detoxification of xenobiotic substances. The biotransformation pathway comprises three phases: I oxidation, II conjugation, and III excretion. Glutathione S-transferases (GSTs) are among the major enzymes involved in phase II biotransformation and negate oxidative stress by reducing free radicals and conjugating phase I metabolites for further excretion (Lohning & Salinas, 1999). For the neonicotinoid imidacloprid, previous research has identified *Glutathione-S-Transferase 3* (*GST3)* as a potential gene expression biomarker in the soil ecotoxicological model species *Folsomia candida* (Collembola) (Sillapawattana & Schäffer, 2017). However, marked differences exist between the toxicity of individual neonicotinoids to non-target invertebrates, and distinct molecular mechanisms mediating their toxicity (Buszewski et al., 2019).

Two neonicotinoids with large differential toxicity to the fecundity and survival of springtails are imidacloprid and thiacloprid (de Lima e Silva et al., 2017, 2020, 2021). In various bee species, the differential toxicity of these insecticides has been attributed to a more readily biotransformation of thiacloprid compared to imidacloprid (Beadle et al., 2019; Manjon et al., 2018). Therefore, in order to apply *GST3* as a biomarker for neonicotinoid exposure, its gene expression should be a

reliable indicator for multiple neonicotinoids and, in particular, for imidacloprid and thiacloprid.

Neonicotinoid toxicity is mediated, in part, by GST enzyme activity although it remains unclear what the exact mechanism is (Sillapawattana & Schäffer, 2017). Three possible mechanisms are: (1) direct metabolism of phase I biotransformation products, (2) negation of oxidative stress caused by neonicotinoid metabolism or toxicity, and (3) a combination of these two mechanisms (Lohning & Salinas, 1999; Sillapawattana & Schäffer, 2017). One finite resource, the co-factor glutathione (GSH), limits the extent by which GST enzymes can carry out these roles at any moment (Lohning & Salinas, 1999). Moreover, various putative biomarkers for neonicotinoid pollution identified in the honey bee and *F. candida* (Bakker et al., 2022; Christen et al., 2018; Christen & Fent, 2017) are also involved in their response to oxidative stress, in particular; *Heat Shock Protein 70 (HSP70)*, responsible for the refolding of proteins, and *Vitellogenin (Vg)*, involved in egg-yolk protein production (King & Macrae, 2015; Perez & Lehner, 2019; Seehuus et al., 2006). Therefore, increased oxidative stress conditions by altered GST activity may impact the reliability of key neonicotinoid biomarkers in indicating exposure.

We aimed at investigating the expression of *HSP70*, *GST3* and the *Vitellogenin Receptor (VgR)*, as biomarkers under the mutual exposure of imidacloprid or thiacloprid with diethyl maleate (DEM), which depletes cellular GSH levels, thereby limiting GST-mediated negation of oxidative stress (Plummer et al., 1981). By choosing DEM over pollutants found in the soil, we ensure the observed effects on gene expression are the result of increased oxidative stress conditions and not of additional toxic effects with unknown molecular mechanisms. In this way, DEM serves as a "stress-test" that can provide evidence for the role of GST-mediated detoxification in neonicotinoid toxicity and its reliability as a biomarker for indicating neonicotinoid exposure. Additionally, the target receptor of neonicotinoids, *nicotinic Acetylcholine Receptor (nAchR),* was also tested as it was proven to be a prominent neonicotinoid biomarker in previous studies on the honey bee (Christen et al., 2016) and *F. candida* (Bakker et al., 2022). First, we determined the influence of DEM on neonicotinoid toxicity to springtail fecundity. Second, we surveyed the gene expression of four biomarkers under mutual exposure of the two neonicotinoids with DEM.

Methods

Animals, chemicals and test soil

Folsomia candida were obtained from inhouse cultures at the Vrije Universiteit Amsterdam, Amsterdam Institute for Life and Environment (A-LIFE) (Berlin strain). Rearing and age synchronization of the individuals has been described in de Lima e Silva et al. (2017; 2020).

Imidacloprid and thiacloprid, both > 98% purity, were provided by Bayer CropSciences, Monheim, Germany. Diethyl maleate (DEM; >98% purity) was obtained from Sigma-Aldrich, the Netherlands.

The LUFA2.2 test soil originated from Lufa, Speyer, Germany. The soil attributes, reported by the supplier, were: total organic carbon content 2.1%, water-holding-capacity (WHC) 46.5% (w/w), and soil pH 5.5 (0.01 M $CaCl_2$). Imidacloprid was directly dissolved in ultra-pure water. Thiacloprid was first dissolved in acetone amounting to 3 % of the total stock solution volume consisting of ultra-pure water. Both stock solutions were stirred overnight at 300 rounds per minute, in the dark and at room temperature. Water controls were included in all tests by moistening LUFA2.2 soil with demineralized water to 50 % of its WHC and mixed thoroughly. For other treatments, 10 % of the dry soil per treatment was completely inundated by acetone, with the desired concentration of DEM, in a glass jar and stirred every half hour for two hours, in the dark, covered with aluminum foil. Hereafter, the soil was left overnight in a fume hood to allow complete evaporation of the acetone. The remaining soil was added, mixed, and moistened and mixed again as described above. All test soils were prepared the day before the springtails were added. The concentrations for the DEM single exposure were: 0, 1.1, 3.3, 10, 30, 90 mg kg^{-1} dry soil. The concentrations for mutual exposure with neonicotinoids were 1 and 6 mg DEM kg^{-1} dry soil; 0, 0.25, 0.5, 1, 2, 4, 8 and 16 mg thiacloprid kg^{-1} dry soil; 0, 0.05, 0.1, 0.2, 0.4, 0.8, 1.6 mg imidacloprid kg^{-1} dry soil. For the control groups of the neonicotinoid toxicity tests, DEM concentrations were roughly equal to the Effect Concentrations (EC_x) reducing the number of juveniles by 1 and 25 %. To calculate the pesticide recoveries and accuracy of their application, 3-5 gram portions of test soil were stored at -20 °C and sent to Groen Agro Control, Delfgauw, the Netherlands. Here, the pesticide soil concentrations were measured following a certified protocol and with a detection limit of 0.01 mg kg^{-1}.

For the gene expression assay, *ad hoc* chosen DEM concentrations of 0, 10 and 20 mg DEM kg^{-1} dry soil were combined with 0, 0.1, 0.2 and 0.4 mg imidacloprid kg^{-1} dry soil or 0, 0.5, 1 and 2 mg thiacloprid kg^{-1} dry soil. The neonicotinoid concentrations represented roughly the neonicotinoid EC_{10}, EC_{25} and EC_{50} for effects on springtail fecundity from earlier studies in our laboratory (de Lima e Silva et al., 2020, 2021).

Toxicity tests

The toxicity tests followed OECD guidelines 232 for Collembolan reproduction testing in soil (OECD, 2016) with two deviations: the duration of the test was shortened from 28 to 21 days, and the initial age of the animals was increased from 11-13 to 21-23 days. At the end of the toxicity tests, the samples were emptied into plastic beakers and their contents waterlogged using tap water, stirred gently and left to rest for at least 5 minutes to allow all animals to come floating to the surface. The surface was photographed by a Nikon Coolpix P510 and the *F. candida* adults and juveniles were counted using Image-J based software Fiji (v. 1.52p) with the Cell Counter plugin (Kurt de Vos, version from 2010).

Gene Expression Assay.

Two-day exposures of roughly 30 age-synchronized, 21-23 day old, *F. candida*, followed by RNA isolation, cDNA transcription and quantitative real-time PCR were carried out as previously described (M. E. de Boer et al., 2009, 2011). The selected genes were: *nicotinic Acetylcholine Receptor-subunit alpha1* (nAchR), the binding site of neonicotinoids; *Heat Shock Protein 70* (*HSP70*), involved in protein refolding after endured stressors, such as oxidative stress (King & Macrae, 2015); *Vitellogenin Receptor (VgR*), which activation leads to egg yolk production and transport, but has been linked to oxidative stress response as well (Perez & Lehner, 2019; Seehuus et al., 2006); *Glutathione-S-Transferase 3* (*GST3*), which negates oxidative stress by reducing reactive compounds: and two reference genes; *Tyrosine 3-Monooxygenase* (YWHAZ) and *Eukaryotic Transcription Initiation Factor 1A* (ETIF). The primer sets for nAchR (Bakker et al., 2022), *YWHAZ*, *ETIF*, *HSP70* and *VgR* were taken from earlier work (M. E. de Boer et al., 2011; Roelofs et al., 2012). The *GST3* primer set was custom made for this work with Primer BLAST (Ye et al., 2012), based on the *GTS3* gene described in (Nakamori et al., 2010; Sillapawattana & Schäffer, 2017). Normalized gene expression values were obtained using the qPCR

accompanying software CFX manager by creating a gene study and exporting the untransformed values. For the primer sequences and efficiencies, see Table S5.1 in the Supplementary Information.

Data analysis.

All statistics were carried out in the *R* programming language v4.0.0 (R Core Team, 2019). Three parameter logistic concentration-response curves were fitted over the number of juveniles or adult *F. candida* to calculate the effect concentrations for survival and reproduction using the R-package *drc* v3.0-1 (Ritz et al., 2015). Models constrained and unconstrained in their EC_{50}-estimate, i.e. concentration reducing juvenile counts by 50 %, were compared using the loglikelihood ratio test. Graphics were generated using *ggplot2* v3.3.5 throughout this work (Wickham, 2016).

For each primer set, a generalized additive model (GAM) was fitted over the log2-transformed normalized gene expression values using the R-package *mgcv* v1.8-37 (Wood, 2011). The null-model considered only neonicotinoid influence on gene expression, equation 1, and the alternative model also included the influence of DEM, equation 2.

$$E = g^{-1}(\beta_0 + \sum_{j=1}^{k_1} \beta_1 s_j(X_j)) \qquad \text{(Eq. 5.1)}$$

$$E = g^{-1}(\beta_0 + \sum_{j=1}^{k_1} \beta_j s_j(x_j) + \sum_{p=1}^{k_2} \beta_p s_p(X_p)) \qquad \text{(Eq. 5.2)}$$

in which E is the expected value of the log2-normalized expression values, g^{-1} the inverse linkage function, β_0 the intercept, β_j and β_p the coefficients for neonicotinoid (j) and DEM exposure (p), s_j and s_p smooth terms for neonicotinoid (j) and DEM exposure (p) with k the basis size, respectively.

Basis size (k_x) for the neonicotinoid smooth term (k_1) was set to four and for the DEM smooth term (k_2) it was set to three, i.e. the maximum size for this experimental design. Gaussian error distribution of the residuals was assumed, thin plate regression splines and restricted maximum likelihood (REML) were used to fit the models. Models were compared using an F-test of their fits and the alternative model was accepted when $p \leq 0.1$. Adherence of homogeneity of residuals was visually checked by histogram frequency plot and quantile-quantile plots.

Results & Discussion

Soil concentrations

Neonicotinoid concentrations were measured in test soil spiked with concentrations around the EC_{50} for effects on springtail fecundity for imidacloprid (0.2 and 0.4 mg kg^{-1} dry soil) and thiacloprid (1 mg kg^{-1} dry soil). Measured imidacloprid concentrations were on average 87 % (SD 6.7 %, n=6) of the nominal ones (Table S5.2). The measured and nominal concentrations of thiacloprid were highly similar with an average recovery of 98 % (SD 12.5 %, n=3). Imidacloprid degraded to 85 % of its measured concentration between the onset and the end (day 21) of the toxicity test. Thiacloprid degraded almost completely to only 2.5 % of its initial measured concentration within the 21-day test period. Because of the high recovery of both test compounds at the start of the exposures, all data are based on the nominal concentrations.

Test validity

With the exception of two groups, all reference groups, including those treated with 1 or 6 mg DEM kg^{-1} dry soil, met the validity criteria of OECD guideline 232 (OECD, 2016), namely: mean juvenile count > 100, variation in control juvenile counts < 30 %, adult survival > 80%, see Table S5.3. For the single diethyl maleate (DEM) exposures, the variation in the number of juveniles was 36 % in the control and for the thiacloprid toxicity test it was 32 % in the 6 mg DEM kg^{-1} dry soil reference group (i.e. without thiacloprid). A high variation in the number of juveniles is common in *F. candida* reproduction tests (Crouau & Cazes, 2003), and the higher variation was not coincidental to any particular treatment across the three toxicity tests. We therefore conclude that the springtail health was of sufficient quality at the start of the toxicity tests and did not bias the results.

Effects of DEM on springtail fecundity and mortality

DEM reduced the adult springtail survival by 1, 10 and 50 % at 2.99, 6.73 and 14.2 mg DEM kg^{-1} dry soil, i.e. the LC_1, LC_{10} and LC_{50}, respectively, see Figure S5.1 and Table 5.1. DEM, as a single compound, reduced the number of juveniles by 1 % (EC_1) at 1.15 mg kg^{-1} dry soil and had an estimated EC_{10} of 3.7 and EC_{50} of 10.9 mg DEM kg^{-1} dry soil (Table 5.1). The DEM concentrations affecting survival (LC_x) and

fecundity (EC_x) did not differ much, as also shown by the similar concentration-response curves (Figure S5.1) and overlapping 95% confidence intervals (Table 5.1). The close effect concentrations for survival and fecundity suggest that DEM reduces fecundity as a direct consequence of reduced survival and elicits little sublethal toxic effect.

Table 5.1: Toxicity of diethyl maleate (DEM) on reproduction (EC_x) and survival (LC_x) and its effect on the toxicity of imidacloprid and thiacloprid to the reproduction of *Folsomia candida* after 21 days of exposure in LUFA2.2 soil. EC_1, EC_{10} and EC_{50} are effective concentrations reducing juvenile numbers by 1, 10 and 50 % compared to the control, respectively. LC_1, LC_{10} and LC_{50} are lethal concentrations reducing adult survival by 1, 10 and 50 %, respectively. Values in parenthesis are 95% confidence intervals calculated using the delta method.

Exposure	DEM (mg kg^{-1} dry soil)	EC_1 (mg kg^{-1} dry soil)	EC_{10} (mg kg^{-1} dry soil)	EC_{50} (mg kg^{-1} dry soil)
Imidacloprid	0	0.02 (0:0.05)	0.08 (0.03:0.12)	0.24 (0.19:0.29)
	1	0.06 (0.01:0.12)	0.15 (0.08:0.22)	0.32 (0.26:0.37)
	6	0.02 (0:0.04)	0.07 (0.03:0.11)	0.24 (0.17:0.30)
Thiacloprid	0	0.09 (-0.02:0.19)	0.44 (0.14:0.74)	1.94 (1.35:2.53)
	1	0.12 (-0.02-0.19)	0.52 (0.18:0.85)	1.96 (1.41:2.50)
	6	0.20 (-0.02:0.43)	0.72 (0.28:1.16)	2.28 (1.71:2.86)
DEM	NA	1.15 (-1.90:4.21)	3.70 (-1.75:9.16)	10.8 (5.49:16.1)
DEM	NA	2.99 (0.31:5.66)	6.73 (3.63:9.83)	14.18 (10.61:17.75)

Effects of DEM on neonicotinoid toxicity to springtail fecundity

The neonicotinoids thiacloprid and imidacloprid did not cause sufficiently high adult mortality at their test highest concentrations, therefore no LC_{50} values could be calculated. Thiacloprid reduced juvenile counts with EC_1, EC_{10}, and EC_{50} values of 0.09, 0.44, and 1.94 mg kg^{-1} dry soil, respectively (Table 5.1). The EC_x values were not affected by DEM exposure as their 95 % confidence intervals were overlapping. The concentration-response curves for each level of DEM were overlapping or at least adjacent, see Figure 5.1. Also, the EC_{50} estimates did not differ between the levels of DEM exposure (p=0.66, Loglikelihood Ratio Test). Combined, the results indicate no influence of DEM exposure on the toxicity of thiacloprid to springtail fecundity.

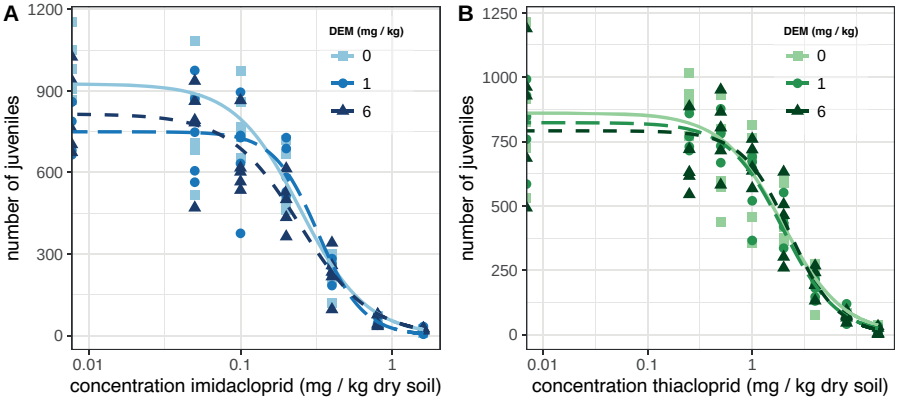

Figure 5.1: The effect of diethyl maleate (DEM) on the toxicity of the neonicotinoids imidacloprid (A) and thiacloprid (B) to the fecundity of the springtail *Folsomia candida* after 21 days exposure in LUFA2.2 soil. Juvenile counts per sample are shown as markers. Lines show the fit to the data of the three-parameter logistic model. Line and marker type vary per level of DEM: solid lines and squares for 0 mg kg^{-1} dry soil, long-dashed lines and circles for 1 mg DEM kg^{-1} dry soil and short-dashed lines and triangles for 6 mg DEM kg^{-1} dry soil.

In the absence of DEM, the estimated EC_1, EC_{10}, and EC_{50} values for the effects of imidacloprid on springtail fecundity were 0.02, 0.08, and 0.24 mg kg^{-1} dry soil, respectively (Table 5.1). The EC_x-estimates for the effects of imidacloprid on springtail fecundity showed overlapping 95 % confidence intervals between the different levels of DEM exposure, see Table 5.1. The concentration-response curves largely overlapped for intermediate till high concentrations of imidacloprid, i.e. 0.1 mg kg^{-1} dry soil and above, indicating similar effects of imidacloprid on springtail fecundity independent of DEM exposure. The comparison of the EC_{50}-values between the levels of DEM showed moderate effects of DEM on imidacloprid toxicity (p=0.07, Loglikelihood Ratio Test). However, as the 95% confidence intervals of the EC_x values largely overlapped, we conclude that DEM also did not alter the toxicity of imidacloprid to springtail fecundity.

Our data indicate that when applied in combination with the two neonicotinoids, DEM did not alter the toxicity of either thiacloprid or imidacloprid. Most research investigating the influence of DEM exposure on neonicotinoid toxicity has been performed on neonicotinoid-resistant insect pests with the aim to provide evidence that increased GST enzymatic activity contributes to neonicotinoid resistance. Imidacloprid is the most well studied neonicotinoid in this body of research. No

influence of DEM on the survival of the neonicotinoid susceptible strains of brown planthopper, melon/cotton aphid (*Aphis gossypii*), sweet potato whitefly (*Bemisia tabaci*) or the English grain aphid (*Sitobion avenae*) under imidacloprid exposure was found (Bao et al., 2016; Salehi-Sedeh et al., 2020; Seyedebrahimi et al., 2016; B. Z. Zhang et al., 2020). DEM also did not influence the toxicity of the neonicotinoid dinotefuran to the survival of the melon/cotton aphid *A. gossypii* (A. Chen et al., 2020). Lastly, no influence was found of DEM on the toxicity of the neonicotinoid acetamiprid to the honey bee (*Apis mellifera)* and the Iwasa sweet potato whitefly (*B. tabaci*) (Feng et al., 2010; Iwasa et al., 2004). Therefore, our results are in line with previous findings that GST inhibition by DEM does not increase the toxicity of neonicotinoids to insects and related organisms like springtails.

Gene expression responses to DEM and neonicotinoids.

For gene expression responses, the adherence of the Generalized Additive Models' fit to homogeneity was confirmed by inspecting frequency and quantile-quantile plots, see Figure S5.2 and Figure S5.3. No noteworthy deviation from the residuals to homogeneity was found.

Neonicotinoid exposure did not influence the gene expression of *VgR* and *GST3*, see Figure 5.2. Both neonicotinoids enhanced the expression of *nAchR* and imidacloprid also enhanced the expression of *HSP70*. The gene expression patterns upon thiacloprid exposure are different from those under imidacloprid exposure by one key aspect: imidacloprid induced gene expression in a concentration-dependent manner, while gene expression upon thiacloprid exposures was at maximum or minimum at intermediate exposure levels and returned to control levels at high exposure concentrations (see Figure 5.2). Similarly, previous findings in *F. candida* found enhanced gene expression of *nAchR* under the exposure of both neonicotinoids and non-linear gene expression patterns of various biomarkers upon thiacloprid exposure (Bakker et al., 2022). Previous findings and the results of this work indicate that different molecular mechanisms mediate the toxicity of the two neonicotinoids at higher exposure levels.

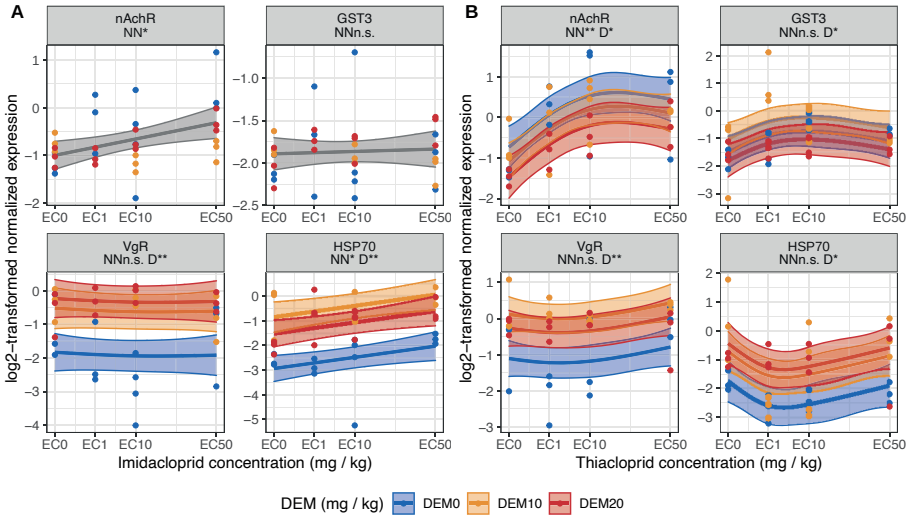

Figure 5.2: The influence of diethyl maleate (DEM) on the gene expression of the springtail *Folsomia candida* induced by 48 hours exposure to the neonicotinoids imidacloprid (A) or thiacloprid (B) in LUFA2.2 soil. Each panel represents the results of one gene, the abbreviations are listed in the portrait headers: *nicotinic Acetylcholine Receptor subunit alpha1* (*nAchR*), *Glutathione-s-Transferase 3* (*GST3*), *Vitellogenin Receptor* (*VgR*) and *Heat Shock Protein 70* (*HSP70*). Below the names are the significance levels of the generalized additive models (GAMs) smooth terms of neonicotinoid (NN) and DEM (D). Significance levels of the smooth terms are depicted by the following symbols: p>0.1 "N.S", p<= 0.1 ".", p<= 0.05 "*", p<=0.01 "**". GAM mean functions are shown in solid lines, the 95 % confidence intervals as outlined transparent bands, and dots depict the log2-transformed normalized expression values. Each level of DEM exposure is shown as a separate color, i.e. blue, orange and red for 0, 10 and 20 mg DEM kg^{-1} dry soil, respectively. Mean function and confidence interval outlined bands are shown in grey when the influence of DEM was not included in the GAM model fit.

DEM increased the expression of *HSP70* and *VgR* under the mutual exposure with both neonicotinoids, see Figure 5.2. For both genes, expression was increased by DEM exposure compared to neonicotinoid exposure in the absence of DEM. The extent by which DEM induced the expression of *VgR* and *HSP70* was similar between the two levels of DEM as indicated by overlapping confidence intervals, see Figure 5.2. The influence of DEM on *nAchR* and *GST3* was different in the mutual exposures to the two neonicotinoids. Under mutual exposure with thiacloprid, DEM decreased the expression of *nAchR* and altered the expression of *GST3*. *GST3* expression was increased at 10 mg DEM kg^{-1} dry soil and decreased by 20 mg DEM kg^{-1} dry soil under co-exposure with thiacloprid, showing a non-linear response of *GST3* to DEM exposure. Hence, the results indicate that thiacloprid toxicity exerts a stronger oxidative stress response compared to imidacloprid because the gene

expression of all four biomarkers was altered only following mutual exposure to DEM with thiacloprid.

Sillapawattana & Schäffer (2017) observed *GST3* upregulation and increased GST enzymatic activity under imidacloprid exposure. They offered three scenarios for their findings: 1) GSTs bind neonicotinoids or their toxic metabolites without metabolism, similar to how GSTs mediate pyrethroid insecticide toxicity (Ketterman et al., 2011); 2) GSTs are directly involved in the metabolism of neonicotinoids or their metabolites by conjugation with GSH; 3) GSTs remove Reactive Oxygen Species (ROS) produced by neonicotinoid metabolism or its toxic effects. In this work, we observed no upregulation of the *GST3* by the two neonicotinoids. Therefore, we found no evidence to supports these scenarios. We did find that oxidative stress conditions were increased by DEM. Support for this comes from the expression of *VgR* and *HSP70*. Both genes perform a diverse set of functions (Perez & Lehner, 2019; Wu et al., 2021) and have both been linked to the oxidative stress response (King & Macrae, 2015; Seehuus et al., 2006). Various GSTs are encoded by *F. candida* and it is possible that other GSTs are involved in the direct metabolism of neonicotinoids or its metabolites and respond to neonicotinoid exposure. Future research into the expression of these GSTs under neonicotinoid exposure is needed to refute or support the three scenarios. For the biomarker *GST3*, we found that its gene expression was no reliable indicator of neonicotinoid exposure, neither for imidacloprid nor for thiacloprid.

The gene-expression results suggest that DEM exposure increases oxidative stress conditions and altered the gene-expression patterns of all candidate biomarkers under mutual exposure with at least one neonicotinoid. However, for both neonicotinoids no effects of DEM exposure were found on neonicotinoid toxicity to *F. candida* fecundity. Toxicity is multifaceted and can relate to, among others, behavior, reproduction or survival. A possible explanation for the observed effect of DEM on gene expressions and not fecundity, could be that DEM has little sublethal effects and, hence, has fewer interaction effects with neonicotinoids affecting reproduction. Secondly, the gene-expression is a more specific and sensitive metric of pesticide exposure compared to fecundity and precedes effects observed on the phenotype. Therefore, effects can be observed not (yet) affecting downstream phenotypic measures of toxicity.

The effects of toxics on gene expression is diverse and, hence, multiple biomarkers have to be combined in order to provide a reliable read-out of pesticide soil pollution (Lionetto et al., 2019). No suitable selection of candidate biomarkers has been identified in this study to indicate neonicotinoid exposure. However, the aim of this study was to investigate the influence of oxidative stress on biomarker reliability not provide a comprehensive panel of biomarkers. In our previous study, we found that the expressions of *nAchR* and *Sodium-Coupled Monocarboxylate Transporter* (*SMCT*) *1* were reliable indicators of neonicotinoid exposure when used in combination (Bakker et al., 2022). Therefore, future studies should attempt to incorporate novel biomarkers into a panel that includes *nAchR* and *SMCT* for neonicotinoid exposure. The current work provides a tool, i.e. mutual exposure with DEM, for testing the resulting biomarker reliability under varying oxidative stress conditions.

Conclusion

Our goal was to investigate the reliability of *Folsomia candida* (springtail) biomarkers as indicators of neonicotinoid exposure in soil under increased oxidative stress conditions exerted by co-exposure to DEM, a metabolic inhibitor of GST enzymes. In particular, we surveyed the previously described imidacloprid biomarker *GST3* (Sillapawattana & Schäffer, 2017). We found that DEM did not influence the toxicity of two neonicotinoids, i.e. imidacloprid and thiacloprid, to springtail fecundity. Moreover, both neonicotinoids did not affect the expression of *GST3*. However, DEM exposure influenced the gene expression of *VgR* and *HSP70* under mutual exposure with both neonicotinoids. Combined, the results indicate that GST enzyme activity does not strongly mediate neonicotinoid toxicity to springtail fecundity and that the expression of *GST3* is not a reliable biomarker for neonicotinoid exposure. Additionally, we observed that the gene expression of all considered candidate biomarkers was altered by DEM co-exposure, at least for one of the two neonicotinoids. This suggests that increased oxidative stress conditions are an important factor for the reliability of biomarkers indicating neonicotinoid exposure. Therefore, our data support the hypothesis that DEM could provide a "stress-test" to study biomarker reliability under such conditions. The results of this work give insights into the influence of GST-mediated biotransformation on neonicotinoid toxicity and indicate that different molecular mechanisms mediate the toxicity of imidacloprid and thiacloprid in an important soil ecotoxicological model species.

Acknowledgements

The authors would like to thank Rudo A. Verweij, Astrid Ekelmans and Janine Mariën for their help in conducting the experiments of this work. Also, we wish to extend our gratitude for our consortium partners and user committee members of our Applied and Engineering Sciences (NWO/TTW) research project for their insights during the conceptualization of this work.

Statements and Declarations

Ethical Approval

Not applicable.

Consent to Participate

Not applicable.

Consent to Publish

All authors and participants of the funding consortium have approved publication.

Funding

This research was financed by the Dutch Research Council (NWO) domain Applied and Engineering Sciences (TTW) (Project number 15494).

Competing Interests

The authors declare they have no known financial or non-financial interests to disclose that could have influenced the work.

Availability of data and materials

The authors are committed to publish material, such as R-code, and data alongside the publication.

Author contributions

All authors have contributed to the conceptualization of the work. Ruben Bakker: Data Curation, Formal Analysis, Supervision, Investigation, Visualization, Methodology, Writing – original draft. Liyan Xie and Riet Vooijs: Methodology, Investigation. Katja Hoedjes: Supervision, Writing – review & editing, Dick Roelofs and Cornelis A.M. van Gestel: Project administration, Writing – review & editing, Funding acquisition.

Chapter 5: supplementary information

Table S5.1: Summary of the primer sets used in quantitative PCR to determine the effects of neonicotinoid and/or DEM exposure on the gene expression of *Folsomia candida* in LUFA2.2 soil. The name of the primer sets used, the primer direction, oligo sequence, the description of the primer set target, the target gene id according to Ensembl Metazoa release version 50 (Cunningham et al., 2019) and the efficiency at which the sets amplify the DNA fragments at each cycle shown as percentages.

name	direction	oligo sequence	description	gene id	Efficiency (%)
YWHAZ	Forward	CCTACAAAAACGTCGTCGGTG	*Tyrosine 3-Monooxygenase*	Fcan01_06830	89.3
	Reverse	TGTTGCTTTCGTTCGAACC			
ETIF	Forward	TGATTCTGGAGATCTTCGCGAG	*Eukaryotic Transcription Initiation Factor 1A*	Fcan01_13627	94.9
	Reverse	ACAGTGCAAAGGATTTCCCGA			
GST3	Forward	CAACGATCTCTTTGAGCAGTGG	*Glutathione-S-Transferase 3*	Fcan01_00498	93.2
	Reverse	CTTCCAAGCATTTAGGCGCA			
VgR	Forward	TGTCCCGTAGGGATGTATCTTGA	*Vitellogenin Receptor*	Fcan01_04244, Fcan01_04245	85.6
	Reverse	GATTGTGTTGTTGTACCCGATGAC			
HSP70	Forward	TTGGTCGACGTAGCTCCACTCT	*Heat Shock Protein 70*	Fcan01_10020	98.1
	Reverse	TGGGCTTGTTTGCATGGAAT			
nAchR	Forward	CGTGGACCAGGACAGAGAAA	*nicotinic Acetylcholine Receptor subunit alpha 1*	Fcan01_01431	85.6
	Reverse	TTGCAGACCCCCATAGTCTG			

Table S5.2: Concentrations of imidacloprid and thiacloprid in LUFA2.2 soil measured on the day of soil spiking and the end of the 21-day exposure of *Folsomia candida*. Recovery was calculated by dividing the measured over the nominal concentration and expressing it as a percentage. The recovery is not calculated for the samples analyzed after 21 days exposure, or if the nominal concentration was zero (shown as NA, not applicable).

neonicotinoid	nominal concentration (mg kg^{-1} dry soil)	day	measured concentration (mg kg^{-1} dry soil)	Recoveries (%)
Imidacloprid	0	0	0	NA
	0.2	0	0.18	90
	0.2	0	0.17	84
	0.2	0	0.19	96
	0.4	0	0.36	90
	0.4	0	0.31	78
	0.4	0	0.32	81
	0.4	21	0.28	NA
Thiacloprid	0	0	0	NA
	2	0	2.04	102
	2	0	1.68	84
	2	0	2.16	108
	2	21	0.05	NA

Table S5.3: Reference group (control) performance of *Folsomia candida* in LUFA2.2 soil in toxicity tests with diethyl maleate (DEM) and/or the neonicotinoids imidacloprid or thiacloprid. Reference groups were exposed to soils only treated with demineralized water, pretreated with acetone or pretreated with acetone and either 1 or 6 mg DEM kg^{-1}: abbreviated as water, acetone and DEM 1 or DEM 6, respectively. Also added are the validity criteria according to the OECD guideline 232 (OECD, 2016). The reference group of DEM 6 in the thiacloprid test and water control of the DEM test are marked in bold as they did not meet these criteria with a coefficient of variance of 32 and 36 %, respectively.

Compounds	Control type	Mean adult mortality (%)	Mean juvenile count	Coefficient of variance (%)
Imidacloprid and DEM	water	20	964	11
	acetone	8	991	11
	DEM 1	18	771	12
	DEM 6	10	820	19
Thiacloprid and DEM	water	8	743	18
	acetone	16	843	30
	DEM 1	6	822	19
	DEM 6	6	852	**32**
DEM	water	10	670	**36**
	acetone	8	695	21
OECD validity criteria		< 20 %	>100	<30

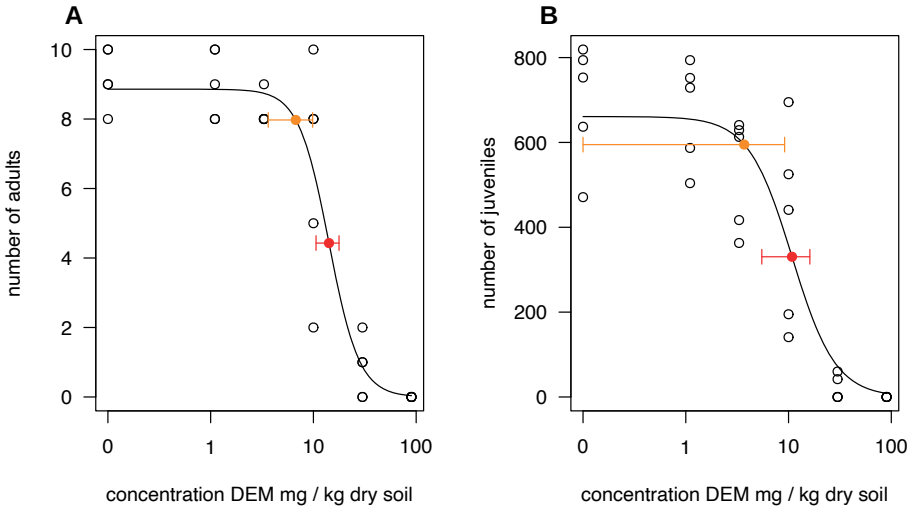

Figure S5.1: The effects of diethyl maleate (DEM) on the survival (A) and reproduction (B) of *Folsomia candida* after 21 days exposure in LUFA 2.2 soil. The juvenile and adult counts are shown as circles on the panels, the solid line shows the fit of a three-parameter logistic model. Concentrations affecting survival and reproduction by 10 % and 50 %, LC_{10} and LC_{50} (A) or EC_{10} and EC_{50} (B) respectively, are shown as red and orange. Whiskers show the 95% confidence interval estimators as obtained using the delta method.

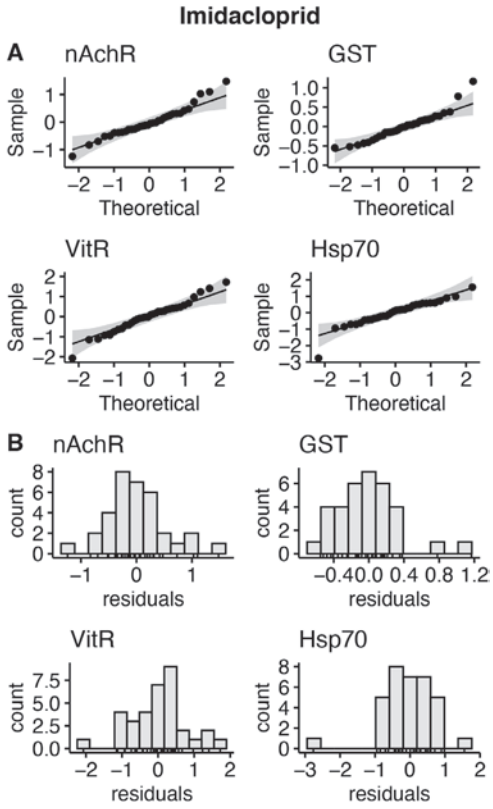

Figure S5.2: Adherence of the residual distribution to homogeneity shown as quantile-quantile plots (A) and histogram frequency plots (B) for all Generalized Additive Models (GAMs) fitted on log2-transformed normalized gene expression measured by qPCR from *Folsomia candida* exposed for 48 hours to imidacloprid and diethyl maleate (DEM) in LUFA2.2 soil. Residuals are shown as dots on the quantile-quantile plot panels (A), a solid black line indicates perfect adherence to homogeneity with grey bands indicating 95 % confidence intervals. Residuals are shown as ticks on the x-axis of the histogram frequency plots (B) with their frequency of occurrence indicated by the height of the bars. Each plot shows the result of one primer set, their names are abbreviated above the panels: *nicotinic Acetylcholine Receptor subunit alpha 1* (*nAchR*), *Glutathione-S-Transferase 3* (*GST3*), *Vitellogenin Receptor* (*VgR*) and *Heat Shock Protein 70* (*HSP70*).

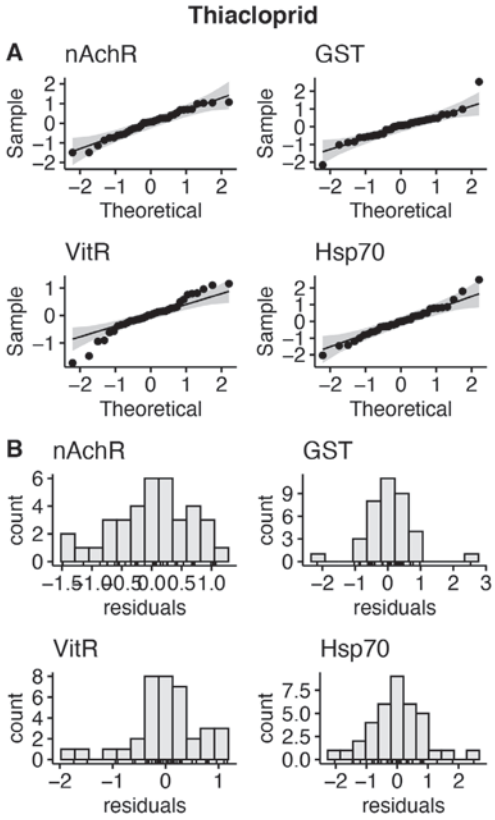

Figure S5.3: Adherence of the residual distribution to homogeneity shown as quantile-quantile plots (A) and histogram frequency plots (B) for all Generalized Additive Models (GAMs) fitted on log2-transformed normalized gene expression measured by qPCR from *Folsomia candida* exposed for 48 hours to thiacloprid and diethyl maleate (DEM) in LUFA2.2 soil. Residuals are shown as dots on the quantile-quantile plot panels (A), a solid black line indicates perfect adherence to homogeneity with grey bands indicating 95 % confidence intervals. Residuals are shown as ticks on the x-axis on the histogram frequency plots (B) with their frequency of occurrence indicated by the height of the bars. Each plot shows the result of one primer set, their names are abbreviated above the panels: *nicotinic Acetylcholine Receptor subunit alpha 1* (*nAchR*), *Glutathione-S-Transferase 3* (*GST*3), *Vitellogenin Receptor* (*VgR*) and *Heat Shock Protein 70* (*HSP70*).

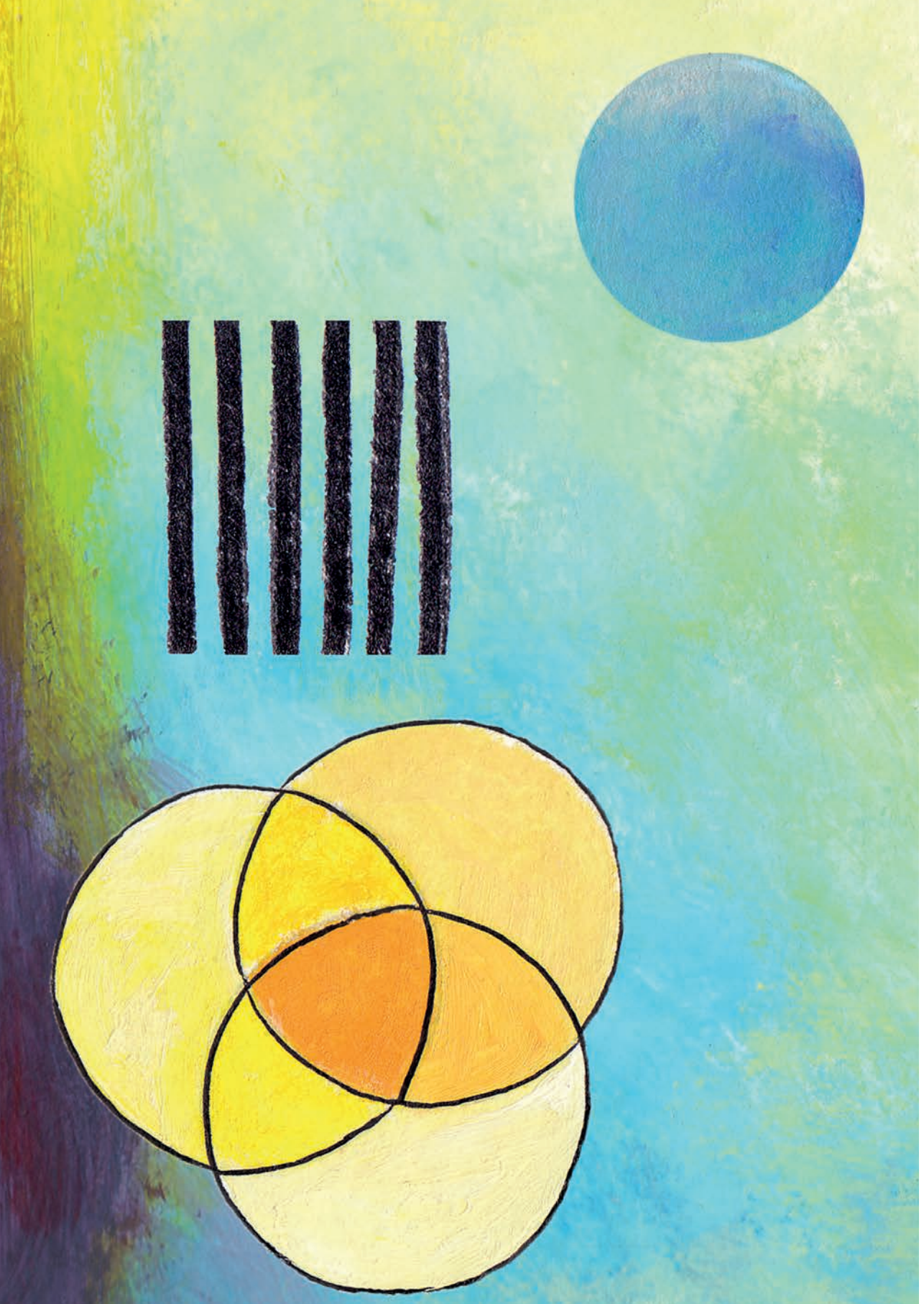

Chapter 6

General Discussion and Conclusions

In this Ph.D. thesis, I investigated various aspects of the toxicogenomic fingerprint identification and subsequent biomarker development in the springtail *Folsomia candida* (Collembola) for assessing pesticide contamination in soil.

My research questions were divided into two categories:

1. How to identify toxicogenomic fingerprints?
2. Are biomarkers derived from toxicogenomic fingerprints robust indicators of neonicotinoid exposure under various stress conditions?

How to identify toxicogenomic fingerprints?

This work addressed various questions for toxicogenomic fingerprint identification.

1. What is the most opportune exposure duration for toxicogenomic fingerprint identification?
2. Can multiple omics data types be combined for toxicogenomic fingerprint identification?
3. Are the current statistical methods suitable for identifying toxicogenomic fingerprints?

What is the most opportune exposure duration for toxicogenomic fingerprint identification?

I sought to identify toxicogenomic fingerprints for diagnosing pesticide-soil pollution. In chapter 2, I analyzed time-resolved transcriptomic and proteomic data from *F. candida* under imidacloprid exposure and found that the most opportune timepoint for toxicogenomic fingerprint identification was 48 hours post the onset of exposure. Remarkably, this timepoint was already the most commonly used exposure duration for *F. candida* gene-expression surveys (M. E. de Boer et al., 2009, 2011; T. E. de Boer et al., 2010; Nota et al., 2009; Sillapawattana & Schäffer, 2017). One might argue that a standardized exposure duration for toxicants with varying toxicodynamics and toxicokinetics would hamper our ability to link omics results obtained under such a timepoint to toxicity occurring on the phenotype. In other words, every toxicant has a different rate of uptake, distribution, metabolism, and excretion and, therefore, differential rates at which its mechanisms of toxic action occur (Aschieri et al., 2003; Jager, 2020). These differential rates may hamper our ability to link the cause and consequence of toxic exposure from responses observed at the molecular level to adverse effects

on the phenotype, e.g., reproduction. Additionally, in the discussion of chapter 2, I have argued that the differential transcript and protein abundances observed at the 48h timepoint could be the result of the influence of imidacloprid on the response of *F. candida* to its transfer from a culture on Paris plaster into test soil. When this is true, it further erodes the biological relevance of the 48h timepoint for toxicogenomic fingerprint identification as it is not solely indicative of toxic mechanisms that mediate imidacloprid toxicity.

Resolving the toxicodynamics and toxicokinetics of toxicants is essential to the prognosis of the possible risk of a toxicant as it improves our prediction of the mechanisms of interaction that mediate its toxicity. Improving our understanding of these mechanisms forms the basis for pollution prognosis and diagnosis. However, it is difficult to extrapolate such findings to field-relevant conditions as environmental pollution is complex, and soil type, climatic factors, and mixture components will influence the toxicodynamics and toxicokinetics of every toxicant in a mixture (van Gestel, 2012). Therefore, resolving toxicodynamics and toxicokinetics when pursuing pollution diagnosis is somewhat fruitless. Perhaps, omics data may one day provide a single high-throughput source for identifying toxicogenomic fingerprints, toxicodynamics, and toxicokinetics (Spurgeon et al., 2010). Until then, the 48h exposure duration, however arbitrary, provides a pragmatic way forward to standardize gene and protein surveys in *F. candida*.

Can multi-omics data be combined for toxicogenomic fingerprint identification?

The underlying "quantitative assumption" of multi-omics data integration is that conserved shifts of biomolecule abundances across multiple levels of biological organization lend more relevance to their associated molecular functions (Rohart et al., 2017; Yugi et al., 2016). In chapter 2, I demonstrated that the shifts in transcript and protein abundances from the same gene occurred in the absence of a time lag. Although this finding seems to provide credibility to the quantitative assumption of multi-omics data integration, in chapter 2, I also reported two findings counter to the assumption. First, I did not observe a conserved signature between the omics data of the affected molecular function of *F. candida* to imidacloprid exposure. Second, I found that only a small proportion of the entire transcriptome and proteome correlated (269 out of 4364 overlapping genes).

My findings suggest that we should combine the results of multiple omics data analyses rather than aiming at an integrative approach.

A possible solution for optimizing the quantitative correspondence between omics data is implementing more advanced models to account for any nonlinear relationship between shifts in the transcript and protein abundances (X. Zhang et al., 2018). Although I am confident that this will improve multi-omics integration, this approach does not address my most fundamental concern. In chapter 1, I discussed that shifts in the transcript and protein abundances have different meanings. Transcription occurs within minutes, while protein levels are affected in hours (Canzler et al., 2020). Meanwhile, transcripts have a high turnover and proteins a slow turnover, i.e., minutes or hours to months (Canzler et al., 2020). Lastly, the relationship between the transcript's abundances and its function is strongly correlated. In contrast, the protein abundance does not indicate its function, e.g., enzymatic activity. Therefore, I concluded in chapter 2 that the transcriptome can be seen as a direct proxy of energy expenditure, the proteome of energy investment. In light thereof, the true power of multi-omics data analysis is not their quantitative correspondence, i.e., integration, but rather their ability to provide information on separate processes that coincide. Combining the results of omics data analysis is more valuable to understanding mechanisms that mediate toxicity than when their analysis is forced into one integrated approach.

Are the current statistical methods suitable for identifying toxicogenomic fingerprints?

For the application of toxicogenomic fingerprints in diagnosing pesticide soil contamination, the reliability of gene expression patterns in indicating pollution should be monitored under varying exposure conditions, such as pesticide mixtures and stress intensities. Exposure conditions however, are highly variable in agricultural soils (Pelosi et al., 2021; Silva et al., 2019). Therefore, in chapter 3, I obtained transcriptomic data from *F. candida* under mixture exposure of two neonicotinoids, imidacloprid and clothianidin, or imidacloprid and cyproconazole (an azole fungicide). The exposures were in a grid design finely resolved for stress intensities. From these data, I obtained toxicogenomic fingerprints for neonicotinoids and cyproconazole, and validated that biomarkers derived from these toxicogenomic fingerprints remained robust indicators for the exposure of either imidacloprid or cyproconazole even under combined exposure.

Transcriptomic data obtained under the mixture exposure contains high variability of gene expression, nonlinear concentration-expression patterns, and genetic interaction effects (Altenburger et al., 2012). In chapter 3, I argued that current differential gene expression analysis methods are unsuitable for assessing transcriptomic data primarily due to their implementation of parametric models. Therefore, we implemented Gaussian Process models to identify differential gene-expression patterns for the type of pesticide exposure, even from data that contains all three challenges of mixture transcriptomic data. The new approach was successful in the identification of toxicogenomic fingerprints for both neonicotinoid and cyproconazole exposure.

After identifying toxicogenomic fingerprints, further measures are required to assess their reliability in indicating the exposure intensity. To explain how this can be done, I have to refer again to the dynamic energy budget (Jager, 2020). At any given moment, an organism's energy uptake and storage limit its actions, i.e., its energy budget. The energy budget expenditure consists of three parts: first, in the absence of stress, energy will be distributed between resource acquisition, development, and reproduction. Second, under severe stress, the universal stress response is prioritized. Third, under mild stress, the specific-stress response is dominant - the latter consists of specific actions that vary between types of stress, i.e., the toxicogenomic fingerprints. Therefore, the ratios between these three types of energy expenditure can provide a read-out of the type and intensity of toxic exposure (Murphy et al., 2018). The transcriptome would be ideal as it captures the broadest spectrum of these actions from any omics data type, and transcript performance, i.e., protein synthesis, is more directly relatable to the transcript's abundance than proteins or metabolites (Canzler et al., 2020). Even though transcriptomics does not provide a direct measure of energy storage in lipids, proteins, or metabolites, it can measure the proportion of the transcriptome involved in energy extraction from or deposition in storage. By relating toxicogenomic fingerprints (i.e., exposure indicators) to the dynamic energy budget expenditure, toxicogenomic fingerprints become not only an exposure indicator but also an effect-based indicator. In summary, after identifying toxicogenomic fingerprints, i.e., the specific stress response, their expression must be related to the energy budget before the intensity of exposure can be determined.

In order to infer shifts in the dynamic energy budget from transcriptomics, new methods must be developed. These shifts can only be detected when the relative

expression of genes under one condition can be compared to the same relative expression in another condition. Currently, a method based on weighted gene co-expression network analysis (WGCNA) is one of the few that allows for such an assessment (Langfelder & Horvath, 2008). This framework calculates the correlation between gene expression in an assay and compares the resulting correlation network in various conditions. This approach is referred to as differential network analysis (Shojaie, 2021). However, the method of WGCNA is over 14 years old and ill-adapted to large experiments due to computational constraints when calculating the correlation of gene-to-gene expressions and subsequent comparison of the gene co-expression networks. Feature compression can resolve these constraints by combining genes based on their expression patterns and sequence similarity. Calculating the correlation of the expression patterns of all genes (n) in an assay is a computational cost of n^2: i.e., the computation cost increases exponentially per gene. When comparing networks between conditions, the size of the network n^2 is compared to a network of n^2 in another condition. Likewise, per gene, the computational costs for network comparison grow exponentially. The computational cost savings of feature compression is exponential for two computationally intense steps of the WGCNA approach. Moreover, the WGCNA software currently only accommodates assessing a linear correlation between gene cluster expression and an experimental condition (Langfelder & Horvath, 2008). Future endeavors should seek to implement nonlinear experimental-condition to gene-expression relationships. Implementing both additions to the WGCNA approach would prove a powerful tool for tracking the correlation of gene clusters and their molecular function under varying stress conditions. The improved WGCNA differential network analysis will allow scientists to track gene expression between conditions and relative to each other. This may provide a means to link toxicogenomic fingerprint expression to other expenditures of the dynamic energy budget.

Are biomarkers derived from toxicogenomic fingerprints robust indicators of neonicotinoid exposure?

In chapters 2 and 3, I identified toxicogenomic fingerprints and derived various biomarkers for neonicotinoid exposure. In chapters 4 and 5, I have demonstrated a high variability of these biomarker expressions under mutual exposure of two neonicotinoids, imidacloprid and thiacloprid, together with two metabolic inhibitors

piperonyl butoxide (PBO) and diethyl maleate (DEM). I elected imidacloprid and thiacloprid as these have differential toxicity to springtail reproduction and survival (de Lima e Silva et al., 2017, 2021). In bee species, this differential toxicity is attributed to varying rates of detoxification of these neonicotinoids by biotransformation enzymes (Beadle et al., 2019; Manjon et al., 2018). The metabolomic inhibitors provided a "stress-test" by their probable inhibition of biotransformation enzymes. Chapters 4 and 5 sought to identify biomarkers that remained reliable indicators for both neonicotinoids even under metabolic inhibition of their primary route of detoxification. Using the same statistical approach based on Generalized Additive Models (GAMs), I investigated biomarker reliability for indicating exposure to both neonicotinoids. I found that no biomarker could reliably indicate the exposure of both neonicotinoids in the presence of both metabolic inhibitors. For example, the expression of the neonicotinoid target site, *nicotinic acetylcholine receptor* (*nAChR*), was overall increased by exposure to either neonicotinoid. However, under metabolic inhibition, *nAChR* expression varied; hence, the expression did not reliably indicate neonicotinoid exposure intensity in all cases. Therefore, I concluded that multiple biomarkers must be integrated into a single panel for diagnosing neonicotinoid soil pollution. When combined, these biomarkers remain robust indicators of neonicotinoid pollution.

I am not alone in proposing multiple biomarker integration into a single panel for diagnosing environmental pollution (Fontanetti et al., 2011; Lionetto et al., 2019). We argue that the effects of toxic exposure vary; therefore, multiple biomarkers must be incorporated into a single panel to capture this range of effects. However, extending a biomarker panel by including various genes for each pollutant type is impractical when diagnosing pesticide pollution. Unlike pollutants that activate pathways solely for exogenic compound detoxification (such as metals), pesticides inhibit or enhance pathways already expressed in the absence of stress and synergize with key processes of concern (Hawkins et al., 2019). Baseline expression of pesticide biomarkers based on endogenous pathways already varies in the absence of pesticide exposure. Therefore, biomarker expression must not only be related to its expression under control conditions but also to the expression of other biomarkers that represent various pathways and key processes of concern. Following this line of logic, a pesticide exposure biomarker panel must assess the expression of a vast number of biomarkers. However, these biomarkers are measured by Real-Time quantitative PCR (qPCR), which imposes practical

limitations on the possible number of biomarkers in a panel, simply because there is limited space on qPCR machines, and the labor and material costs of these surveys increase with the number of biomarkers measured.

A yet not existing methodology to forgo practical limitations on the number of biomarkers is to measure the transcriptome directly. The advantage is that this data is unconstrained in any way to the number of genes surveyed and, thereby, it can remain indicative of the exposure to any (novel) contaminant. However, the drawback of unconstrained customization is that a method requires a high degree of expertise and optimization whenever applied to a new type of pollution. A promising middle ground between gene-expression biomarkers by qPCR and transcriptomic data for diagnosing pollution is the EcoToxChip. The ExoToxChip is based on qPCR. However, instead of one gene per well, it measures the expression of 30 genes per well on a mass-produced 96-well plate (Basu et al., 2019). As these 96-well plates are mass-produced, labor intensity, the complexity of the data analysis, and the material costs of EcoToxChip are low. Regrettably, the EcoToxChip only accommodates (semi-)aquatic organisms missing a vital section of the terrestrial ecosystem, i.e., the soil. Moreover, whether this method remains indicative for any type of novel contaminant remains unknown as it has been developed recently. Developing an EcoToxChip for *F. candida* risk assessors will gain clear metrics of soil pollution that can bridge the gap until the academic community provides a standardized implementation of transcriptomic data for diagnosing environmental pollution.

The solution to the low reliability of a single biomarker in indicating pesticide pollution is multiple biomarker integration into a panel. The solution to the low scalability of incorporating multiple biomarkers into a panel can be the application of transcriptomic data or an EcoToxChip in diagnosing pesticide soil pollution. In both cases, we are no longer measuring biomarkers but toxicogenomic fingerprints. No single gene is measured, rather the expression of entire pathways or processes of concern is assessed. Therefore, in this section, I argued that we should move from biomarkers to toxicogenomic fingerprints for diagnosing complex environmental pollution mixtures.

The future of ecotoxicogenomics

In the previous sections, I have discussed and given my opinion on various improvements and future perspectives for toxicogenomic fingerprint identification and its implementation in environmental risk assessment. Therefore, I will limit my discussion to one final future perspective of ecotoxicogenomics. My opinions mentioned above were:

1. The practical benefit of standardized exposure duration for *F. candida* gene expression surveys outweighs concerns over differences in toxicant toxicodynamics and toxicokinetics when applying gene expression for diagnosing environmental pollution.
2. The combined results of multiple omics data analysis are more valuable than their integrative assessment.
3. Methodologies are required to assess energy budget allocation by tracking shifts in gene expression and their molecular function over various exposure conditions.
4. We should move from biomarkers to toxicogenomic fingerprints for diagnosing complex environmental pollution mixtures.

If my vision is attenable and successful, toxicogenomic fingerprints could identify the type of exposure and its intensity. These outcomes match the aims of Adverse Outcome Pathways (AOPs). However, I believe AOPs remain essential for the acceptability of, e.g., toxicogenomic fingerprints as a tool for environmental risk assessment. That the necessity of AOPs is questionable does indicate its main pitfall: are AOPs a tool for environmental risk assessors or for academics? Of course, AOPs do not require to submit to either role. Nevertheless, the development of AOPs will speed up, and its acceptability by a broader community will improve when we clarify the envisioned role of AOPs.

A crucial first step for the acceptability of AOPs by risk assessors is to identify and align AOPs to their mindset. The debate surrounding the acceptability of AOPs by risk assessors often focuses on how mechanisms underlying toxic effects can be incorporated more accurately into AOPs or their various possible applications (Garcia-Reyero & Perkins, 2011). I believe we should invert the discussion, not focus on what is possible but on what is crucial for the end users. Not focus on possible application, but: what will AOPs allow risk assessors to achieve they

currently cannot? Not focus on how risk assessors can apply AOPs, but when will AOPs have failed.

The term toxicogenomic fingerprints convey two crucial aspects: i.e., what it is and what it does. Toxicogenomic fingerprints are genome-wide molecular imprints by which we can identify toxic exposure akin to fingerprints for human identification. In contrast, the term AOP only conveys what it is and not what it does. Other AOP terminology also does not convey the purpose of its components. For example, Key Events are defined as necessary and relevant responses of the organism to toxic exposure (OECD, 2018). Better terminology would be: Key Evens are reliable and informative responses of the organism allowing the environmental risk assessment of pollutants. We cannot only improve the current AOP acceptability by improving terminology, but the end goal should also be to help prioritize technical developments. Originally, AOPs were designed to be species and chemical agnostic to allow broad application (Ankley et al., 2010). However, worthwhile pursuits will allow for quantitative (qAOPs) and domain-specific AOPs (Becker et al., 2015; LaLone et al., 2013). In other words, it seeks to accurately correlate responses across different levels of biological organization and allow species-specific AOPs. First, a qAOP cannot be developed in a species agnostic manner as the quantitative correspondence between the layers of biological organization is inevitably not conserved between species. Second, an end-user can only apply an AOP confidently when assured that the information it provides is reliable for their species. Therefore, both domain-specific AOPs and qAOPs will improve the acceptability of the AOP concept as they inform the end-users of the AOP reliability and in which cases this is ensured. Succinctly, there is a discrepancy between the developers and users of technology, academics, and risk assessors, respectively. The developers ask what problem they can solve with their invention. The users ask whether this technology allows them to achieve their goals more effectively and reliably.

Conclusion

This thesis provided statistical and methodological approaches to identify toxicogenomic fingerprints to assess pesticide-soil contamination. First, I identified the 48h time point as the most opportune moment for toxicogenomic fingerprint identification. Second, I argued that the results of multiple types of omics data

could be combined in toxicogenomic fingerprint identification. Third, I proposed Gaussian Process models for toxicogenomic fingerprint identification. Lastly, the biomarkers derived from these toxicogenomic fingerprints are "stress-tested" under metabolic inhibition and deemed robust indicators for neonicotinoid exposure.

In the general discussion, I am dismissive of toxicodynamics, toxicokinetics, and certain developments of AOPs without putting the end-user experience first. In academia, we tend to describe and inform on the technical limitation we face rather than critically assess the intent that drives our work. Academia focuses on finding technical solutions and accurately describing complex processes. This tendency is highly understandable because this is the monopoly of academia in society. However, one might forget that hidden in my thesis's figures, tables, equations, and jargon-riddled pages, my research aimed to contribute to methods to *diagnose* complex environmental pollution. When concerned with technical details, it is easy to forget that the world is experiencing its sixth extinction event, and pesticides contribute to this rapid loss of biodiversity (Eldredge, 2009; FAO, ITPS, GSBI, 2020). We are running out of time to develop high-throughput methods to diagnose pesticide pollution and guide abatement efforts. I firmly believe that by letting the envisioned end-goal guide our research, we can speed up the development and acceptability of new methodology to this end. Therefore, I want to conclude my thesis: we are running out of time; let us put intent first.

References

Afgan, E., Baker, D., van den Beek, M., Blankenberg, D., Bouvier, D., Čech, M., Chilton, J., Clements, D., Coraor, N., Eberhard, C., Grüning, B., Guerler, A., Hillman-Jackson, J., Von Kuster, G., Rasche, E., Soranzo, N., Turaga, N., Taylor, J., Nekrutenko, A., & Goecks, J. (2016). The Galaxy platform for accessible, reproducible and collaborative biomedical analyses: 2016 update. *Nucleic Acids Research*, *44*(W1), W3–W10. https://doi.org/10.1093/nar/gkw343

Altenburger, R., Scholz, S., Schmitt-Jansen, M., Busch, W., & Escher, B. I. (2012). Mixture toxicity revisited from a toxicogenomic perspective. *Environmental Science and Technology*, *46*(5), 2508–2522. https://doi.org/10.1021/es2038036

Anand, S., Foot, N., Ang, C. S., Gembus, K. M., Keerthikumar, S., Adda, C. G., Mathivanan, S., & Kumar, S. (2018). Arrestin-Domain Containing Protein 1 (Arrdc1) Regulates the Protein Cargo and Release of Extracellular Vesicles. *Proteomics*, *18*(17), 1–6. https://doi.org/10.1002/pmic.201800266

Ankley, G. T., Bennett, R. S., Erickson, R. J., Hoff, D. J., Hornung, M. W., Johnson, R. D., Mount, D. R., Nichols, J. W., Russom, C. L., Schmieder, P. K., Serrrano, J. A., Tietge, J. E., & Villeneuve, D. L. (2010). Adverse outcome pathways: A conceptual framework to support ecotoxicology research and risk assessment. *Environmental Toxicology and Chemistry*, *29*(3), 730–741. https://doi.org/10.1002/etc.34

Apitz, S. E., Davis, J. W., Finkelstein, K., Hohreiter, D. W., Hoke, R., Jensen, R. H., Jersak, J., Kirtay, V. J., Mack, E. E., Magar, V. S., Moore, D., Reible, D., & Stahl, R. G. (2005). Assessing and managing contaminated sediments: part I, developing an effective investigation and risk evaluation strategy. *Integrated Environmental Assessment and Management*, *1*(1), 2–8. https://doi.org/10.1897/IEAM_2004a-002.1

Aschieri, P., Jurčo, B., Schupp, P., & Wess, J. (2003). Noncommutative GUTs, Standard Model and C,P,T. *Nuclear Physics B*, *651*(1–2), 45–70. https://doi.org/10.1016/S0550-3213(02)00937-9

Bakker, R., Ekelmans, A., Xie, L., Vooijs, R., Roelofs, D., Ellers, J., Hoedjes, K. M., & van Gestel, C. A. M. (2022). Biomarker development for neonicotinoid exposure in soil under interaction with the synergist piperonyl butoxide in *Folsomia candida*. *Environmental Science and Pollution Research*, 1–17. https://doi.org/10.1007/s11356-022-21362-z

Bakker, R., Xie, L., Vooijs, R., Hoedjes, K. M., & van Gestel, C. A. M. (n.d.). Validation of biomarkers for neonicotinoid exposure in *Folsomia candida* under mutual exposure to diethyl maleate. *Environmental Science and Pollution Research*, 1–16. https://doi.org/10.21203/rs.3.rs-1489709/v1

Bao, H., Gao, H., Zhang, Y., Fan, D., Fang, J., & Liu, Z. (2016). The roles of CYP6AY1 and CYP6ER1 in imidacloprid resistance in the brown planthopper: Expression levels and detoxification efficiency. *Pesticide Biochemistry and Physiology*, *129*, 70–74. https://doi.org/10.1016/j.pestbp.2015.10.020

Barsnes, H., & Vaudel, M. (2018). SearchGUI: A Highly Adaptable Common Interface for Proteomics Search and de Novo Engines. *Journal of Proteome Research*, *17*(7), 2552–2555. https://doi.org/10.1021/acs.jproteome.8b00175

Basu, N., Crump, D., Head, J., Hickey, G., Hogan, N., Maguire, S., Xia, J., & Hecker, M. (2019). EcoToxChip: A next-generation toxicogenomics tool for chemical prioritization and environmental management. *Environmental Toxicology and Chemistry*, *38*(2), 279–288. https://doi.org/10.1002/etc.4309

Beadle, K., Singh, K. S., Troczka, B. J., Randall, E., Zaworra, M., Zimmer, C. T., Hayward, A., Reid, R., Kor, L., Kohler, M., Buer, B., Nelson, D. R., Williamson, M. S., Davies, T. G. E., Field, L. M., Nauen, R., & Bass, C. (2019). Genomic insights into neonicotinoid sensitivity in the solitary bee *Osmia bicornis*. *PLOS Genetics*, *15*(2), e1007903. https://doi.org/10.1371/journal.pgen.1007903

Becker, R. A., Ankley, G. T., Edwards, S. W., Kennedy, S. W., Linkov, I., Meek, B., Sachana, M., Segner, H., Van Der Burg, B., Villeneuve, D. L., Watanabe, H., & Barton-Maclaren, T. S. (2015). Increasing Scientific Confidence in Adverse Outcome Pathways: Application of Tailored Bradford-Hill Considerations for Evaluating Weight of Evidence. *Regulatory Toxicology and Pharmacology*, *72*(3), 514–537. https://doi.org/10.1016/j.yrtph.2015.04.004

Beckman, R. J., & Weisberg, S. (1987). Applied Linear Regression. In *Technometrics* (Vol. 29, Issue 1). https://doi.org/10.2307/1269895

Bielow, C., Mastrobuoni, G., & Kempa, S. (2016). Proteomics Quality Control: Quality Control Software for MaxQuant Results. *Journal of Proteome Research*, *15*(3), 777–787. https://doi.org/10.1021/acs.jproteome.5b00780

Binukumar, B. K., & Gill, K. D. (2010). Cellular and molecular mechanisms of dichlorvos neurotoxicity: Cholinergic, nonchlolinergic, cell signaling, gene expression and therapeutic aspects. *Indian Journal of Experimental Biology*, *48*(7), 697–709.

Bonmatin, J. M., Giorio, C., Girolami, V., Goulson, D., Kreutzweiser, D. P., Krupke, C., Liess, M., Long, E., Marzaro, M., Mitchell, E. A., Noome, D. A., Simon-Delso, N., & Tapparo, A. (2015). Environmental fate and exposure; neonicotinoids and fipronil. *Environmental Science and Pollution Research*, *22*(1), 35–67. https://doi.org/10.1007/s11356-014-3332-7

Borsuah, J. F., Messer, T. L., Snow, D. D., Comfort, S. D., & Mittelstet, A. R. (2020). Literature review: Global neonicotinoid insecticide occurrence in aquatic environments. *Water (Switzerland)*, *12*(12), 1–17. https://doi.org/10.3390/w12123388

Brack, W. (2003). Effect-directed analysis: A promising tool for the identification of organic toxicants in complex mixtures? *Analytical and Bioanalytical Chemistry*, *377*(3), 397–407. https://doi.org/10.1007/s00216-003-2139-z

Buszewski, B., Bukowska, M., Ligor, M., & Staneczko-Baranowska, I. (2019). A holistic study of neonicotinoids neuroactive insecticides—properties, applications, occurrence, and analysis. *Environmental Science and Pollution Research*, 34723–34740. https://doi.org/10.1007/s11356-019-06114-w

Camp, A. A., & Lehmann, D. M. (2021). Impacts of Neonicotinoids on the Bumble Bees *Bombus terrestris* and *Bombus impatiens* Examined through the Lens of an Adverse Outcome Pathway Framework. *Environmental Toxicology and Chemistry*, *40*(2), 309–322. https://doi.org/10.1002/etc.4939

Canzler, S., Schor, J., Busch, W., Schubert, K., Rolle-Kampczyk, U. E., Seitz, H., Kamp, H., von Bergen, M., Buesen, R., & Hackermüller, J. (2020). Prospects and challenges of multi-omics data integration in toxicology. *Archives of Toxicology*, *94*(2), 371–388. https://doi.org/10.1007/s00204-020-02656-y

Casida, J. E. (2011). Neonicotinoid metabolism: Compounds, substituents, pathways, enzymes, organisms, and relevance. *Journal of Agricultural and Food Chemistry*, *59*(7), 2923–2931. https://doi.org/10.1021/jf102438c

Chambers, M. C., MacLean, B., Burke, R., Amodei, D., Ruderman, D. L., Neumann, S., Gatto, L., Fischer, B., Pratt, B., Egertson, J., Hoff, K., Kessner, D., Tasman, N., Shulman, N., Frewen, B., Baker, T. A., Brusniak, M. Y., Paulse, C., Creasy, D., … Mallick, P. (2012). A cross-platform toolkit for mass spectrometry and proteomics. *Nature Biotechnology*, *30*(10), 918–920. https://doi.org/10.1038/nbt.2377

Chen, A., Zhang, H., Shan, T., Shi, X., & Gao, X. (2020). The overexpression of three cytochrome P450 genes CYP6CY14, CYP6CY22 and CYP6UN1 contributed to metabolic resistance to dinotefuran in melon/cotton aphid, *Aphis gossypii* Glover. *Pesticide Biochemistry and Physiology*, *167*(March), 104601. https://doi.org/10.1016/j.pestbp.2020.104601

Chen, G., de Boer, T. E., Wagelmans, M., van Gestel, C. A. M., van Straalen, N. M., & Roelofs, D. (2014). Integrating transcriptomics into triad-based soil-quality assessment. *Environmental Toxicology and Chemistry*, *33*(4), 900–909. https://doi.org/10.1002/etc.2508

Christen, V., & Fent, K. (2017). Exposure of honey bees (Apis mellifera) to different classes of insecticides exhibit distinct molecular effect patterns at concentrations that mimic environmental contamination. *Environmental Pollution*, *226*, 48–59. https://doi.org/10.1016/j.envpol.2017.04.003

Christen, V., Mittner, F., & Fent, K. (2016). Molecular Effects of Neonicotinoids in Honey Bees (*Apis mellifera*). *Environmental Science and Technology*, *50*(7), 4071–4081. https://doi.org/10.1021/acs.est.6b00678

Christen, V., Schirrmann, M., Frey, J. E., & Fent, K. (2018). Global Transcriptomic Effects of Environmentally Relevant Concentrations of the Neonicotinoids Clothianidin, Imidacloprid, and Thiamethoxam in the Brain of Honey Bees (*Apis mellifera*). *Environmental Science and Technology*, *52*(13), 7534–7544. https://doi.org/10.1021/acs.est.8b01801

Chua, J. P., De Calbiac, H., Kabashi, E., & Barmada, S. J. (2021). Autophagy and ALS: mechanistic insights and therapeutic implications. *Autophagy*, *00*(00), 1–29. https://doi.org/10.1080/15548627.2021.1926656

Claudianos, C., Ranson, H., Johnson, R. M., Biswas, S., Schuler, M. A., Berenbaum, M. R., Feyereisen, R., & Oakeshott, J. G. (2006). A deficit of detoxification enzymes: Pesticide sensitivity and environmental response in the honeybee. *Insect Molecular Biology*, *15*(5), 615–636. https://doi.org/10.1111/j.1365-2583.2006.00672.x

Cragg, R. G., & Bardgett, R. D. (2001). *ScienceDirect - Soil Biology and Biochemistry How changes in soil faunal diversity and composition within a trophic group influence decomposition processes*. *33*, 2073–2081.

Crouau, Y., & Cazes, L. (2003). What causes variability in the *Folsomia candida* reproduction test? *Applied Soil Ecology*, *22*(2), 175–180. https://doi.org/10.1016/S0929-1393(02)00128-2

Cunningham, F., Achuthan, P., Akanni, W., Allen, J., Amode, M. R., Armean, I. M., Bennett, R., Bhai, J., Billis, K., Boddu, S., Cummins, C., Davidson, C., Dodiya, K. J., Gall, A., Girón, C. G., Gil, L., Grego, T., Haggerty, L., Haskell, E., … Flicek, P. (2019). Ensembl 2019. *Nucleic Acids Research*, *47*(D1), D745–D751. https://doi.org/10.1093/nar/gky1113

Dastogeer, K. M. G., Tumpa, F. H., Sultana, A., Akter, M. A., & Chakraborty, A. (2020). Plant microbiome–an account of the factors that shape community composition and diversity. *Current Plant Biology*, *23*(April), 100161. https://doi.org/10.1016/j.cpb.2020.100161

de Boer, M. E., Berg, S., Timmermans, M. J. T. N., den Dunnen, J. T., van Straalen, N. M., Ellers, J., & Roelofs, D. (2011). High throughput nano-liter RT-qPCR to classify soil contamination using a soil arthropod. *BMC Molecular Biology*, *12*. https://doi.org/10.1186/1471-2199-12-11

de Boer, M. E., de Boer, T. E., Mariën, J., Timmermans, M. J. T. N., Nota, B., van Straalen, N. M., Ellers, J., & Roelofs, D. (2009). Reference genes for QRT-PCR tested under various stress conditions in *Folsomia candida* and *Orchesella cincta* (Insecta, Collembola). *BMC Molecular Biology*, *10*. https://doi.org/10.1186/1471-2199-10-54

de Boer, M. E., Ellers, J., Van Gestel, C. A. M., Den Dunnen, J. T., Van Straalen, N. M., & Roelofs, D. (2013). Transcriptional responses indicate attenuated oxidative stress in the springtail *Folsomia candida* exposed to mixtures of cadmium and phenanthrene. *Ecotoxicology*, *22*(4), 619–631. https://doi.org/10.1007/s10646-013-1053-1

de Boer, T. E., Holmstrup, M., van Straalen, N. M., & Roelofs, D. (2010). The effect of soil pH and temperature on *Folsomia candida* transcriptional regulation. *Journal of Insect Physiology*, *56*(4), 350–355. https://doi.org/10.1016/j.jinsphys.2009.11.004

de Lima e Silva, C., Brennan, N., Brouwer, J. M., Commandeur, D., Verweij, R. A., & van Gestel, C. A. M. (2017). Comparative toxicity of imidacloprid and thiacloprid to different species of soil invertebrates. *Ecotoxicology*, *26*(4), 555–564. https://doi.org/10.1007/s10646-017-1790-7

de Lima e Silva, C., Rooij, W., Verweij, R. A., & Gestel, C. A. M. (2020). Toxicity in Neonicotinoids to *Folsomia candida* and *Eisenia andrei*. *Environmental Toxicology and Chemistry*, *39*(3), 548–555. https://doi.org/10.1002/etc.4634

de Lima e Silva, C., van Haren, C., Mainardi, G., de Rooij, W., Ligtelijn, M., van Straalen, N. M., & van Gestel, C. A. M. (2021). Bringing ecology into toxicology: Life-cycle toxicity of two neonicotinoids to four different species of springtails in LUFA 2.2 natural soil. *Chemosphere*, *263*. https://doi.org/10.1016/j.chemosphere.2020.128245

de Matthews, A. G., van der Wilk, M., Nickson, T., Fujii, K., Boukouvalas, A., León-Villagrá, P., Ghahramani, Z., & Hensman, J. (2017). GPflow: A Gaussian Process Library using TensorFlow Mark van der Wilk. *Journal of Machine Learning Research*, *18*, 1–6. https://jmlr.org/papers/v18/16-537.html

Dean, R. T., & Dunsmuir, W. T. M. (2016). Dangers and uses of cross-correlation in analyzing time series in perception, performance, movement, and neuroscience: The importance of constructing transfer function autoregressive models. *Behavior Research Methods*, *48*(2), 783–802. https://doi.org/10.3758/s13428-015-0611-2

Durinck, S., Spellman, P. T., Birney, E., & Huber, W. (2009). Mapping identifiers for the integration of genomic datasets with the R/ Bioconductor package biomaRt. *Nature Protocols*, *4*(8), 1184–1191. https://doi.org/10.1038/nprot.2009.97

Duvenaud, D. K. (2014). Automatic Model Construction with Gaussian Processes. *PhD Thesis, University of Cambridge*, *June*, XIII, 144. https://www.repository.cam.ac.uk/handle/1810/247281%0Ahttps://www.cs.toronto.edu/~duvenaud/thesis.pdf

EASAC. (2015). *Ecosystem Services, Agriculture and Neonicotinoids* (Issue April).

Eldredge, N. (2009). *Eldridge-6th-extinction*. 1–6.

Escher, B. I., Stapleton, H. M., & Schymanski, E. L. (2020). Tracking complex mixtures of chemicals in our changing environment. *Science*, *367*(6476), 388–392. https://doi.org/10.1126/science.aay6636

Ewald, J., Soufan, O., Xia, J., & Basu, N. (2021). FastBMD: an online tool for rapid benchmark dose–response analysis of transcriptomics data. *Bioinformatics*, *37*(7), 1035–1036. https://doi.org/10.1093/bioinformatics/btaa700

Ewels, P., Magnusson, M., Lundin, S., & Käller, M. (2016). MultiQC: Summarize analysis results for multiple tools and samples in a single report. *Bioinformatics*, *32*(19), 3047–3048. https://doi.org/10.1093/bioinformatics/btw354

Faddeeva-Vakhrusheva, A., Kraaijeveld, K., Derks, M. F. L., Anvar, S. Y., Agamennone, V., Suring, W., Kampfraath, A. A., Ellers, J., Le Ngoc, G., van Gestel, C. A. M., Mariën, J., Smit, S., van Straalen, N. M., & Roelofs, D. (2017). Coping with living in the soil: The genome of the parthenogenetic springtail *Folsomia candida*. *BMC Genomics*, *18*(1). https://doi.org/10.1186/s12864-017-3852-x

FAO, ITPS, GSBI, S. and E. (2020). State of knowledge of soil biodiversity - Status, challenges and potentialities. In *Soil in the Environment*. FAO. https://doi.org/10.4060/cb1928en

Feng, Y., Wu, Q., Wang, S., Chang, X., Xie, W., Xu, B., & Zhang, Y. (2010). Cross-resistance study and biochemical mechanisms of thiamethoxam resistance in b-biotype *bemisia tabaci* (Hemiptera: Aleyrodidae). *Pest Management Science*, *66*(3), 313–318. https://doi.org/10.1002/ps.1877

Fent, K., Schmid, M., Hettich, T., & Schmid, S. (2020). The neonicotinoid thiacloprid causes transcriptional alteration of genes associated with mitochondria at environmental concentrations in honey bees. *Environmental Pollution*, *266*, 115297. https://doi.org/10.1016/j.envpol.2020.115297

Feyereisen, R. (2018). Toxicology: Bee P450s Take the Sting out of Cyanoamidine Neonicotinoids. *Current Biology*, *28*(9), R560–R562. https://doi.org/10.1016/j.cub.2018.03.013

Fontanetti, Carmem, S., Nogarol, Larissa, R., de Souza, Raphael, B., Perex, Danielli, G., & Maziviero, Guilherme, T. (2011). Bioindicators and Biomarkers in the assessment of soil toxicity. *Soil Contamination*, 143–169.

Fountain, M. T., & Hopkin, S. P. (2005). *Folsomia candida* (Collembola): A "standard" soil arthropod. *Annual Review of Entomology*, *50*(February 2005), 201–222. https://doi.org/10.1146/annurev.ento.50.071803.130331

Garcia-Reyero, N., & Perkins, E. J. (2011). Systems biology: Leading the revolution in ecotoxicology. *Environmental Toxicology and Chemistry*, *30*(2), 265–273. https://doi.org/10.1002/etc.401

Gatto, L., & Lilley, K. S. (2012). Msnbase-an R/Bioconductor package for isobaric tagged mass spectrometry data visualization, processing and quantitation. *Bioinformatics*, *28*(2), 288–289. https://doi.org/10.1093/bioinformatics/btr645

Glavan, G., & Bozic, J. (2013). The synergy of xenobiotics in honey bee *Apis mellifera*: mechanisms and effects. *Acta Biologica Slovenica*, *56*(October 2015), 11–25.

Godfray, H. C. J., Beddington, J. R., Crute, I. R., Haddad, L., Lawrence, D., Muir, J. F., Pretty, J., Robinson, S., Thomas, S. M., & Toulmin, C. (2010). Food Security: The Challenge of Feeding 9 Billion People. *Science*, *327*(5967), 812–818. https://doi.org/10.1126/science.1185383

Goeminne, L. J. E., Sticker, A., Martens, L., Gevaert, K., & Clement, L. (2020). MSqRob Takes the Missing Hurdle: Uniting Intensity- And Count-Based Proteomics. *Analytical Chemistry*, *92*(9), 6278–6287. https://doi.org/10.1021/acs.analchem.9b04375

Gomez-Eyles, J. L., Svendsen, C., Lister, L., Martin, H., Hodson, M. E., & Spurgeon, D. J. (2009). Measuring and modelling mixture toxicity of imidacloprid and thiacloprid on *Caenorhabditis elegans* and *Eisenia fetida*. *Ecotoxicology and Environmental Safety*, *72*(1), 71–79. https://doi.org/10.1016/j.ecoenv.2008.07.006

Gornall, J., Betts, R., Burke, E., Clark, R., Camp, J., Willett, K., & Wiltshire, A. (2010). Implications of climate change for agricultural productivity in the early twenty-first century. *Philosophical Transactions of the Royal Society B: Biological Sciences*, *365*(1554), 2973–2989. https://doi.org/10.1098/rstb.2010.0158

Goulson, D. (2013). An overview of the environmental risks posed by neonicotinoid insecticides. *Journal of Applied Ecology*, *50*(4), 977–987. https://doi.org/10.1111/1365-2664.12111

Gradish, A. E., Van Der Steen, J., Scott-Dupree, C. D., Cabrera, A. R., Cutler, G. C., Goulson, D., Klein, O., Lehmann, D. M., Lückmann, J., O'Neill, B., Raine, N. E., Sharma, B., & Thompson, H. (2019). Comparison of Pesticide Exposure in Honey Bees (Hymenoptera: Apidae) and Bumble Bees (Hymenoptera: Apidae): Implications for Risk Assessments. *Environmental Entomology*, *48*(1), 12–21. https://doi.org/10.1093/ee/nvy168

Gunstone, T., Cornelisse, T., Klein, K., Dubey, A., & Donley, N. (2021). Pesticides and Soil Invertebrates: A Hazard Assessment. *Frontiers in Environmental Science*, *9*(May), 1–21. https://doi.org/10.3389/fenvs.2021.643847

Haas, J., & Nauen, R. (2021). Pesticide risk assessment at the molecular level using honey bee cytochrome P450 enzymes: A complementary approach. *Environment International*, *147*, 106372. https://doi.org/10.1016/j.envint.2020.106372

Haider, S., & Pal, R. (2013). Integrated Analysis of Transcriptomic and Proteomic Data. *Current Genomics*, *14*(2), 91–110. https://doi.org/10.2174/1389202911314020003

Hawkins, N. J., Bass, C., Dixon, A., & Neve, P. (2019). The evolutionary origins of pesticide resistance. *Biological Reviews*, *94*(1), 135–155. https://doi.org/10.1111/brv.12440

Hodgson, E., & Levi, P. E. (1999). Interactions of Piperonyl Butoxide with Cytochrome P450. In *Piperonyl Butoxide* (pp. 41–II). Elsevier. https://doi.org/10.1016/B978-012286975-4/50005-X

Innocenti, G., & Sabatini, M. A. (2018). Collembola and plant pathogenic, antagonistic and arbuscular mycorrhizal fungi: A review. *Bulletin of Insectology*, *71*(1), 71–76.

Iwasa, T., Motoyama, N., Ambrose, J. T., & Roe, R. M. (2004). Mechanism for the differential toxicity of neonicotinoid insecticides in the honey bee, *Apis mellifera*. *Crop Protection*, *23*(5), 371–378. https://doi.org/10.1016/j.cropro.2003.08.018

Jager, T. (2020). Revisiting simplified DEBtox models for analysing ecotoxicity data. *Ecological Modelling*, *416*(December 2019), 108904. https://doi.org/10.1016/j.ecolmodel.2019.108904

Kalaitzis, A. A., & Lawrence, N. D. (2011). A simple approach to ranking differentially expressed gene expression time courses through Gaussian process regression. *BMC Bioinformatics*, *12*. https://doi.org/10.1186/1471-2105-12-180

Kaufman, L., & Rousseeuw, P. J. (1990). Finding Groups in Data. In L. Kaufman & P. J. Rousseeuw (Eds.), *Finding Groups in Data: An introduction to Cluster Analysis*. John Wiley & Sons, Inc. https://doi.org/10.1002/9780470316801

Ketterman, A. J., Saisawang, C., & Wongsantichon, J. (2011). Insect glutathione transferases. *Drug Metabolism Reviews*, *43*(2), 253–265. https://doi.org/10.3109/03602532.2011.552911

Kim, S., & Pevzner, P. A. (2014). MS-GF+ makes progress towards a universal database search tool for proteomics. *Nature Communications*, *5*. https://doi.org/10.1038/ncomms6277

King, A. M., & Macrae, T. H. (2015). Insect heat shock proteins during stress and diapause. *Annual Review of Entomology*, *60*, 59–75. https://doi.org/10.1146/annurev-ento-011613-162107

LaLone, C. A., Villeneuve, D. L., Burgoon, L. D., Russom, C. L., Helgen, H. W., Berninger, J. P., Tietge, J. E., Severson, M. N., Cavallin, J. E., & Ankley, G. T. (2013). Molecular target sequence similarity as a basis for species extrapolation to assess the ecological risk of chemicals with known modes of action. *Aquatic Toxicology*, *144–145*, 141–154. https://doi.org/10.1016/j.aquatox.2013.09.004

LaLone, C. A., Villeneuve, D. L., Wu-Smart, J., Milsk, R. Y., Sappington, K., Garber, K. V., Housenger, J., & Ankley, G. T. (2017). Weight of evidence evaluation of a network of adverse outcome pathways linking activation of the nicotinic acetylcholine receptor in honey bees to colony death. *Science of the Total Environment*, *584–585*, 751–775. https://doi.org/10.1016/j.scitotenv.2017.01.113

Langfelder, P., & Horvath, S. (2008). WGCNA: An R package for weighted correlation network analysis. *BMC Bioinformatics*, *9*. https://doi.org/10.1186/1471-2105-9-559

Larras, F., Billoir, E., Baillard, V., Siberchicot, A., Scholz, S., Wubet, T., Tarkka, M., Schmitt-Jansen, M., & Delignette-Muller, M. L. (2018). DRomics: A Turnkey Tool to Support the Use of the Dose-Response Framework for Omics Data in Ecological Risk Assessment. *Environmental Science and Technology*, *52*(24), 14461–14468. https://doi.org/10.1021/acs.est.8b04752

Lee, J. W., Won, E. J., Raisuddin, S., & Lee, J. S. (2015). Significance of adverse outcome pathways in biomarker-based environmental risk assessment in aquatic organisms. *Journal of Environmental Sciences (China)*, *35*, 115–127. https://doi.org/10.1016/j.jes.2015.05.002

Leung, K. M. Y. (2018). Joining the dots between omics and environmental management. *Integrated Environmental Assessment and Management*, *14*(2), 169–173. https://doi.org/10.1002/ieam.2007

Levitsky, L. I., Ivanov, M. V., Lobas, A. A., Bubis, J. A., Tarasova, I. A., Solovyeva, E. M., Pridatchenko, M. L., & Gorshkov, M. V. (2018). IdentiPy: An Extensible Search Engine for Protein Identification in Shotgun Proteomics. *Journal of Proteome Research*, *17*(7), 2249–2255. https://doi.org/10.1021/acs.jproteome.7b00640

Lionetto, M. G., Caricato, R., & Giordano, M. E. (2019). Pollution Biomarkers in Environmental and Human Biomonitoring. *The Open Biomarkers Journal*, *9*(1), 1–9. https://doi.org/10.2174/1875318301909010001

Lohning, A. E., & Salinas, A. E. (1999). Glutathione S-transferases--a review. *Current Medicinal Chemistry*, *6*(January), 279–309.

Love, M. I., Huber, W., & Anders, S. (2014). Moderated estimation of fold change and dispersion for RNA-seq data with DESeq2. *Genome Biology*, *15*(12), 1–21. https://doi.org/10.1186/s13059-014-0550-8

Manjon, C., Troczka, B. J., Zaworra, M., Beadle, K., Randall, E., Hertlein, G., Singh, K. S., Zimmer, C. T., Homem, R. A., Lueke, B., Reid, R., Kor, L., Kohler, M., Benting, J., Williamson, M. S., Davies, T. G. E., Field, L. M., Bass, C., & Nauen, R. (2018). Unravelling the Molecular Determinants of Bee Sensitivity to Neonicotinoid Insecticides. *Current Biology*, *28*(7), 1137-1143.e5. https://doi.org/10.1016/j.cub.2018.02.045

Martin, M. (2011). Cutadapt removes adapter sequences from high-throughput sequencing reads. *EMBnet.Journal*, *17*(1), 10. https://doi.org/10.14806/ej.17.1.200

Mehta, S., Easterly, C. W., Sajulga, R., Millikin, R. J., Argentini, A., Eguinoa, I., Martens, L., Shortreed, M. R., Smith, L. M., McGowan, T., Kumar, P., Johnson, J. E., Griffin, T. J., & Jagtap, P. D. (2020). Precursor intensity-based label-free quantification software tools for proteomic and multi-omic analysis within the galaxy platform. *Proteomes*, *8*(8), 1–15. https://doi.org/10.3390/PROTEOMES8030015

Mellacheruvu, D., Wright, Z., Couzens, A. L., Lambert, J. P., St-Denis, N. A., Li, T., Miteva, Y. V, Hauri, S., Sardiu, M. E., Low, T. Y., Halim, V. A., Bagshaw, R. D., Hubner, N. C., Al-Hakim, A., Bouchard, A., Faubert, D., Fermin, D., Dunham, W. H., Goudreault, M., … Nesvizhskii, A. I. (2013). The CRAPome: A contaminant repository for affinity purification-mass spectrometry data. *Nature Methods*, *10*(8), 730–736. https://doi.org/10.1038/nmeth.2557

Moriya, Y., Itoh, M., Okuda, S., Yoshizawa, A. C., & Kanehisa, M. (2007). KAAS: An automatic genome annotation and pathway reconstruction server. *Nucleic Acids Research*, *35*(SUPPL.2), 182–185. https://doi.org/10.1093/nar/gkm321

Murphy, C. A., Nisbet, R. M., Antczak, P., Garcia-Reyero, N., Gergs, A., Lika, K., Mathews, T., Muller, E. B., Nacci, D., Peace, A., Remien, C. H., Schultz, I. R., Stevenson, L. M., & Watanabe, K. H. (2018). Incorporating Suborganismal Processes into Dynamic Energy Budget Models for Ecological Risk Assessment. *Integrated Environmental Assessment and Management*, *14*(5), 615–624. https://doi.org/10.1002/ieam.4063

Nakamori, T., Fujimori, A., Kinoshita, K., Ban-nai, T., Kubota, Y., & Yoshida, S. (2010). mRNA expression of a cadmium-responsive gene is a sensitive biomarker of cadmium exposure in the soil collembolan *Folsomia candida*. *Environmental Pollution*, *158*(5), 1689–1695. https://doi.org/10.1016/j.envpol.2009.11.022

Nota, B., Bosse, M., Ylstra, B., van Straalen, N. M., & Roelofs, D. (2009). Transcriptomics reveals extensive inducible biotransformation in the soil-dwelling invertebrate *Folsomia candida* exposed to phenanthrene. *BMC Genomics*, *10*, 1–13. https://doi.org/10.1186/1471-2164-10-236

OECD. (2016). Collembolan reproduction test in soil. *Guidelines for Testing Chemicals 232*, *July*.

OECD. (2018). *Users Handbook supplement to the Guidance Document for developing and assessing Adverse Outcome Pathways*. *1*, 60. https://doi.org/https://doi.org/10.1787/5jlv1m9d1g32-en

Pantano, L. (2020). *DEGreport: Report of DEG analysis*. http://lpantano.github.io/DEGreport/

Pathiraja, D., Wee, J., Cho, K., & Choi, I. G. (2022). Soil environment reshapes microbiota of laboratory-maintained Collembola during host development. *Environmental Microbiomes*, *17*(1), 1–14. https://doi.org/10.1186/s40793-022-00411-7

Patro, R., Duggal, G., Love, M. I., Irizarry, R. A., & Kingsford, C. (2017). Salmon provides fast and bias-aware quantification of transcript expression. *Nature Methods*, *14*(4), 417–419. https://doi.org/10.1038/nmeth.4197

Pelosi, C., Bertrand, C., Daniele, G., Coeurdassier, M., Benoit, P., Nélieu, S., Lafay, F., Bretagnolle, V., Gaba, S., Vulliet, E., & Fritsch, C. (2021). Residues of currently used pesticides in soils and earthworms: A silent threat? *Agriculture, Ecosystems and Environment*, *305*(September 2020). https://doi.org/10.1016/j.agee.2020.107167

Perez, M. F., & Lehner, B. (2019). Vitellogenins - Yolk Gene Function and Regulation in *Caenorhabditis elegans*. *Frontiers in Physiology*, *10*(August). https://doi.org/10.3389/fphys.2019.01067

Pfaff, J., Reinwald, H., Ayobahan, S. U., Alvincz, J., Göckener, B., Shomroni, O., Salinas, G., Düring, R. A., Schäfers, C., & Eilebrecht, S. (2021). Toxicogenomic differentiation of functional responses to fipronil and imidacloprid in *Daphnia magna. Aquatic Toxicology*, *238*(July). https://doi.org/10.1016/j.aquatox.2021.105927

Pisa, L. W., Amaral-Rogers, V., Belzunces, L. P., Bonmatin, J. M., Downs, C. A., Goulson, D., Kreutzweiser, D. P., Krupke, C., Liess, M., Mcfield, M., Morrissey, C. A., Noome, D. A., Settele, J., Simon-Delso, N., Stark, J. D., Van Der Sluijs, J. P., Van Dyck, H., & Wiemers, M. (2014). Effects of neonicotinoids and fipronil on non-target invertebrates. *Environmental Science and Pollution Research*, *22*(1), 68–102. https://doi.org/10.1007/s11356-014-3471-x

Pitombeira de Figueirêdo, L., Daam, M. A., Mainardi, G., Mariën, J., Espíndola, E. L. G., van Gestel, C. A. M., & Roelofs, D. (2019). The use of gene expression to unravel the single and mixture toxicity of abamectin and difenoconazole on survival and reproduction of the springtail *Folsomia candida*. *Environmental Pollution*, *244*, 342–350. https://doi.org/10.1016/j.envpol.2018.10.077

Plummer, J. L., Smith, B. R., Sies, H., & Bend, J. R. (1981). Chemical depletion of glutathione in vivo. In *Methods in Enzymology* (Vol. 77, pp. 50–59). https://doi.org/10.1016/S0076-6879(81)77010-1

Qiao, M., Wang, G. P., Zhang, C., Roelofs, D., van Straalen, N. M., & Zhu, Y. G. (2015). Transcriptional profiling of the soil invertebrate *Folsomia candida* in pentachlorophenol-contaminated soil. *Environmental Toxicology and Chemistry*, *34*(6), 1362–1368. https://doi.org/10.1002/etc.2930

Raimets, R., Karise, R., Mänd, M., Kaart, T., Ponting, S., Song, J., & Cresswell, J. E. (2017). Synergistic interactions between a variety of insecticides and an ergosterol biosynthesis inhibitor fungicide in dietary exposures of bumble bees (*Bombus terrestris L.*). *Pest Management Science*, *December*. https://doi.org/10.1002/ps.4756

Redler, R. L., & Dokholyan, N. V. (2012). The complex molecular biology of Amyotrophic Lateral Sclerosis (ALS). In *Progress in Molecular Biology and Translational Science* (Vol. 107). https://doi.org/10.1016/B978-0-12-385883-2.00002-3

Reeb, P. D., & Steibel, J. P. (2013). Evaluating statistical analysis models for RNA sequencing experiments. *Frontiers in Genetics*, *4*(SEP), 1–9. https://doi.org/10.3389/fgene.2013.00178

Rehberger, K., Kropf, C., & Segner, H. (2018). In vitro or not in vitro: a short journey through a long history. *Environmental Sciences Europe*, *30*(1). https://doi.org/10.1186/s12302-018-0151-3

Ren, X., & Kuan, P. F. (2020). Negative binomial additive model for RNA-Seq data analysis. *BMC Bioinformatics*, *21*(1), 1–15. https://doi.org/10.1186/s12859-020-3506-x

Ritchie, M. E., Phipson, B., Wu, D., Hu, Y., Law, C. W., Shi, W., & Smyth, G. K. (2015). Limma powers differential expression analyses for RNA-sequencing and microarray studies. *Nucleic Acids Research*, *43*(7), e47. https://doi.org/10.1093/nar/gkv007

Ritz, C., Baty, F., Streibig, J. C., & Gerhard, D. (2015). Dose-response analysis using R. *PLoS ONE*, *10*(12), 1–13. https://doi.org/10.1371/journal.pone.0146021

Robinson, M. D., McCarthy, D. J., & Smyth, G. K. (2009). edgeR: A Bioconductor package for differential expression analysis of digital gene expression data. *Bioinformatics*, *26*(1), 139–140. https://doi.org/10.1093/bioinformatics/btp616

Roelofs, Aarts, M. G. M., Schat, H., & Van Straalen, N. M. (2008). Functional ecological genomics to demonstrate general and specific responses to abiotic stress. In *Functional Ecology*. https://doi.org/10.1111/j.1365-2435.2007.01312.x

Roelofs, D., de Boer, M., Agamennone, V., Bouchier, P., Legler, J., & van Straalen, N. (2012). Functional environmental genomics of a municipal landfill soil. *Frontiers in Genetics*, *3*(MAY), 1–11. https://doi.org/10.3389/fgene.2012.00085

Rohart, F., Gautier, B., Singh, A., & Lê Cao, K. A. (2017). mixOmics: An R package for 'omics feature selection and multiple data integration. *PLoS Computational Biology*, *13*(11), 1–19. https://doi.org/10.1371/journal.pcbi.1005752

Rusek, J. (1998). Biodiversity of Collembola and their functional role in the ecosystem. *Biodiversity and Conservation*, *7*(9), 1207–1219. https://doi.org/10.1023/A:1008887817883

Ruttan, V. W. (2002). Productivity Growth in World Agriculture: Sources and Constraints. *Journal of Economic Perspectives*, *16*(4), 161–184. https://doi.org/10.1257/089533002320951028

Salehi-Sedeh, F., Khajehali, J., Nematollahi, M. R., & Askari-Saryazdi, G. (2020). Imidacloprid resistance status and role of detoxification enzymes in *Bemisia tabaci* (Hemiptera: Aleyrodidae) populations from Iran. *Journal of Agricultural Science and Technology*, *22*(5), 1267–1277.

Seehuus, S. C., Norberg, K., Gimsa, U., Krekling, T., & Amdam, G. V. (2006). Reproductive protein protects functionally sterile honey bee workers from oxidative stress. *Proceedings of the National Academy of Sciences of the United States of America*, *103*(4), 962–967. https://doi.org/10.1073/pnas.0502681103

Seyedebrahimi, S. S., Talebi Jahromi, K., Imani, S., Hosseini Naveh, V., & Hesami, S. (2016). Characterization of imidacloprid resistance in *Aphis gossypii* (Glover) (Hemiptera: Aphididae) in Southern Iran. *Turkish Journal of Entomology*, *39*(4). https://doi.org/10.16970/ted.67424

Sgolastra, F., Medrzycki, P., Bortolotti, L., Renzi, M. T., Tosi, S., Bogo, G., Teper, D., Porrini, C., Molowny-Horas, R., & Bosch, J. (2017). Synergistic mortality between a neonicotinoid insecticide and an ergosterol-biosynthesis-inhibiting fungicide in three bee species. *Pest Management Science*, *73*(6), 1236–1243. https://doi.org/10.1002/ps.4449

Shapovalova, Y., Heskes, T., & Dijkstra, T. (2022). Non-parametric synergy modeling of chemical compounds with Gaussian processes. *BMC Bioinformatics*, *23*(1), 1–30. https://doi.org/10.1186/s12859-021-04508-7

Shi, Z., Tang, Z., & Wang, C. (2017). A brief review and evaluation of earthworm biomarkers in soil pollution assessment. *Environmental Science and Pollution Research*, *24*(15), 13284–13294. https://doi.org/10.1007/s11356-017-8784-0

Shojaie, A. (2021). Differential network analysis: A statistical perspective. *WIREs Computational Statistics*, *13*(2), 1–16. https://doi.org/10.1002/wics.1508

Sillapawattana, P., & Schäffer, A. (2017). Effects of imidacloprid on detoxifying enzyme glutathione S-transferase on *Folsomia candida* (Collembola). *Environmental Science and Pollution Research*, *24*(12), 11111–11119. https://doi.org/10.1007/s11356-016-6686-1

Silva, V., Mol, H. G. J., Zomer, P., Tienstra, M., Ritsema, C. J., & Geissen, V. (2019). Pesticide residues in European agricultural soils – A hidden reality unfolded. In *Science of the Total Environment* (Vol. 653, pp. 1532–1545). https://doi.org/10.1016/j.scitotenv.2018.10.441

Simões, T., Novais, S. C., Natal-da-Luz, T., Devreese, B., de Boer, T., Roelofs, D., Sousa, J. P., van Straalen, N. M., & Lemos, M. F. L. (2019). Using time-lapse omics correlations to integrate toxicological pathways of a formulated fungicide in a soil invertebrate. *Environmental Pollution*, *246*, 845–854. https://doi.org/10.1016/j.envpol.2018.12.069

Simon-Delso, N., Amaral-Rogers, V., Belzunces, L. P., Bonmatin, J. M., Chagnon, M., Downs, C., Furlan, L., Gibbons, D. W., Giorio, C., Girolami, V., Goulson, D., Kreutzweiser, D. P., Krupke, C. H., Liess, M., Long, E., Mcfield, M., Mineau, P., Mitchell, E. A., Morrissey, C. A., … Wiemers, M. (2015). Systemic insecticides (Neonicotinoids and fipronil): Trends, uses, mode of action and metabolites. *Environmental Science and Pollution Research*, *22*(1), 5–34. https://doi.org/10.1007/s11356-014-3470-y

Simon, E., Van Velzen, M., Brandsma, S. H., Lie, E., Løken, K., De Boer, J., Bytingsvik, J., Jenssen, B. M., Aars, J., Hamers, T., & Lamoree, M. H. (2013). Effect-directed analysis to explore the polar bear exposome: Identification of thyroid hormone disrupting compounds in plasma. *Environmental Science and Technology*, *47*(15), 8902–8912. https://doi.org/10.1021/es401696u

Solntsev, S. K., Shortreed, M. R., Frey, B. L., & Smith, L. M. (2018). Enhanced Global Post-translational Modification Discovery with MetaMorpheus [Research-article]. *Journal of Proteome Research*, *17*(5), 1844–1851. https://doi.org/10.1021/acs.jproteome.7b00873

Soneson, C., Love, M. I., & Robinson, M. D. (2016). Differential analyses for RNA-seq: Transcript-level estimates improve gene-level inferences. *F1000Research*, *4*, 1–23. https://doi.org/10.12688/F1000RESEARCH.7563.2

Spurgeon, D. J., Jones, O. A. H., Dorne, J. L. C. M., Svendsen, C., Swain, S., & Stürzenbaum, S. R. (2010). Systems toxicology approaches for understanding the joint effects of environmental chemical mixtures. *Science of the Total Environment*, *408*(18), 3725–3734. https://doi.org/10.1016/j.scitotenv.2010.02.038

Storey, J. D., Bass, A. J., Dabney, A., & Robinson, D. (2020). *qvalue: Q-value estimation for false discovery rate control*. http://github.com/jdstorey/qvalue

Suchail, S., De Sousa, G., Rahmani, R., & Belzunces, L. P. (2004). In vivo distribution and metabolisation of 14C-imidacloprid in different compartments of *Apis mellifera L*. *Pest Management Science*, *60*(11), 1056–1062. https://doi.org/10.1002/ps.895

Taillebois, E., & Thany, S. H. (2022). The use of insecticide mixtures containing neonicotinoids as a strategy to limit insect pests : Efficiency and mode of action. *Pesticide Biochemistry and Physiology*, *184*(May), 105126. https://doi.org/10.1016/j.pestbp.2022.105126

Tange, O. (2011). GNU Parallel: the command-line power tool. *The USENIX Magazine*, *36*(1), 42–47. https://www.usenix.org/publications/login/february-2011-volume-36-number-1/gnu-parallel-command-line-power-tool

van Gestel, C. A. M. (2012). Soil ecotoxicology: State of the art and future directions. *ZooKeys*, *176*(SPECIAL ISSUE), 275–296. https://doi.org/10.3897/zookeys.176.2275

van Straalen, N. M., & Roelofs, D. (2008). Genomics technology for assessing soil pollution. *Journal of Biology*, *7*(6), 19. https://doi.org/10.1186/jbiol80

van Straalen, N. M., & Roelofs, D. (2011). Stress responses. In *An Introduction to Ecological Genomics*. Oxford University Press. https://doi.org/10.1093/acprof:oso/9780199594689.003.0201 LK - https://vu.on.worldcat.org/oclc/5564637021

Vaudel, M., Burkhart, J. M., Zahedi, R. P., Oveland, E., Berven, F. S., Sickmann, A., Martens, L., & Barsnes, H. (2015). PeptideShaker enables reanalysis of MS-derived proteomics data sets: To the editor. *Nature Biotechnology*, *33*(1), 22–24. https://doi.org/10.1038/nbt.3109

Wall, D. H., Nielsen, U. N., & Six, J. (2015). Soil biodiversity and human health. *Nature*, *528*(7580), 69–76. https://doi.org/10.1038/nature15744

Wang, D., Hensman, J., Kutkaite, G., Toh, T. S., Galhoz, A., Dry, J. R., Saez-Rodriguez, J., Garnett, M. J., Menden, M. P., & Dondelinger, F. (2020). A statistical framework for assessing pharmacological responses and biomarkers using uncertainty estimates. *ELife*, *9*, 1–21. https://doi.org/10.7554/ELIFE.60352

Wickham, H. (2016). *ggplot2: Elegant Graphics for Data Analysis*. Springer-Verlag New York. https://ggplot2.tidyverse.org

Willis Chan, D. S., Prosser, R. S., Rodríguez-Gil, J. L., & Raine, N. E. (2019). Assessment of risk to hoary squash bees (*Peponapis pruinosa*) and other ground-nesting bees from systemic insecticides in agricultural soil. *Scientific Reports*, *9*(1), 1–13. https://doi.org/10.1038/s41598-019-47805-1

Wood, S. N. (2011). Fast stable restricted maximum likelihood and marginal likelihood estimation of semiparametric generalized linear models. *Journal of the Royal Statistical Society. Series B: Statistical Methodology*, *73*(1), 3–36. https://doi.org/10.1111/j.1467-9868.2010.00749.x

Wooten, D. J., Meyer, C. T., Lubbock, A. L. R., Quaranta, V., & Lopez, C. F. (2021). MuSyC is a consensus framework that unifies multi-drug synergy metrics for combinatorial drug discovery. *Nature Communications*, *12*(1). https://doi.org/10.1038/s41467-021-24789-z

Wu, Z., Yang, L., He, Q., & Zhou, S. (2021). Regulatory Mechanisms of Vitellogenesis in Insects. *Frontiers in Cell and Developmental Biology*, *8*(January), 1–11. https://doi.org/10.3389/fcell.2020.593613

Ye, J., Coulouris, G., Zaretskaya, I., Cutcutache, I., Rozen, S., & Madden, T. L. (2012). Primer-BLAST: A tool to design target-specific primers for polymerase chain reaction. *BMC Bioinformatics*, *13*(1), 134. https://doi.org/10.1186/1471-2105-13-134

Young, M. D., Wakefield, M. J., Smyth, G. K., & Oshlack, A. (2010). Gene ontology analysis for RNA-seq: accounting for selection bias. *Genome Biology*, *11*(2). https://doi.org/10.1186/gb-2010-11-2-r14

Yugi, K., Kubota, H., Hatano, A., & Kuroda, S. (2016). Trans-Omics: How To Reconstruct Biochemical Networks Across Multiple "Omic" Layers. *Trends in Biotechnology*, *34*(4), 276–290. https://doi.org/10.1016/j.tibtech.2015.12.013

Zhang, B. Z., Su, X., Xie, L. F., Zhen, C. A., Hu, G. L., Jiang, K., Huang, Z. Y., Liu, R. Q., Gao, Y. F., Chen, X. L., & Gao, X. W. (2020). Multiple detoxification genes confer imidacloprid resistance to *Sitobion avenae* Fabricius. *Crop Protection*, *128*(November 2019). https://doi.org/10.1016/j.cropro.2019.105014

Zhang, Q. Q., & Qiao, M. (2020). Transcriptional response of springtail (Folsomia candida) exposed to decabromodiphenyl ether-contaminated soil. *Science of the Total Environment*, *719*, 134859. https://doi.org/10.1016/j.scitotenv.2019.134859

Zhang, X., Xia, P., Wang, P., Yang, J., & Baird, D. (2018). Omics advances in Ecotoxicology. *Environmental Science & Technology*, acs.est.7b06494. https://doi.org/10.1021/acs.est.7b06494

Summary

Most agricultural soils are polluted with pesticide mixtures. In part, this pesticide pollution has led to a global decline in invertebrates, which provide ecosystem services essential to sustainable agriculture. Rapid and cost-effective tools are necessary to determine the environmental risk of pesticide soil contamination and guide pesticide abatement efforts to protect these non-target invertebrate populations. Conventional environmental risk assessment measures the soil concentration of an extensive panel of pesticides using chemical analysis. This labor-intensive process does not indicate the bioavailable fraction of pesticides or the hazard they pose to non-target invertebrates. Bioanalytical tools can supplement conventional chemical screening to assess the environmental risk of bioavailable and hazardous fractions of the pesticide pollution mixtures.

One bioanalytical tool is gene regulation biomarkers, i.e., transcripts or proteins. For the successful implementation of biomarkers in assessing pesticide mixture pollution, they should indicate the type of toxic exposure, even under synergistic interaction with other pollutants and over a range of exposure intensities. To this end, the molecular mechanisms that mediate pesticide toxicity must be elucidated. Without understanding these mechanisms, it is impossible to determine if the observed gene regulation patterns are unique identifiers of the type of pollution or part of a broader stress response elicited by multiple pollutants. The characteristic molecular functions affected by toxic exposure are called toxicogenomic fingerprints. In comparison, biomarkers are the single genes derived from toxicogenomic fingerprints that provide a read-out of its occurrence.

Under toxicogenomic fingerprint-based pesticide monitoring, soil samples are sent to a testing facility where lab-reared animals are exposed. These sentinels can provide a read-out of their response to toxic exposure and function as a living probe to assess the bioavailable and hazardous fraction of the pollutant mixture. *Folsomia candida* (springtails) would be ideal for this role; it is easily reared in the lab, requires a small amount of soil compared to other model species, and has been a soil ecotoxicological model for decades. I choose to focus on toxicogenomic fingerprint development for neonicotinoid soil pollution as neonicotinoids are the most commonly used type of insecticides of the past three decades and among the most toxic class of pesticides to invertebrates.

My research questions were divided into two categories: (1) How to identify toxicogenomic fingerprints? (2) Are biomarkers derived from toxicogenomic

fingerprints robust indicators of neonicotinoid exposure under various stress conditions?

In **chapter 2**, I investigated what would be most optimal exposure time to obtain transcriptomic and proteomic (omic) data for toxicogenomic fingerprint identification in *Folsomia candida*. Moreover, I investigated if shifts in transcript and protein abundances from the same gene occurred simultaneously or were delayed and whether this delay would hamper the combined analysis of both omics data. To this end, I obtained transcriptomic and proteomic data from *Folsomia candida* exposed to the neonicotinoid imidacloprid or control conditions every 12 hours for a total of 72 hours. I found that the 48-hour time point had the most differential gene regulation between control and treatment, marking the most opportune moment for toxicogenomic fingerprint identification. The results indicated no time lag between gene expression (transcripts) and regulation (proteins) relevant for the combined analysis of the omics data. The results contribute to the identification of toxicogenomic fingerprints, i.e., research question 1, by identifying the most opportune time point and facilitating justification for combining the results of omics data obtained at the same time point.

Toxicogenomic fingerprints should remain reliable indicators for pesticide exposure over various stress intensities and in mixtures with other pesticides. Gene expression patterns in transcriptomic data obtained under mixture exposure commonly are: non-linear (1), highly variable (2), and under genetic interaction (3). These three common characteristics impede the correct identification of characteristic gene-expression patterns, i.e., toxicogenomic fingerprints, with conventional statistical software based on generalized linear models. In **chapter 3**, I sought to identify toxicogenomic fingerprints from the transcriptomic data obtained from *Folsomia candida* exposed to two binary mixtures of pesticides that were finely resolved for stress intensity. I studied a mixture of two neonicotinoids (imidacloprid and clothianidin) and a mixture of a neonicotinoid (imidacloprid) combined with an azole fungicide (cyproconazole). Together with co-authors, I employed a statistical framework based on Gaussian Process (GP) models to analyze the binary mixture data jointly and identify toxicogenomic fingerprints for either neonicotinoids or cyproconazole. In turn, I identified putative biomarkers from these toxicogenomic fingerprints. These biomarkers remained indicative of their target pesticide type even under combined exposure with the other

pesticide type in spiked soils. The results demonstrated the validity of GP models for toxicogenomic fingerprint identification, i.e., research question 1, and can overcome the three common characteristics of transcriptomic data obtained under mixture exposures.

Toxicogenomic fingerprints, and derived biomarkers, should remain reliable indicators of neonicotinoid exposure under various stress conditions (research question 2). The cytochrome P450 enzymes (CYPs), which are key enzymes involved in biotransformation processes, mediate neonicotinoid toxicity and commonly form points of synergistic interaction with other pollutants in various invertebrates. In **chapter 4**, I investigated the influence of CYP-mediated metabolism on neonicotinoid biomarker reliability. I exposed *Folsomia candida* to two neonicotinoids (imidacloprid and thiacloprid) and a metabolic inhibitor of CYP enzymes: piperonyl butoxide (PBO). First, I found that putative inhibition of CYP metabolism by PBO enhanced the neonicotinoid toxicity to *Folsomia candida* reproduction in spiked soil. Second, only two biomarkers provided a reliable indication of the exposure to both neonicotinoids under metabolic inhibition of CYP enzymes. The results indicate that a panel of biomarkers is required for assessing neonicotinoid soil contamination.

Previous research proposed *glutathione-S-transferase* (*GST*) gene expression as a biomarker for neonicotinoid exposure in *Folsomia candida*. However, this group of enzymes has many cross-functional roles and is part of the oxidative stress response, a hallmark of the universal stress response. For their application in assessing neonicotinoid soil pollution, biomarkers should remain robust even under the effects of other stressors, such as increased oxidative stress conditions. As these genes are part of the universal stress response, I sought to determine their reliability in indicating neonicotinoid exposure. In **chapter 5**, I used the metabolic inhibitor diethyl maleate (DEM), which inhibits GST enzymes. I exposed *Folsomia candida* to two neonicotinoids (imidacloprid, thiacloprid) and DEM in spiked soil. I found no effect of DEM exposure on neonicotinoid toxicity to springtail reproduction. Then, I demonstrated that oxidative stress response genes, such as a GST, did not reliably indicate exposure to both neonicotinoids. The results suggest that oxidative stress response can greatly impact biomarker reliability and, therefore, DEM can prove as a valuable validation step in biomarker development.

In **chapter 6**, I discuss future perspectives for toxicogenomic fingerprint identification and application for the purpose of diagnosing pesticide soil pollution, and formulate four key recommendations. First, the practical benefit of standardized exposure duration for *Folsomia candida* gene expression surveys outweighs concerns over differences in toxicant toxicodynamics and toxicokinetics when applying gene expression for diagnosing environmental pollution. Second, the combined results of multiple omics data analysis are more valuable than their integrative assessment. Third, new methodologies are required to assess energy budget allocation by tracking shifts in gene expression and their molecular function over various exposure conditions. Four, as a discipline, we should move from biomarkers to toxicogenomic fingerprints to diagnosing complex environmental pollutant mixtures.

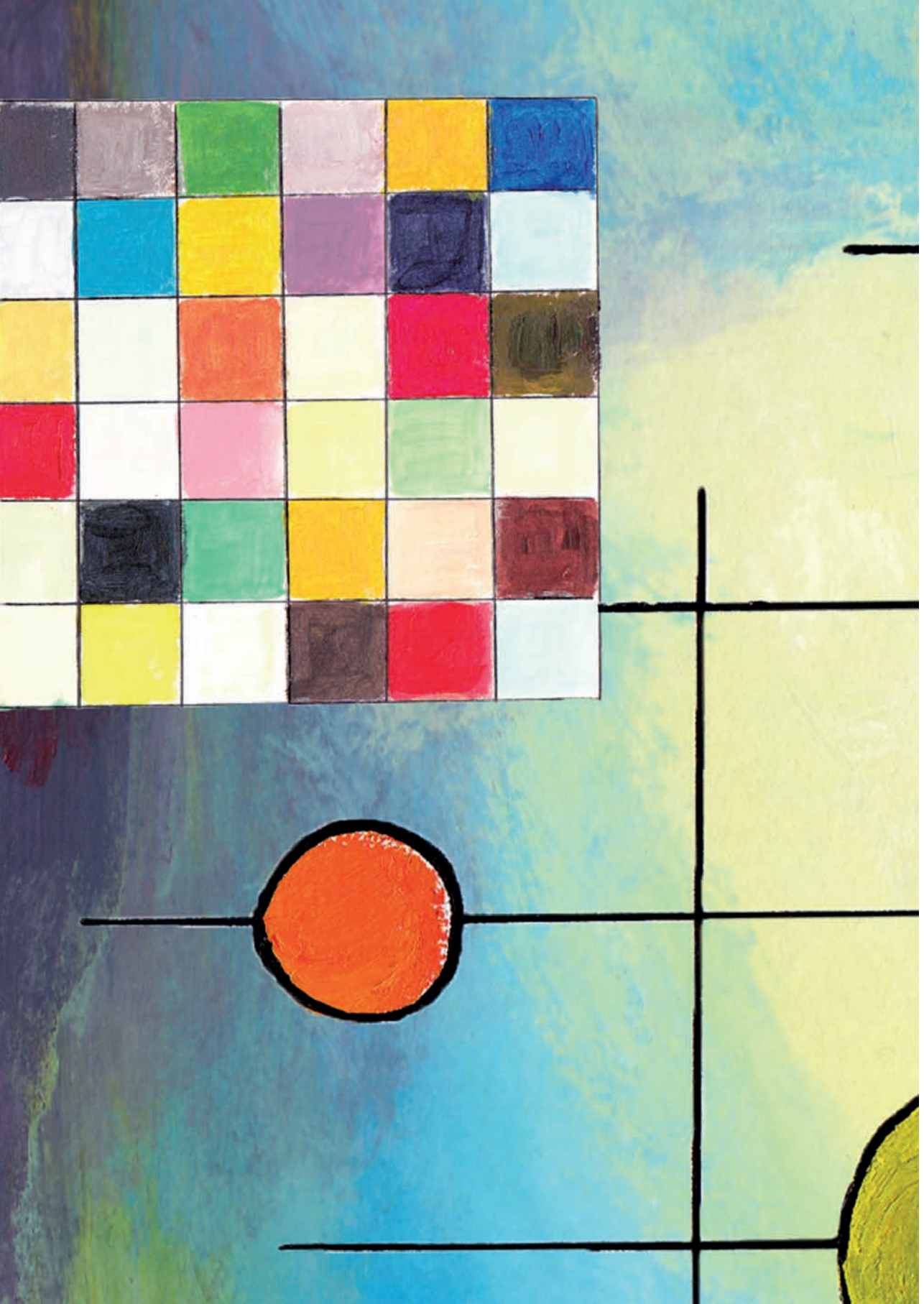

Samenvatting

De meeste landbouwgronden zijn vervuild met een mengsel van bestrijdingsmiddelen, ofwel pesticiden. Deze verontreiniging draagt bij aan de wereldwijde afname van ongewervelde dieren, zoals insecten, die cruciaal zijn voor een duurzame landbouw. Snelle en kostenbesparende methoden zijn nodig om de milieurisico's van deze bodemverontreiniging in kaart te brengen en daarmee maatregelingen te kunnen nemen die kunnen leiden tot een afname van de risico's. Deze maatregelen kunnen ongewervelde dieren en andere bodemorganismen beschermen die bevorderlijk zijn voor de landbouw. De gangbare risicobeoordeling van bodemverontreiniging met pesticiden is gebaseerd op het meten van de concentraties van een heel scala aan pesticiden in de bodem door middel van chemische analyse. Dit is een dure en arbeidsintensieve aangelegenheid die echter geen inzicht geeft in de fractie van het pesticidemengsel dat risicodragend of biologisch beschikbaar is voor ongewervelde dieren en andere bodemleven. Bio-analytische methoden kunnen deze tekortkoming van de gangbare chemische analyse aanvullen en zijn wel in staat de risicodragende en biologische beschikbare fractie van de pesticideverontreiniging vast te stellen.

Eén bio-analytische methode die voor dit doel geschikt is, zijn genetische biomarkers, zoals genexpressie (transcriptomic) of eiwitexpressie (proteomic) niveaus. Voor een succesvolle implementatie van deze biomarkers in de risicobeoordeling van pesticiden moeten zij een indicatie kunnen geven van het type verontreiniging, ook in aanwezigheid van andere mogelijk giftige stoffen. De moleculaire mechanismen die de giftigheid van pesticiden voor ongewervelde dieren bepalen moeten opgehelderd worden voor het succesvol ontwikkelen van deze biomarkers. Dit is nodig omdat anders niet bepaald kan worden of de waargenomen patronen van genexpressie of eiwitexpressie uniek zijn voor het type verontreiniging of onderdeel vormen van een algemene stressreactie. Karakteristieke moleculaire reacties voor een type giftige blootstelling worden toxicogenomische vingerafdrukken genoemd. Ter vergelijking, biomarkers zijn gebaseerd op de reactie van één gen en zijn een middel om toxicogenomische vingerafdrukken waar te nemen.

Toxicogenomisch-gebaseerde bepalingen van pesticiden beginnen met het sturen van bodemmonsters naar een testcentrum. Hier worden in het laboratorium gekweekte dieren aan de bodemmonsters blootgesteld. Deze dieren kunnen dienen als levende sondes die een indicatie geven van de risicodragende en biologisch

beschikbare fractie van het mengsel aan pesticiden in het bodemmonster. De springstaart *Folsomia candida* is uiterst geschikt voor deze functie, omdat dit dier gemakkelijk gekweekt kan worden in het laboratorium, weinig bodem nodig heeft in vergelijking tot andere bodemdieren en al sinds decennia als modelorganisme wordt gebruikt voor bodem-ecotoxicologisch onderzoek. Ik heb mij gericht op het bepalen van de toxicogenomische vingerafdruk van neonicotinoïden, een groep van insecticiden die wereldwijd veel is gebruikt in de afgelopen drie decennia en die behoren tot de meest giftige pesticiden voor ongewervelden, met name voor insectachtigen.

Mijn onderzoekvragen waren verdeeld in twee categorieën: (1) Hoe kunnen toxicogenomische vingerafdrukken bepaald worden? (2) Kunnen de biomarkers afkomstig van toxicogenomische vingerafdrukken een betrouwbare indicatie geven van bodemverontreiniging en zijn ze in staat dit ook te blijven doen onder wisselende stressomstandigheden?

In het **hoofdstuk 2** van mijn proefschrift onderzocht ik de optimale duur van blootstelling van *Folsomia candida* voor het verkrijgen van genexpressie (transcriptomic) en eiwitexpressie (proteomic) data. Deze omics data kunnen de basis vormen voor het bepalen van toxicogenomische vingerafdrukken van pesticiden. Verder wilde ik onderzoeken of er een vertraging plaats vond tussen de veranderingen in het niveau van genexpressie en eiwitexpressie. Een vertraging hiervan kan de gecombineerde analyse van de twee typen omics data belemmeren. Om dit te onderzoeken, stelde ik *Folsomia candida* gedurende 72 uur bloot aan het neonicotinoïd imidacloprid en een niet behandelde controle. Hierbij nam ik elke 12 uur monsters. De genexpressie- en eiwitexpressie-niveaus verschilden het meest tussen de imidacloprid-behandeling en de controle na 48 uur blootstelling. Hiermee was dit tijdstip het meest geschikt voor het verkrijgen van omics data en het bepalen van toxicogenomische vingerafdrukken. Verder vond ik dat veranderingen van de genexpressie- en eiwitexpressie niveaus van hetzelfde gen synchroon verliepen. Ik concludeerde daarom dat deze twee typen omics data samen geanalyseerd kunnen worden. Dit hoofdstuk draagt bij aan onderzoekvraag 1, omdat ik het meest gunstigste tijdstip voor het meten van de toxicogenomische vingerafdruk bepaalde en verantwoording verleen voor de gecombineerde analyse van de twee typen omics data.

Toxicogenomische vingerafdrukken moeten betrouwbare indicatoren zijn voor pesticide-blootstelling, ook wanneer er sprake is van blootstelling aan verscheidende stressfactoren of meerdere chemische stoffen (mengsels). Er zijn echter drie algemeen voorkomende aspecten van genexpressie-patronen verkregen bij blootstelling van organismen aan mengsels van stoffen: deze genexpressie-patronen zijn niet lineair (1), zeer variabel (2) en zijn onderhevig aan genetische interactie (3). Deze drie aspecten belemmeren de toepassing van de huidige methodiek gebaseerd op generalistische lineaire statistische modellen voor het bepalen van toxicogenomische vingerafdrukken. In **hoofdstuk 3** richtte ik mij op het identificeren van toxicogenomische vingerafdrukken in genexpressie data. De transcriptomic data waren afkomstig van een bloostelling aan twee binaire pesticide mengsels, ieder met een zeer verfijnde reeks aan concentraties (stress-intensiteiten). Deze mengsels bestonden uit twee neonicotinoïden (imidacloprid en clothianidin) of een neonicotinoïd (imidacloprid) en een fungicide (cyproconazole). Samen met coauteurs gebruikte ik een statische aanpak gebaseerd op zogenaamde Gaussian Proces (GP) modellen die de data van de twee mengselblootstellingen gecombineerd analyseerden. Hiermee identificeerde ik kandidaat-biomarkers voor blootstelling aan neonicotinoïden of aan cyproconazole. Deze biomarkers bleken indicatief voor het bedoelde pesticide zelfs in mengsel met het andere type pesticide in bodems die in het laboratorium waren behandeld. Deze resultaten lieten zien dat GP-modellen ingezet kunnen worden voor het bepalen van toxicogenomische vingerafdrukken (onderzoeksvraag 1). Verder konden met de GP-modellen de drie veel voorkomende uitdagingen worden overwonnen, die veel voorkomen in transcriptomic data verkregen bij blootstelling aan mengsels van stoffen.

Toxicogenomische vingerafdrukken, en hun afgeleide biomarkers, moeten betrouwbare indicatoren zijn voor neonicotoïden, zelfs onder blootstelling aan verscheidende stressoren (onderzoeksvraag 2). De biotransformatie-enzymen van de familie van de cytochroom P450s (CYPs) zijn betrokken bij het mediëren van de giftigheid van pesticiden, maar spelen ook vaak een rol in het optreden van synergistische interacties met andere verontreinigende stoffen. In **hoofdstuk 4** onderzocht ik de invloed van het CYP-gemedieerde metabolisme op de betrouwbaarheid van biomarkers voor neonicotinoïden. Ik stelde *Folsomia candida* bloot aan twee neonicotoïden (imidacloprid en thiacloprid) en een remmer van CYP-enzymen: piperonyl butoxide (PBO). Ten eerste vond ik dat de waarschijnlijke

CYP-remming door PBO de giftigheid van neonicotoïden versterkte, gemeten als een verlaagde voortplanting van *Folsomia candida*. Ten tweede gaven slechts twee biomarkers een betrouwbare meting van de blootstelling aan beide neonicotoïden en onder metabolische remming van CYP-enzymen. Dit toont aan dat meerdere biomarkers nodig zijn voor een betrouwbare bepaling van de blootstelling aan neonicotoïden.

Voorgaand onderzoek had de genexpressie van het enzym *glutathione-S-transferase* (*GST*) aangewezen als een biomarker voor blootstelling aan neonicotinoïden in *Folsomia candida*. Dit enzym heeft echter verscheidende functies en is het betrokken bij de oxidatieve stressreactie, een zeer kenmerkend onderdeel van de universele stressreactie in organismen. Voor de toepassing als biomarkers voor pesticiden in de bodem, moeten zij een betrouwbare indicatie geven van de blootstelling aan neonicotoïden ook bij aanwezigheid van andere stressoren, zoals verhoogde oxidatieve stress. Omdat GSTs ook betrokken zijn bij de universele stressreactie, wilde ik hun betrouwbaarheid onderzoeken als biomarkers voor blootstelling aan neonicotoïden. In **hoofstruk 5**, gebruikte ik een metabolische remmer van GSTs: diethyl maleate (DEM). Ik stelde *Folsomia candida* bloot aan twee neonicotoïden (imidacloprid en thiacloprid) en DEM in bodems die in het laboratorium waren behandeld. Ik vond geen effect van DEM op de giftigheid van de neonicotoïden voor de voortplanting van *Folsomia candida*. Daarna toonde ik aan dat genen die betrokken waren bij de oxidatieve stressreactie, zoals GSTs, geen betrouwbare indicatie gaven van de blootstelling aan beide neonicotoïden. Deze resultaten suggereerden dat de oxidatieve stressreactie grote invloed heeft op de betrouwbaarheid van de biomarker. Daardoor kan DEM van grote waarde zijn bij het valideren van biomarkers voor pesticidenblootstelling.

In **hoofdstuk 6** heb ik perspectieven besproken voor de toepassing van toxicogenomische vingerafdrukken voor het bepalen van de risico's van bodems verontreinigd met pesticiden. Ik heb daarbij vier belangrijke aanbevelingen gedaan. Ten eerste, het praktische voordeel van een gestandaardiseerde blootstellingsduur voor genexpressie-bepalingen is van groter belang dan mogelijke zorgen over verschillen in toxicodynamiek (opnamesnelheid) en toxicokinetiek (snelheid van het zichtbaar worden van effecten) tussen verontreinigende stoffen. Ten tweede, de resultaten van een gecombineerde analyse van meerdere typen omics-data zijn meer informatief dan de resultaten van een geïntegreerde analyse. Ten

derde, nieuwe methoden zijn nodig om veranderingen in het energiebudget van organismen waar te nemen op het niveau van genexpressie en voor gelijktijdige blootstellingen aan verscheidene typen stressoren of aan mengsels van chemische stoffen. Ten vierde, als een onderzoeksgemeenschap zouden wij onze focus moeten verleggen van biomarkers naar toxicogenomische vingerafdrukken voor het bepalen van de milieurisico's van complexe mengsels van verontreinigende stoffen.

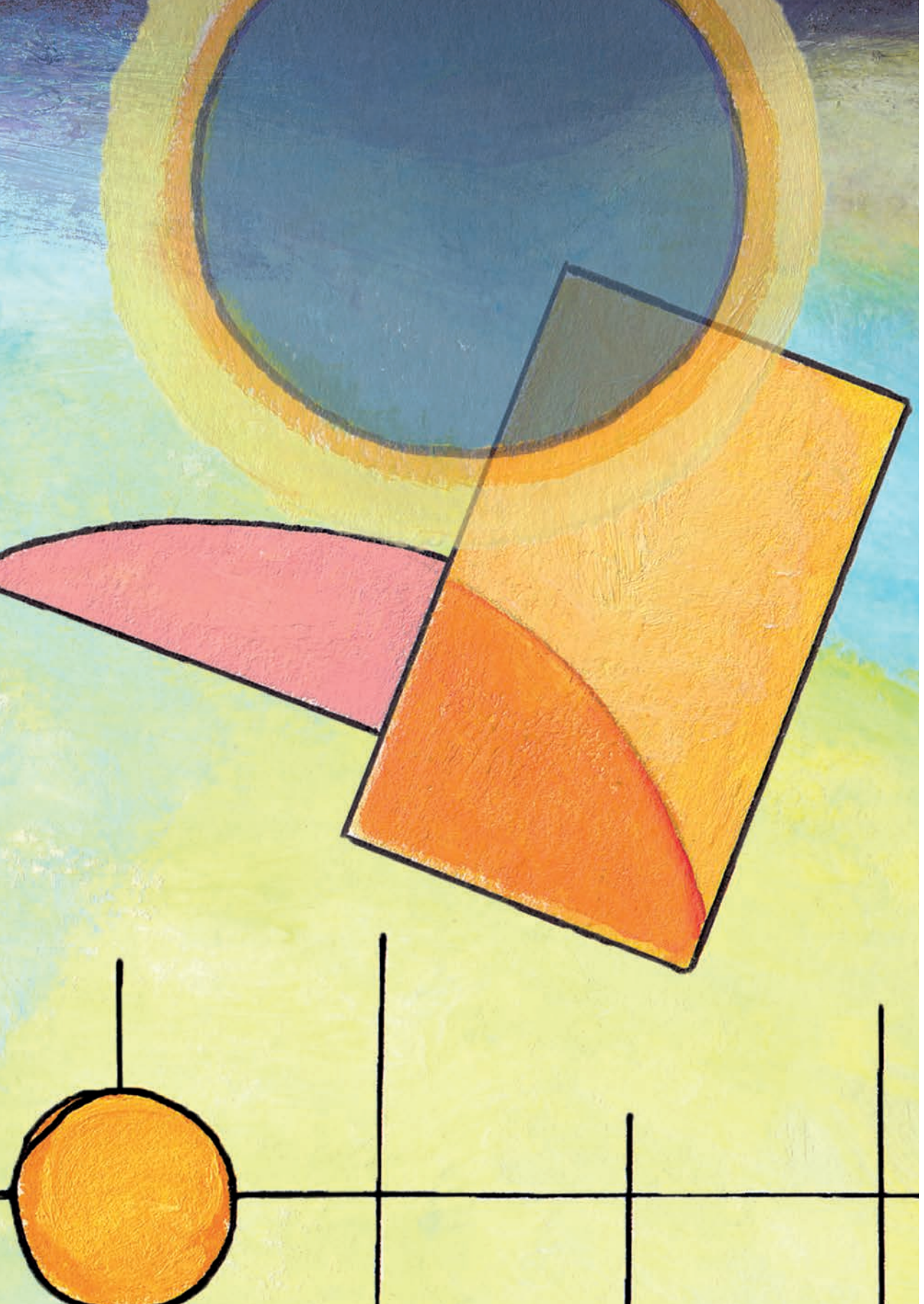

Acknowledgements

My Ph.D. research project marked some of my best years. However, the COVID-19 pandemic and the inevitable grind of the last years challenged me personally and professionally. Luckily, I had an incredibly supportive network of colleagues, supervisors, friends, and family to rely on, and I met many more wonderful people along the way. They have significantly impacted me and the dissertation you are currently reading. If you doubt, however slightly, if you are among these people, I can assure you: you most definitely are! Chances are, you do not even know half the praise you deserve. The help and support I received from you ranged from a simple conversation over a coffee to weeks of hands-on sweat and toil in the laboratory, writing and revisions. Without this support, I would never have managed to complete my Ph.D. program. Naming those involved will result in me forgetting a few among you that played a crucial role. Therefore, here I want to thank you all! From the bottom of my heart, thank you for being there for me in ways big and small!

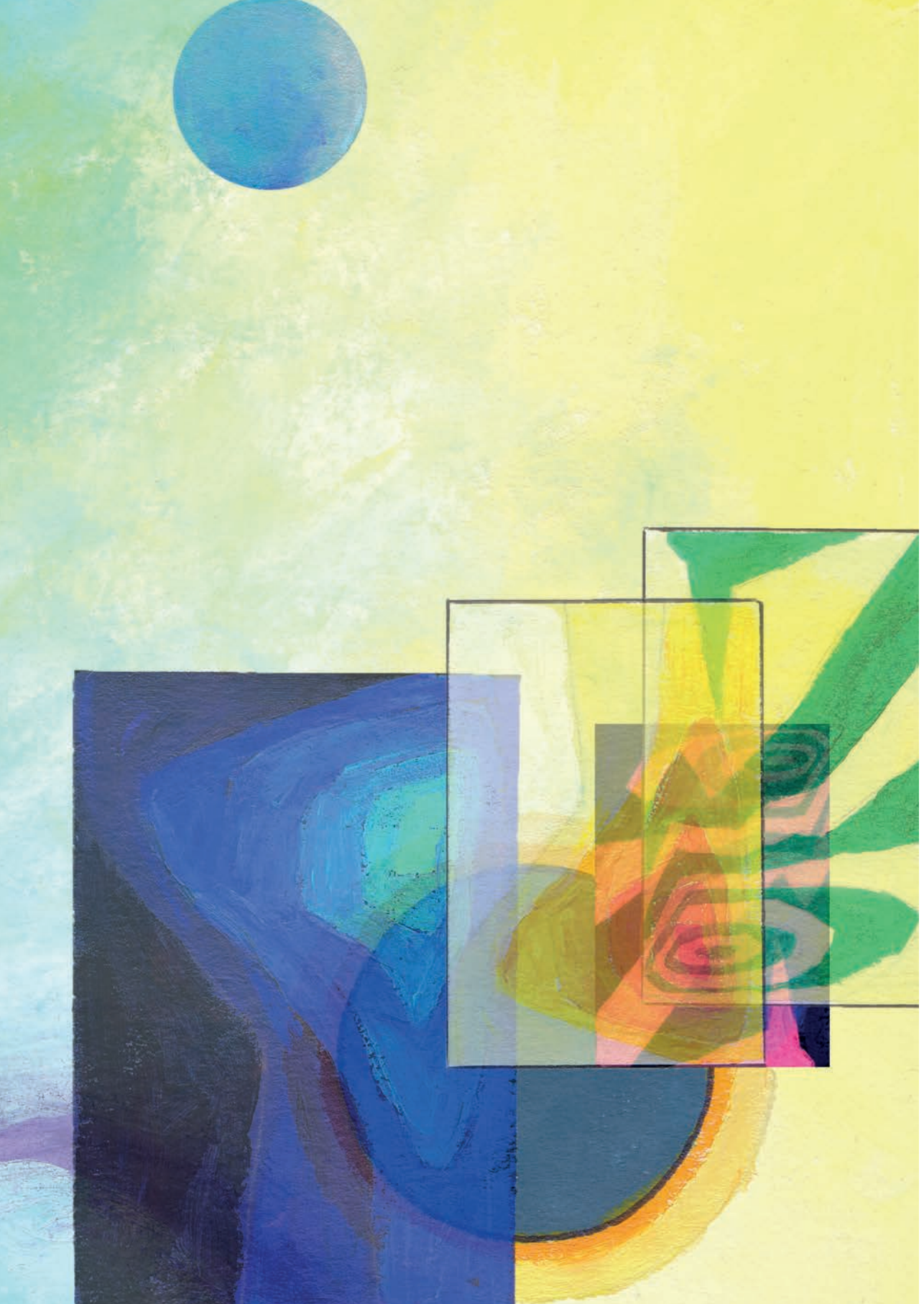

List of Publications

Bakker, R., Ekelmans, A., Xie, L., Vooijs, R., Roelofs, D., Ellers, J., Hoedjes, K. M., & van Gestel, C. A. M. (2022). Biomarker development for neonicotinoid exposure in soil under interaction with the synergist piperonyl butoxide in *Folsomia candida*. Environmental Science and Pollution Research, 1–17. https://doi.org/10.1007/s11356-022-21362-z

Bakker, R., Xie, L., Vooijs, R., Hoedjes, K. M., & van Gestel, C. A. M. (*under review*). Validation of biomarkers for neonicotinoid exposure in *Folsomia candida* under mutual exposure to diethyl maleate. Environmental Science and Pollution Research, 1–16. https://doi.org/10.21203/rs.3.rs-1489709/v1

Dai, W., Holmstrup, M., Slotsbo, S., **Bakker, R.**, Damgaard, C. & van Gestel, C.A.M. (*under review*). Heat stress delays detoxification of phenanthrene in the springtail *Folsomia candida*. Chemosphere

Bakker, R., Ellers, J., Roelofs, D., Vooijs, R., Dijkstra, T., van Gestel, C. A. M. & Hoedjes, K. M. (*under review*). Combining time-resolved transcriptomics and proteomics data for Adverse Outcome Pathway refinement in ecotoxicology. Science of the Total Environment.

Bakker, R., Shapovola, Y., Dijkstra, T., Heskes, T., van Gestel, C. A. M. & Hoedjes, K. M. (*in preparation*). A Gaussian Processes Approach Facilitates the Identification of Robust Biomarkers for Exposure to Complex Pesticide Mixtures.

Fernandes, S., Buskermolen, K., Ilyaskina, D., **Bakker, R.**, van Gestel, C.A.M. (*in preparation*). Effects of Life Stage on the Sensitivity of *Folsomia candida* to Four Pesticides.